STUIDES OF IMPROVING THERAPEUTIC OUTCOMES OF BREAST CANCER THROUGH DEVELOPMENT OF PERSONALIZED TREATMENTS AND CHARACTERIZATION OF GENE INTERACTIONS

By

Jing-Ru Jhan

A DISSERTATION

Submitted to
Michigan State University
in partial fulfillment of the requirements
for the degree of

Cell and Molecular Biology- Doctor of Philosophy

2016

ABSTRACT

STUIDES OF IMPROVING THERAPEUTIC OUTCOMES OF BREAST CANCER THROUGH DEVELOPMENT OF PERSONALIZED TREATMENTS AND CHARACTERIZATION OF GENE INTERACTIONS

By

Jing-Ru Jhan

With an understanding of the heterogeneity of breast cancer, patients with luminal or HER2 breast cancer have more specific treatment options other than traditional chemotherapy, the standard therapy for triple-negative breast cancer (TNBC) patients. However, the response to current treatments as well as the prognosis have been clinical challenges. In fact, breast cancer consists of more than subtypes routinely used based on gene expression. In addition, gene expression is highly correlated with response to treatment and prognosis. This suggests that the development of personalized treatment with targeted therapy could improve the outcomes, especially for the TNBC subtype. To address this need, I used two approaches, the development of pathway-guided individualized treatment and an understanding of the interactions of potential genes for targeted therapy. Considering the complexity of gene and pathway interactions, the probability of pathway activation was predicted using pathway signatures generated by comparing gene expression differences between cells overexpressing interested genes and those expressing GFP. This approach was validated in two subtypes of mouse mammary tumors from MMTV-Myc mice, and then further validated in human TNBC patient-derived xenografts (PDXs). The inhibition of tumor growth in mouse mammary tumors and the regression of tumors in PDXs were observed. These proof-of-principle experiments demonstrated the flexibility of pathway-guided personalized treatment. Because this approach needs the combination of different targeted therapies, it is necessary to understand the characteristics of these targeted genes and therapies,

such as gene-gene interactions. To meet this demand, I studied the effects of Stat3 in Myc-driven tumors. Here, MMTV-Myc mice with conditional knockout Stat3 mice was generated. I noted that the deletion of Stat3 in MMTV-Myc mice accelerated the tumorigenesis as well as delayed the tumor growth with an alteration in the frequency of histological subtypes. These tumors also had deficient angiogenesis. Unexpectedly, mice with this genotype had lactation deficiencies and the lethality of pups was found.

This model shared some of the same effects of loss of Stat3 in other oncogene-induced tumors and also had distinct effects compared with other models. This suggests that the oncogene drivers determine the roles of Stat3, an oncogene or tumor suppressor, and emphasizes again the importance of understanding the pathways and interactions in the development of treatment.

In sum, these studies demonstrate the potential of guiding individualized treatments in preclinical platforms using bioinformatics analyses. Combined with other genomic profiles, this approach could offer more complete assessments before being translated to practice. In addition, this could be further applied in adaptive clinical trials through matching with mouse models.

This thesis is dedicated to Mom.
Thanks for supporting my life.
Appreciate the contributions of all animals involved in these studies.

ACKNOWLEDGEMENTS

I would like to express my deep appreciation to my mentor, Dr. Eran Andrechek. He has been the one who is always willing to answer my questions and polish my writings. I appreciate his enormous supports in the past years. I thank all my committee members, Dr. Christina Chan, Dr. Sue Conrad, Dr. Kathleen Gallo, and Dr. Hua Xiao for their great advice in my research.

Thank you to current and previous members in Andrechek lab. Thank you to my big brother in bioinformatics, Dr. Daniel Hollern, for teaching me bioinformatic analyses. Thank you to Dr. Inez Yuwanita for her supports. Thank you to Jordan Honeysett and Kelian Sun for helping our lab operating properly. I would like to thank all partners in my second lab (mouse rooms).

A special acknowledgement to the awesome veterinarian Dr. Danielle Ferguson. Thanks for her patience and quick response to the mouse issues I encountered. I would like to thank Dr. Sandra O'Relliy for her suggestions in mouse experiments. Thank ULAR staffs for taking cares of my mice. Thank Don Herrington for sharing some experiences of working with mice. Thank Amy Porter and Kathy Joseph for helping histology experiments.

I would like to thank all helps from my home program, Cell and Molecular Biology Program, and the home of our lab, Department of Physiology. I also thank all past and current members in cancer research network for their suggestions and supports.

Thank all my friends and those people for being there for me whenever I needed them. Without them, I would not be able to go through difficult times before writing this thesis.

Finally, I thank my mother for generous supports in my life. Her enthusiasm and braveness have helped me go through many challenges. I would like to dedicate this thesis work to her.

TABLE OF CONTENTS

LIST OF TABLES

LIST OF FIGURES

KEY TO SYMBOLS OR ABBREVIATIONS

ALT	Alanine Aminotransferase
AST	Aspartate Aminotransferase
BFRM	Bayesian Factor Regression Modelling
BL-1	Basal-Like 1
BL-2	Basal-Like 2
BLG	Beta-Lactoglobulin
BRCA	Breast Cancer Gene
BrdU	5-Bromo-2'-Deoxyuridine
Chk1	Checkpoint Kinase 1
CK	Cytokeratin
CKO	Conditional Knockout
CRD	Coding Region Determinant
CRD-BP	CRD-Binding Protein
DCIS	Ductal Carcinoma In Situ
DERE	Distant Estrogen Response Elements
DMEM	Dulbecco's Modified Essential Medium
DMSO	Dimethyl Sulfoxide
E6.5	Embryonic Day 6.5
EGFR	Epithelial Growth Factor Receptor
EMT	Epithelial Mesenchymal Transition
EpCAM	Epithelial Cell Adhesion Molecule

ER	Estrogen Receptor
FBS	Fetal Bovine Serum
FDA	Food and Drug Administration
GFP	Green Fluorescent Protein
GGI	Genomic Grade Index
GSEA	Gene Set Enrichment Analysis
GSK3	Glycogen Synthase Kinase-3
HER2	Human Epithelial Growth Factor Receptor 2
HER3	Human Epithelial Growth Receptor 3
IDC	Invasive Ductal Carcinoma
IDFS	Invasive Disease-Free Survival Rate
IM	Immunomodulatory
I-SPY	Investigation of Series Studies to Predict Your Therapeutic Response with Imaging And Molecular Analysis
KEGG	Kyoto Encyclopedia of Gene and Genomics
KIF14	Kinesin Family Member 14
LAR	Luminal Androgen Receptor
LCIS	Lobular Carcinoma In Situ
M	Metastasis
MAPK	Mitogen-Activated Protein Kinase
Mas 5	Microarray Suite 5.0
MCSCs	MET-Like Cancer Stem Cells
MGI	Molecular Grade Index
MMTV	Mouse Mammary Tumor Virus

MSL	Mesenchymal Stem-Like
N	Node
ncRNAs	Non-Coding RNAs
PAI-1	Plasminogen Activator Inhibitors
PAM50	Prediction Analysis of Microarray 50
PARP	Poly ADP Ribose Polymerase
PBS	Phosphate-Buffered Saline
PCA	Principle Component Analysis
PCD	Programmed Cell Death
PDX	Patient-Derived Xenograft
PI3K	Phosphoinositide 3-Kinase
PIAS	Protein Inhibitors of Activated Stats
PR	Progesterone Receptor
PyVmT	Polyomavirus Middle T Antigen
RMA	Robust Multi-Array Analysis
RPPA	Reverse Phase Protein Array Data
S1PR1	Shingsosine-1-Phosphate Receptor-1
S62	Serine 62
SAM	Significant Analysis of Microarrays
SERMs	Selective Estrogen Receptor Modulators
SOCS	Suppressors of Cytokine Signaling
SVD	Singular Value Decomposition
T	Tumor

T58	Threonine 58
T-DM1	Ado-Trastuzumab Emtansine
TEB	Terminal End Bud
Tet	Tetracycline
TICs	Tumor-Initiated Cells
TLN1	Talin
TNBC	Triple-Negative Breast Cancer
uPA	Urokinase Plasminogen Activator
VEGF	Vascular Endothelial Growth Factor
WAP	Whey Acidic Protein

CHAPTER 1

GENERAL INTRODUCTION

1-1. Mammary gland development, mammary stem cells, and tumors

Mammary gland development consists of a series of stages. In mouse embryos, the development of the mammary gland starts from embryonic day (E) 10.5 to E18.5 (Veltmaat, Mailleux et al. 2003, Cowin and Wysolmerski 2010). Mammary placodes are formed first, followed by the transformation of placodes into buds at E12.5, surrounded by the mammary mesenchyme. At E15.5, the mammary sprouts are formed by the elongation of the buds, followed by the branch growth toward the fat pad. These ducts are composed of the outer layer cells (myoepithelial cells) and the inner layer cells (luminal cells). The second stage of the mammary gland development occurs during puberty, including formation of terminal end buds (TEB), bifurcation of TEBs, and side branching (Wiseman and Werb 2002). The TEBs consist of the outer cells (cap cells) and the inner cells (body cells). The cap cells, also called stem cells, divide into cap cells and progenitors (discussed later), and the body cells are differentiated into luminal cells as well as undergo apoptosis to generate the lumen. The TEBs guide the mammary ducts to grow and invade the fat pad and then disappear. The third stage of the development starts during pregnancy, including the increase of side branching and formation of alveolar buds and alveoli, producing and secreting milk during lactation (Macias and Hinck 2012). Upon weaning, these alveolar cells are removed during involution (Watson 2006). Involution consists of two phases, including the process of apoptosis and remodeling (Stein, Salomonis et al. 2007). The first 48 hours of involution is apoptosis-only and reversible; in contrast, the second phase, including apoptosis and tissue remodeling, occurs between 72-144 hours after weaning and is irreversible. The apoptosis signaling has been found to be initiated at the end stage of lactation, and is mediated by Stat3. Stat3 increases the uptake of mammary fat globules, which are secreted during lactation. These fat globules are then phagocytosed into the lysosomes, followed by the leakage of

proteases and apoptosis (Sargeant, Lloyd-Lewis et al. 2014). On the other hand, adipocytes around the alveolar cells are differentiated into fat cells to replace their spaces.

The dramatic changes of the structure of the mammary gland occurring at different stages of mammary gland development are due to the signals stimulating mammary stem cells and differentiated mammary epithelial cells. Mammary stem cells divide symmetrically to self-renew stem cells and divide asymmetrically to generate stem cells and bipotent progenitors. These bipotent progenitors generate luminal progenitors and myoepithelial progenitors. The luminal progenitors are differentiated into ductal or alveolar cells, and the myoepithelial progenitors are differentiated into myoepithelial cells (Visvader and Lindeman 2006). Recent lineage-tracing studies showed that mammary stem cells consist of different lineages of stem cells (Van Keymeulen, Rocha et al. 2011, Davis, Lloyd-Lewis et al. 2016). The competition between lineages of stem cells has been observed in duct branching and formation of alveoli (Davis, Lloyd-Lewis et al. 2016). In addition, other cells, such as fibroblasts and vascular cells, are also important in mammary gland development (Inman, Robertson et al. 2015).

Similar with the transformation of normal cells found in the early stage of tumorigenesis, these stem cells are associated with the emerge of cancer stem cells in breast cancer. For instance, mammary stem cells, and cancer stem cells (also called tumor-initiating cells) have higher resistance to DNA damage compared to other mammary epithelial cells(Chang, Zhang et al. 2015). Based on the molecular signatures, mammary stem cells and progenitors have their corresponding subtypes of breast cancer (Lim, Vaillant et al. 2009, Prat and Perou 2009). However, more studies are needed to understand how these mammary stem cells and progenitors transform into different subtypes of tumor cells (Prat and Perou 2011).

1-2. Overview of breast cancer

To date, breast cancer is still the top cancer in women in the United States. The probability of women being diagnosed with breast cancer during their lifetime is 1 in 8. It is estimated that, as of 2016, 29% of newly diagnosed cancer patients have breast cancer in 2016. In addition, the death rate of breast cancer accounts for 14% of women with cancer. Among races, non-Hispanic white and non-Hispanic black women have higher breast cancer incidence and mortality (Siegel, Miller et al. 2016). Several known risk factors of breast cancer include gender, age, race, family history, dense breast tissue, benign breast conditions, and gene mutations. Among the mutated genes, BRCA1 and BRCA2 mutations are frequently noted in inherited breast cancer (Wooster, Neuhausen et al. 1994). The stage of breast cancer and the subtypes are important factors in the determination of the appropriate treatment and evaluation of outcomes. Based on the American Joint Committee on Cancer staging criteria, breast cancer is categorized into stage 0 (carcinoma in situ) and stage I-IV using the TNM (primary tumor/ regional lymph node/ distal metastasis) system. The histological and molecular subtypes of breast cancer reveal that breast cancer is a heterogeneous cancer.

1-2-1. Histological subtypes of breast cancer

Based on the original site, breast cancer can be separated into two groups: in situ carcinoma and invasive carcinoma (Malhotra, Zhao et al. 2010). In situ carcinoma includes lobular and ductal carcinoma. Lobular carcinoma in situ (LCIS) represents abnormal cells found in the lobules, the milk-producing glands. Ductal carcinoma in situ (DCIS) involves abnormal cells in the ducts connecting the lobules to the nipples. Comedo DCIS, characterized by comedo necrosis inside the tumor, is a relative aggressive subtype of DCIS. Cribriform DCIS has evenly disturbed

cells among ducts. Both papillary and micropapillary DCIS have finger-like structures; however, fibrovascular patterns are only present in papillary DCIS (Pal, Lau et al. 2010). Solid DCIS has cancer cells that fill the ducts completely. Invasive carcinoma, also called infiltrating carcinoma, is characterized by cancer cells spreading from the original location to the surrounding breast tissue. Invasive ductal carcinoma (IDC) and invasive lobular carcinoma are the first and second common subtypes of invasive breast cancer. IDC is further categorized into well-differentiated, moderately differentiated, and poorly differentiated types. Some IDCs with lobular features are called invasive ductal lobular carcinoma (Arps, Healy et al. 2013). The rare subgroups of IDCs include tubular, medullary, mucinous (colloid), and papillary. Mucinous IDCs are clusters of cancer cells surrounded by mucin. Medullary IDCs are frequently found in patients with BRCA1 or TP53 mutations (Dossus and Benusiglio 2015). Mutations of CDH1-encoding E-Cadherin and FOXA1, the loss of PTEN, and the activation of AKT are commonly noted in invasive lobular carcinoma (Ciriello, Gatza et al. 2015, Dossus and Benusiglio 2015).

1-2-2. Molecular subtypes of breast cancer

Using gene expression profiling, breast cancer has been categorized into four major subtypes (Perou, Sorlie et al. 2000, Sorlie, Perou et al. 2001, Sorlie, Tibshirani et al. 2003). Luminal subtypes express estrogen receptors (ER) and/ or progesterone receptors (PR), and have enriched expression of luminal markers (keratin 18 and keratin 19). Luminal A tumors usually have a histologically low grade, and luminal B tumors have a high histological grade. HER2-positive subtype has the amplification and overexpression of HER2 as well as a high frequency of gene amplification. Some of luminal B tumors also have HER2-positive expression. Basal subtype, also called triple-negative breast cancer (TNBC), is ER-negative, PR-negative, and HER2-negative.

This subtype has high genomic instability, and high expression of basal markers including keratin 5, keratin 14, and keratin 17. In addition, BRCA1 and BRCA2 mutations were noted in TNBC (Turner, Tutt et al. 2004). BRCA1-mutant tumors have the expression of cytokeratin (CK) 5 and/ or 6, CK14, and CK17, associated with the basal myoepithelial phenotype. Later, claudin-low tumors were identified (Herschkowitz, Simin et al. 2007). The characteristics of this subtype include low expression of claudins, E-cadherin, and luminal genes, and high expression of signature genes of tumor-initiated cells (TICs). The signature genes of TICs are CD24, CD44, CD49f, MUC1, and epithelial cell adhesion molecule (EpCAM). Claudin-low tumors have a poor prognosis (Prat, Parker et al. 2010).

The molecular subtypes of breast cancer can be further stratified into more than five classes based on gene expression pathway signature prediction (West, Blanchette et al. 2001, Bild, Yao et al. 2006). Gatza and colleagues found that breast cancer consists of seventeen subgroups (Gatza, Lucas et al. 2010). Basal, HER2, luminal A, and luminal B subtypes contain three, two, two, and five groups, respectively. There are also four subgroups that represent luminal A/B, and one subgroup with mixed subtypes. In addition, these subgroups showed different DNA copy number changes. Indeed, breast tumors were clustered into 10 groups according to the copy number variation (Curtis, Shah et al. 2012). The deletion of TTK, which is involved in mitosis, in the group that consisted of most basal subtype tumors could be important for the high genomic instability of basal subtype. Further analysis of gene expression profiling showed six classes of TNBC (Lehmann, Bauer et al. 2011).

The heterogeneity of breast cancer has been further studied using multi platforms, including mRNA, miRNA, DNA methylation, copy number variation, and protein expression (Cancer Genome Atlas 2012). Basal and HER2 subtypes are enriched for TP53 mutation. Luminal A, lu-

minal B, and HER2 subtypes have 32-49% PIK3CA mutations. Luminal B, HER2, and basal subtypes have high genomic instability. Basal subtype has 40% Myc focal (a small portion of the chromosome arm) gain, and HER2 subtype has 71% focal ERBB2 amplification. In contrast to the extensive genomic instability in basal and HER2 subtypes, luminal B is enriched for focal amplification. In DNA methylation, luminal B subtype has more hypermethylation. However, basal subtype has more hypomethylation sites. In protein expression, luminal A and luminal B subtypes have high MYB expression, and FOXM1 and MYC, respectively. HER2 subtype has high expression of HER2 and EGFR. Basal subtype is enriched for the expression of DNA repair proteins.

1-3. Gene expression in diagnosis, prognosis, and treatment

In addition to stratifying breast cancer into more than five subtypes, gene expression has been widely used in diagnosis and the prediction of recurrence and drug responses. According to the new American Society of Clinical Oncology clinical guidelines, several assays are included in the determination of adjuvant therapy for breast cancer patients (Harris, Ismaila et al. 2016).

1-3-1. Gene expression-based assay in prognosis

The breast cancer index predicts the recurrence rate based on the expression of HOXB13:IL17BR (Breast cancer gene expression ratio) and the molecular grade index (MGI). MGI includes BUB1B, CENPA, NEK2, RACGAP1, and RRM2. Patients receiving adjuvant endocrine therapy with high HOXB13:IL17BR and MGI haven shown poor survival rates (Ma, Salunga et al. 2008). Oncotype DX is an assay with sixteen cancer genes and five reference genes, such as AURKA, BAG1, BCL2, BIRC5, CCNB1, ERBB2, ESR1, and MMP11 (Cronin, Sangli et al. 2007). The recurrence score generated using Oncotype DX reflects the risks of distant recurrence in hormone receptor-positive patients receiving endocrine therapy (Dowsett, Cuzick et al. 2010). Patients with an intermediate risk of recurrence can be further split into those with a high or low risk by using BreastPRS (a 200-gene signature) (D'Alfonso, van Laar et al. 2013). MammaPrint is a 70-gene platform that determinates the risks of distant metastases in early-stage breast cancer, and the response to adjuvant chemotherapy (Knauer, Mook et al. 2010). Compared with Oncotype DX, a larger population of patients, such as ER-negative ones, are eligible for the MammaPrint test (Ross, Hatzis et al. 2008). PAM50 (Prediction Analysis of Microarray 50; now called Prosigna breast cancer prognostic gene signature assay) contains 50-gene signatures to stratify patients into four intrinsic subtypes, which are not fully consistent with the

immunochemical staining-oriented subtypes (Parker, Mullins et al. 2009). The genomic grade index (GGI) includes 97 genes important in histologic grade (Sotiriou, Wirapati et al. 2006), and the value of GGI is correlated with the therapeutic response to chemotherapy (Liedtke, Hatzis et al. 2009). The EndoPredict test contains 8 signature genes selected from tamoxifen-treated tumors (Filipits, Rudas et al. 2011), and can be applied in the assessment of early and late recurrence (Dubsky, Brase et al. 2013). BluePrint defines the subtypes of breast cancer based on the 80-gene signatures, and predicts sensitivity to chemotherapy (Krijgsman, Roepman et al. 2012, Gluck, de Snoo et al. 2013).

1-3-2. Immunoassay in diagnosis and prognosis

IHC4 is a common tool routinely used for classification of breast cancer based on ER, PR, HER2, and ki67. High expression of urokinase plasminogen activator (uPA) and plasminogen activator inhibitor (PAI-1) is correlated with poor relapse-free survival and overall survival regardless of lymph node status (Look, van Putten et al. 2002). Mammostrat is an assay for detecting the expression of the biomarkers CEACAM5, HTF9C, NDRG1, p53, and SLC7A5. Bartlett and colleagues found that this could be used to evaluate the recurrence risk in ER-positive patients with tamoxifen treatment (Bartlett, Thomas et al. 2010).

1-3-3. Response to treatment

The combination of gene expression and immunochemistry has predicted the response to chemotherapy (Hatzis, Pusztai et al. 2011). The signature genes of resistance and sensitivity to chemotherapy have been selected in ER-positive and ER-negative patients, respectively. In addition to gene expression, another group also analyzed DNA methylation and microRNA in order

to identify seventeen genes for predicting prognosis in TNBC with neoadjuvant therapy (He, Gu et al. 2016). An analysis of patients involved in the I-SPY1 trial (Investigation of Series Studies to Predict Your Therapeutic Response with Imaging and Molecular Analysis) showed that patients with activated wound-healing signatures, the p53 mutation signature, amplification at 17q, or a high ki67 index had a better pathological complete response after neoadjuvant chemotherapy (Esserman, Berry et al. 2012). In addition, kinesin family member 14 (KIF14) and talin (TLN1) were identified to be correlated with the sensitivity to docetaxel treatment through RNA interference screening in MDA-MB-231 cells (Singel, Cornelius et al. 2013). To understand the resistance to tamoxifen, Hsu and colleagues used next-generation sequencing to map regions of distant estrogen response elements (DERE) frequently amplified in luminal breast cancer, and found that the amplification of these regions could be due to the increase of DNA damage response (Hsu, Hsu et al. 2013).

1-4. Treatment of breast cancer

Treatment for breast cancer include radiation, hormone therapy, chemotherapy, targeted therapy, and a combination of treatments. Treatments that are given before surgery are neoadjuvant therapy, and treatments started after surgery are adjuvant therapy. Many factors other than the presence of hormone and HER2 receptors are involved in the decisions regarding appropriate treatments (examples described later).

1-4-1. Hormone therapy

Hormone therapy has been used in the prevention of breast cancer, and neoadjuvant and adjuvant treatment in PR-positive patients. In addition, it is a therapeutic option for patients with chemotherapy-induced amenorrhea or menopause (Bines, Oleske et al. 1996, Lee, Schover et al. 2006). Hormone therapy consists of drugs that block estrogen functions and target the production of estrogen. The major drugs used in blocking estrogen functions are selective estrogen receptor modulators (SERMs). Tamoxifen has been used for over 20 years in breast cancer patients. Toremifene has been approved for metastatic breast cancer patients. Other SERMs include raloxifene and toremifene. Fulvestrant blocks the actions of estrogen as well as mediates the degradation of the estrogen receptors (Long and Nephew 2006). Megestrol acetate is a synthetic derivative of progesterone that interferes with the functions of estrogen. The production of estrogen is prevented by using aromatase inhibitors and gonadotropin-releasing hormone agonists. Aromatase inhibitors, such as letrozole, exemestane, and anastrozole, prevent the production of estrogen. gonadotropin-releasing hormone agonists (ex: Goserlin) suppress the release of pituitary hormones and decrease the production of estrogen in the ovaries.

1-4-2. Chemotherapy

Chemotherapy is still the gold standard for TNBC treatment. Based on the mechanisms of drugs, there are at least five classes, including alkylating agents, antimetabolites, mitotic inhibitors, antifolate drugs, and anthracyclines. Alkylating agents directly attack DNA by attaching to DNA through their alkyl groups. Platinums, such as cisplatin, lead to the crosslinking of DNA through similar reactions without alkyl groups. Antimetabolites consist of analogs of purine, pyrimidine, and nucleoside. Examples include fludarabine and cytarabine which inhibit DNA synthesis, and 5-Fluorouracil which inhibits thymidylate synthase. Taxanes and vinca alkaloids are well-known mitotic inhibitors, which disrupt microtubules. Ixabepilone, which stabilizes microtubule, improved the response of anthracycline- and taxane-resistant patients when combined with capecitabine (Thomas, Gomez et al. 2007). Antifolate drugs inhibit the synthesis of DNA by interfering with the functions of folic acid. Anthracyclines are also called anthracycline antibiotics because of their origins. The mechanisms of anthracyclines include the inhibition of DNA synthesis or topoisomerase II, and the promotion of histone eviction from chromatin (Pang, Qiao et al. 2013).

1-4-3. Targeted therapy

The majority of the population of patients receiving targeted therapy is HER2-positive patients. HER2-targeted therapy includes anti-HER2 antibodies and small molecule inhibitors. Both trastuzumab and pertuzumab are monoclonal antibodies. Trastuzumab interferes with the ligand-independent HER2/HER3/PI3K complexes, and pertuzumab blocks the ligand-induced HER2/HER3 dimerization (Junttila, Akita et al. 2009). Ado-trastuzumab emtansine (T-DM1) is a monoclonal antibody that is linked with a chemotherapy drug. Lapatinib is a small molecule ty-

rosine inhibitor that targets HER2 and EGFR. The combination of trastuzumab, pertuzumab, and docetaxel has been approved in HER2-positive metastatic patients by the U.S. Food and Drug Administration (FDA) (Baselga, Cortes et al. 2012). Recently, advanced hormone receptor-positive and HER2-negative patients have also given options for targeted therapy, such as the combination of hormone therapy and targeted therapy. In 2012, the FDA approved everolimus (mTOR inhibitor) plus exemestane (aromatase inhibitor) for postmenopausal patients who received hormone therapy previously (ClinicalTrials.gov number, NCT00863655). In early 2015, palbociclib (CDK4 and CDK6 inhibitor) plus letrozole (aromatase inhibitor) was approved by the FDA for use in postmenopausal patients without prior hormone therapy (Finn, Crown et al. 2015). In early 2016, the FDA approved that palbociclib plus fulvestrant for patients treated with hormone therapy (Verma, Bartlett et al. 2016).

1-4-4. Miscellaneous treatments

Many target therapies and the combination of targeted therapy and other treatments are recruiting patients or undergoing in clinical trials. For instance, glembatumumab is an antibody-drug conjugate, containing anti-glycoprotein NMB antibody and monomethyl auristatin E (anti-mitotic drug) (Yardley, Weaver et al. 2015). With the emergence of cancer immunotherapy, several clinical trials have been conducted or proposed for breast cancer. NeuVax (Nelipepimut-S) is a peptide vaccine for testing the prevention of the recurrence of breast cancer in patients with HER2 expression (ClinicalTrials.gov number, NCT101479244). Another clinical trial is to assess the benefits of NeuVax in combination with trastuzumab (ClinicalTrials.gov number, NCT02297698). Pembrolizumab (MK-3475) is a PD-1 antibody that binds to the PD-1 on the

surface of T cells to restrain the checkpoint of immune response (ClinicalTrials.gov number, NCT02555657).

1-5. Mouse models for breast cancer research

Mouse models offer opportunities to study breast cancer in each stage of tumor development from various aspects. During the tumor formation, normal cells become transformed cells, requiring the mutation/deletion/overexpression/amplification of genes. These transformed cells need to escape from the immune system to establish their niches (Dunn, Bruce et al. 2002). Angiogenesis is required for tumor growth and metastasis (Folkman 1974, Folkman 2002). In addition, the efficiency of drugs could be increased by targeting the receptors of vessels (Arap, Pasqualini et al. 1998). Though most of models only represent partial of breast cancer, each model has its unique advantage in studies (Vargo-Gogola and Rosen 2007).

1-5-1. Cell line-derived xenografts

Cancer cell lines have been used for several decades; however, the maintenance of the original characteristics of cell lines is still controversial (Wistuba, Behrens et al. 1998, Lacroix and Leclercq 2004, Kao, Salari et al. 2009). The injecting location of cell lines has been found to be related to the changes of cell behavior. Not surprisingly, tumors grown from cell lines injected orthotopically have better vascularization than others (Fleming, Miller et al. 2010). Even though most of cancer cell lines are treated as homogeneous cell lines, some studies have shown the existence of tumor-initiating cells in these cell lines. These cells are characterized as CD44+/CD24-/epithelial-specific antigen+ ones. Compared with cancer cells, these tumor-initiating cells can form tumors from less than a thousand cells (Fillmore and Kuperwasser 2008). However, additional enrichment will be needed for maintaining these cells.

1-5-2. Transgenic mice

With the alteration of gene expression manually, mammary tumors are spontaneously formed in genetically engineered mice. Without the immune barrier between mice and humans, this model is ideal for studying stromal effects and the microenvironment. In addition, the roles of genes in normal mammary gland development and the effects of pregnancy on tumors can be studied. There are four major tissue-specific promoters used in this model, including mouse mammary tumor virus (MMTV), whey acidic protein (WAP), beta-lactoglobulin (BLG), and C3(1). Due to the extensive expression of MMTV promoter (Henrard and Ross 1988), MMTV-LTR promoter is used for selective expression in mammary cells. MMTV promoter was activated by steroid hormones (Grimm and Nordeen 1998). The expression of WAP promoter is enhanced by lactogenic hormones (Andres, Schonenberger et al. 1987). BLG expression is increased during lactation (Simons, McClenaghan et al. 1987). C3(1) promoter represents the 5' flanking region of the rat prostate steroid binding protein, which is expressed in mammary and prostate epithelial cells (Maroulakou, Anver et al. 1994). Moreover, the gene expression of transgenic mice could be also regulated through Tet (Tetracycline)-On/Tet-Off and Cre/LoxP systems (Gunther, Belka et al. 2002, Blakely, Sintasath et al. 2005). Notably, the heterogeneity of tumors in some transgenic mice has been found in gene clustering (Vargo-Gogola and Rosen 2007). Comparison of gene expression between transgenic mice and human breast cancer has shown similarities (Herschkowitz, Simin et al. 2007, Hollern and Andrechek 2014). Additionally, Usary and colleagues showed that transgenic mouse models predicted responses to chemotherapy (Usary, Zhao et al. 2013).

1-5-3. Patient-derived xenografts (PDXs)

PDXs are important tools for translational research in breast cancer. This human-in-mouse model recaptures many characteristics of human breast cancer, such as histology, biomarkers, and gene expression (Marangoni, Vincent-Salomon et al. 2007, DeRose, Wang et al. 2011, Zhang, Claerhout et al. 2013). More importantly, they maintain the heterogeneity of breast cancer (Cassidy, Caldas et al. 2015). Though some single nucleotide variations have been noted, they did not alter the functions of genes (Li, Shen et al. 2013). The sources of tumors for establishing PDX lines are primary breast tumors, pleural effusion, ascites, and other metastasis tissues. Remarkably, the successful rate of establishing ER+ PDX lines is still low compared with PDXs with other subtypes (DeRose, Wang et al. 2011, Cottu, Marangoni et al. 2012, Li, Shen et al. 2013, Zhang, Claerhout et al. 2013). Studies have shown that PDXs also preserve the same response to therapy (Marangoni, Vincent-Salomon et al. 2007, Li, Shen et al. 2013). In addition, Cottu and colleagues found various resistance patterns in luminal PDXs carrying acquired resistance to hormone therapy (Cottu, Bieche et al. 2014). Signatures of rapamycin treatment also predicted the therapeutic responses of mTOR inhibitors in TNBC PDXs (Zhang, Cohen et al. 2014). Mutant p53 sensitized TNBC PDXs to irinotecan (topoisomerase I inhibitor) plus a Chk1 inhibitor treatment (Ma, Cai et al. 2012). The combination of trastuzumab and abemaciclib (a CDK4/6 inhibitor) inhibited tumor growth in HER2+ PDXs which are known to be resistant to trastuzumab (Goel, Wang et al. 2016). Taken together, PDXs are valuable sources for mimicking the therapeutic responses of human breast cancer.

1-6. Bioinformatic analysis of gene expression

As mentioned in Chapter 1-2, gene expression has been widely studied in order to advance our knowledge of breast cancer and improve patient outcomes. Several tools have developed for understanding the interested gene-related networks of interest. For instance, the Kyoto Encyclopedia of Genes and Genomics (KEGG) has annotations for genes and pathways based on literature regardless of organisms (Kanehisa and Goto 2000). Gene Set Enrichment Analysis (GSEA) integrates gene expression datasets from studies to generate collections of enriched genes under specific conditions (Subramanian, Tamayo et al. 2005) and has over 180 gene sets for the oncogenic signatures. This tool ranks genes as well as estimates the false discovery rate. Due to the sources of the data, these signatures are generated in various normal or cancer cells. A potential concern is the organ specificity. For instance, the genes of kras signatures vary between the lung, breast, prostate, and kidney. In this dissertation, I applied another approach: the generation of the signatures of pathway activation using gene expression data of human mammary epithelial cells infected with adenovirus carrying genes or GFP (green fluorescent protein) (Huang, Ishida et al. 2003, Bild, Yao et al. 2006). The signatures have been validated in other datasets.

1-6-1. Microarray and batch effects

Prior to the further analysis of gene expression, microarray data need to be normalized and artificial variance needs to be removed. In Affymetrix microarray, each gene has matched and mismatched probes. Mismatched probes can be used to assess the non-specific hybridization in Mas 5 (Microarray Suite 5.0) normalization. In contrast to normalizing each chip separately, RMA (Robust Multi-Array Analysis) normalizes several chips. In RMA normalization, background signals are removed form observed signals, and signals are $\log_2$-transofrmed. Using

quantile normalization, each chip has an equal distribution of signals. Probe sets are summarized by median polishing. Notably, MAS5.0 and RMA normalizations are for the same batch of microarray data. When analyzing data from multiple batches, such as the comparison of several published datasets, batch effects can be observed by principle component analysis (PCA) and then removed using Bayesian Factor Regression Modeling (BFRM) (Carvalho, Chang et al. 2008).

1-6-2. Signature of pathway activation

For each training dataset, signatures are generated using BinReg. To identify genes with high linear correlations after genes of interest are overexpressed, singular value decomposition (SVD) and PCA are used (West, Blanchette et al. 2001). The gene expression data matrix in SVD consists of gene coefficient vectors, mode amplitudes, and expression level vectors. The metagene, an eigenvector in SVD, represents the lists of genes with distinct gene expression differences between two groups. The number of metagenes is used in Bayesian probit regression model to split samples into the "1 (high probability of pathway activation)" or "0 (low probability of pathway activation)" group. To obtain robust prediction results of the pathway probability in each training dataset, a leave-one-out cross validation, where one sample is left each time, is applied (Huang, Ishida et al. 2003, Bild, Yao et al. 2006, Gatza, Lucas et al. 2010).

1-7. Experimental Rationale

Breast cancer is a heterogeneous disease with both inter-tumor and intra-tumor heterogeneity. Gene expression is known to be a crucial factor in determining therapeutic options. In addition, alterations of genes have been shown to be correlated with the de novo or acquired resistance to current treatments in subtypes of breast cancer. Among these subtypes, traditional chemotherapy is still the primary option for TNBC patients, especially for those ones without BRCA1/2 mutations, accounting for 80% of TNBC. Considering the population of patients and the aggressive status of TNBC, there is an urgent need to improve the therapeutic outcomes of TNBC. Based on this need, the first aim is to *develop a new strategy to guide combinatorial treatment for TNBC*. In the strategy, I integrated bioinformatics methods and the advantages of mouse models in personalized treatments. Instead of selecting targets based on their own alterations, I focused on the signatures of pathways, including genes affected by target genes. To overcome inter- and intra-tumor heterogeneity, I used a transgenic mouse model with heterogeneous tumors. The complete immune system and the similarity of this model to human breast cancer are its strengths. This approach was further tested in patient-derived xenografts reflecting the characteristics of human breast cancer to demonstrate its flexibility.

On the other hand, studies of resistance to target therapies, such as HER2-targeted therapy, outline that the crosstalk of pathways and interactions of genes are underestimated. In light of current knowledge on many target therapies still at the early developmental stage, here I studied the *interactions of Myc and Stat3 in a Myc transgenic mouse model with conditional knockout Stat3* from mammary development to metastases. The findings from this study could lead to a better understanding of the interaction of Myc and Stat3, and have the potential to be applied in the assessment of the administration of target therapies in various conditions.

Taken together, in this thesis, I have worked on advancing the understanding of breast cancer treatment using mouse models from two aspects: the development of personalized therapy and the crosstalk/interaction of potential genes for target therapies. The strategy of developing individualized treatment offers a novel approach to performing a preclinical trial and understanding the potential pitfalls before the clinical trials are started. The details of these studies are shown in Chapters 3 and 4.

CHAPTER 2

MATERIALS AND METHODS

2-1. Animal experiments

All mice were bred and maintained according to guidelines and protocols approved by the Institutional Animal Care and Use Committee in Michigan State University.

2-1-1. Strains

FVB/NJ mice were purchased from Jackson Laboratories (Bar Harbor, ME). $Stat3^{Fl/Fl}$ MMTV-Cre MMTV-Myc and $Stat3^{Fl/Fl}$ MMTV-Cre mice were generated from interbreeding MMTV-Myc (Andrechek, Cardiff et al. 2009), MMTV-Cre, and $Stat3^{Fl/Fl}$ mice generated in the Levy laboratory at New York University (Raz, Lee et al. 1999, Humphreys, Bierie et al. 2002). $Stat3^{Fl/WT}$ mice and MMTV-Cre mice were a generous gift from Dr. William J Muller at McGill University. SCID/Beige mice were purchased from Charles River Laboratories (Wilmington, MA).

2-1-2. DNA extraction and PCR

The tail of the mouse was lysed in lysis buffer (10% Tris-HCl, 5mM EDTA, 0.2% SDS, 0.2M NaCl) with protease K in 55°C. DNA was extracted from the lysates using isopropanol and dissolved in distilled water or 1x TE buffer.

2-1-2-1. Myc PCR

The primers are as follows:

Forward: 5'-GTTGTGCTGGTGAGTGGAGA-3'

Reverse: 5'-TCCTGTACCTCGTCCGATTC-3'

The annealing temperature and time is 52°C and 1 minute, and the number of cycle is 30.

2-1-2-2. Cre PCR

The primers are as follows:

Forward: 5'-GTCGATGCAACGAGTGATGAG-3'

Reverse: 5'-AACCTGGTCGAAATCAGTGCG-3'.

The annealing temperature and time is 52°C and 1 minute, and the number of cycle is 32.

2-1-2-3. Stat3 PCR

The sequences of the primers used in determining Stat3 excision are as follows:

$Stat3^{WT/Fl}$(1): 5'-GCTGCCAACAGCCACTGCCCCAG-3'

$Stat3^{WT/Fl}$ (2): 5' GAAGGCAGGTCTCTCTGGTGCTTC-3'

Stat3 knockout: 5'-CAGAACCAGGCGGCTCGTGGCG-3'.

The annealing temperature and time is 65°C and 45 second, and the number of cycle is 32. Alternatively, the PCR is started with the denature step, 94°C, 5 minutes, and enter the touchdown cycle for 10 cycle. The denature step is 94 °C/ 5 minutes. The start annealing condition is 68°C/ 45 seconds, and gradually decrease 0.5°C in each cycle. The extend step is 72°C/ 45 seconds. After that, regular PCR steps are used. The annealing temperature and time is 66°C and 45 second.

2-1-2-4. kras mutation PCR

PCR for detection of Kras mutation was performed as previously described (Andrechek, Cardiff et al. 2009, Hollern, Yuwanita et al. 2013)

2-1-3. Mammary and human breast tumors

Viably frozen papillary and EMT tumors were collected from MMTV-Myc mice (Andrechek, Cardiff et al. 2009). Tumors from patient-derived xenografts BCM2147 and BCM3887 were obtained from Dr. Michael Lewis' laboratory (Zhang, Claerhout et al. 2013). The freezing medium used were (1) Dulbecco's Modified Essential Medium supplemented with 3.7g/L sodium bicarbonate, 3.5 g/L D-glucose, 10 or 20% fetal bovine serum (FBS), 2.0 mM L-glutamine, and 10% dimethyl sulfoxide (DMSO), or (2) 90% FBS and 10% DMSO. All tumors were cryopreserved by slow freezing in -80°C overnight.

2-1-4. Establishment of cell lines from tumors

Tumors were freshly harvested from mice, and minced in 0.25% trypsin-EDTA solution. The isolated cells were incubated at 37°C with 5% carbon dioxide (Borowsky, Namba et al. 2005). To establish a histological pure EMT cell lines, the cells were divided into subpopulations based on the characteristics of cells, including colony, attachment ability and weight. These established cell lines were injected back to the 4th mammary gland of WT FVB/NJ mice to check the histology. In addition, these cell lines were cryopreserved in the freezing medium as mentioned previously.

2-1-5. Clear fat pad

3-4 week-old female mice were anesthetized and restrained by taping the limbs. The surgical are was sterilized using beta-iodine and normal saline (or PBS). The 4th mammary gland was separated from the skin from the nipple region to the Y-shaped blood vessel junction closed to the lymph node. The connection between separated mammary gland and the remain part of mamma-

ry gland as well as the blood vessel between the four and fifth mammary gland were cauterized (DeRose, Wang et al. 2011, Zhang, Claerhout et al. 2013).

2-1-6. Tumor implantation and cell line injection

2-1-6-1. Preparation of tumors and cells

Fresh harvested tumors and thawed frozen tumors were kept on ice, in 1x PBS or DMEM medium.

2-1-6-2. Recipients

EMT and papillary tumors were implanted into 6-8 week-old WT FVB/NJ female mice. EMT cell lines were injected into the mammary fat pad of WT FVB/NJ female mice. Tumors from human PDX lines were implanted into 3-4 week-old SCID/Beige female mice.

2-1-6-3. Implantation and injection

Mice were anesthetized. The protocol has been modified based on published methods (DeRose, Wang et al. 2011, Zhang, Claerhout et al. 2013).

2-1-7. Body weight and tumor measurement

Body weight of pups and adult mice was measured daily. Tumors were monitored at least twice per week, and were measured using a caliper. Once the diameter of the tumors reached 6 mm, mice were randomized into vehicle and drug-treated groups. Tumor volume was calculated as the shortest diameter^2 × the longest diameter/2. Percentage of tumor volume changes was calculated as (difference of tumor volume at different time points and initial tumor volume)/ initial tumor volume*100. When the tumor size reached 2500mm^3 or the end of the treatment, samples were collected for further analysis.

2-1-8. Drug treatments

VX680 (MK0457), miltefosine, and SB505124 were purchased from Cayman (Ann Arbor, MI, USA). WP1066 was obtained from EMD Biosciences (San Diego, CA, USA). Afatinib and trametinib were purchased from LC Laboratories (Woburn, MA, USA). All drugs except miltefosine were dissolved in DMSO (J.T. Baker, Jackson, TN, USA), and miltefosine was dissolved in PBS. Vehicles here used were poly-ethylene glycol (Sigma-Aldrich #202371, St. Louis, MO, USA), 0.5% methylcellulose (Sigma-Aldrich #274429), 0.4% Tween 80 (Fisher Scientific BP338500, Waltham, MA, USA), or PBS. VX680 (50 or 60 mg/kg, 6 days on, 1 day off), miltefosine (50 mg/kg, 5 days on, 2 days off), and WP1066 (20 mg/kg, 5 days on, 2 days off) were intraperitoneal injected into mice for 21 or 12 days. Afatinib (15 or 12.5 mg/kg daily), trametinib (1 mg/kg daily) and SB505124 (10 mg/kg daily, or 4 days on, 3 days off) were given through oral gavage for 21 or 28 days. The detail regimens are described in the figure legends.

2-1-9. Toxicity and health evaluation

In addition to records of body weight and health condition, the AST (aspartate aminotransferase), ALT (alanine aminotransferase), and creatinine tests were used to evaluate the toxicity of drug treatments. Intracardiac puncture was used to collect blood. The serum sample should be stored at -20°C before being analyzed by Diagnostic Center for Population and Animal Health at Michigan State University.

2-1-10. 5-Bromo-2'-Deoxyuridine (BrdU) staining

For BrdU staining, mice were intraperitoneally injected with BrdU (Acros Organics # 10104810; purchased from Acros organic, New Jersey, USA and dissolved in sterile PBS) 100

mg/kg 2 hours before samples were collected. A piece of guts and tumors were collect and fixed in 10% formaldehyde. BrdU staining was performed by Investigative Histopathology Laboratory at Michigan State University.

2-2. Gene expression, bioinformatics analysis, and statistical methods

2-2-1. RNA, and Microarray

Fresh frozen tumors were homogenized using a Fisher Scientific homogenizer (#14-261-01; Silver Spring, MD, USA), and RNA extraction was conducted using the Qiagen RNeasy Midi kit (#75142; Valencia, CA, USA). Mouse 430A 2.0 microarrays were used (Affymetrix, Santa Clara, CA, USA).

2-2-2. Datasets

Microarray data of mouse mammary tumors includes MMTV-Myc and MMTV-Neu tumors (GSE15904), and papillary tumors after treatment (GSE81284). Microarray data of human breast cancer datasets include GSE1456, GSE1561, GSE3494, GSE18864, GSE19615, GSE20194, and GSE45255. The expression data of patient-derived xenograft samples is GSE46106.

2-2-3. Bioinformatics analysis

Significant analysis of microarrays (SAM) (Tusher, Tibshirani et al. 2001) was used to select signature genes from Stat3 signature expression data (Dauer, Ferraro et al. 2005), and assess fold changes of gene expression in papillary and EMT tumors (p value). Unsupervised clustering was generated using Cluster 3.0 and Java Treeview. Probability of Stat3 pathway activity was generated as described (Andrechek, Cardiff et al. 2009, Gatza, Lucas et al. 2010). Distant metastasis free survival rate was generated using KM plots website (http://kmplot.com). The probability of Myc pathway activity was generated as described previously (Bild, Yao et al. 2006, Gatza, Lucas et al. 2010). Patients were split into two groups based on the median of Myc pathway activi-

ty probability. Patients with high Myc probability were split into two groups based on upper and lower quartile expression of phospho-Stat3 (Y705) from the TCGA RPPA data.

2-2-4. Probability of activation of signaling pathways

To generate probabilities of pathway activation, datasets were first combined and batch effects were removed using Bayesian Factor Regression Modeling (Carvalho, Chang et al. 2008). Gene expression signature training data for each pathway was derived from comparisons between cells overexpressing an oncogene or control cells as previously reported (Gatza, Lucas et al. 2010). Cell signaling signatures were used to calculate the probability of pathway activation, and predictions were previously validated. Detailed information for probability of pathway activation was completed as previously described (West, Blanchette et al. 2001, Bild, Yao et al. 2006, Gatza, Lucas et al. 2010).

2-2-5. Statistical methods

Statistical analyses were performed by two-tailed unpaired Student's t test using GaphPad Prism (GraphPad Software, La Jolla, CA, USA) or Microsoft Excel. Aside from scatter plots showing heterogeneity of samples, all data with error bars represent mean value and SD. $P<0.05$ was considered as statistically significant.

2-3. Protein extraction, immunoblotting, and immunoprecipitation

2-3-1. Protein extraction

Fresh frozen tumor samples were grinded with a mortar and pestle and liquid nitrogen, and lysed in TNE lysis buffer (0.05 M Tris HCl pH 8.0, 0.15 M NaCl, 2 mM EDTA, 0.01 N NaF, and 1% NP40) with proteinase inhibitor (1M Na_3VO_4, 58 uM PMSF, 10 ug/ml aprotinin, and 10 ug/ml leupeptin) (herein called TNE lysis buffer). Protein was quantified using Bradford protein assays (Biorad) and a Nanodrop spectrophotometer (Thermo Scientific, Waltham, MA).

2-3-2. Immunoblotting

Anti-c-Myc (ab32072) and anti-phospho-Smad3 (Serine 423/425; ab52903) were obtained from Abcam (Cambridge, MA). Phospho-Akt (Serine 473; #4060), Akt (#4685), phospho-Erk1/2 (Threonine 202/ Tyrosine 204; #4370), Erk1/2 (#9102), Smad2/3 (#8685; 1:1000), phospho-Stat3 (Tyrosine705; #9145), Stat3 (#9139), beta-Actin (#4967), and beta-Tubulin (#2128) antibodies were purchased from Cell Signaling Technology (Boston, MA). For detections using ECL reagents, secondary goat anti-mouse (BD554002; BD Transduction Laboratories; Lexington, KY) and second goat anti-rabbit antibodies (Abcam ab6721) were used. For samples detected with Odessey imager (LI-COR Biosciences, Lincoln, NE), IRDye 800CW goat anti-rabbit IgG (#925-32211) was used as the secondary antibody.

2-4. Immunohistochemical staining

2-4-1. Immunohistochemical staining

Collected tumor samples were fixed in 4% formaldehyde. Paraffin-embedded sections were used to perform immunohistochemical analyses. Phospho-Erk1/2 antibody (Threonine 202/Tyrosine 204; #4370) was purchased from Cell Signaling Technology (Boston, MA). Ki-67 antibody (Ab15580) was from Abcam (Cambridge, MA, USA). F4/80 antibody (Q61549) was from Serotec (Oxford, United Kingdom). CD31antibody (DIA-310) was from HistoBioTec (Miami beach, FL, USA). Secondary anti-rabbit antibody and the following detection reagents (Vector ABC kit #PK6101 and DAB kit #SK-4100) were obtained from Vector Laboratories (Burlingame, CA). TUNEL staining kit, *In Situ* Cell Death Detection Kit, POD (#11684817910) was obtained from Roche (Indianapolis, IN). BrdU antibody (BD 347580) was from BD Biosciences (San Jose, CA, USA). Positive signals were quantified using ImageJ software (National Institute of Health, Bethesda, MD, USA). When counting and evaluating samples, the experimenter was blinded to the identity.

2-4-2. Mammary gland whole mount staining

The 4th mammary gland was excised and spread on a glass slide. The fat of the mammary gland was removed using acetone, and the gland was stained using Harris's modified hematoxylin.

CHAPTER 3

EFFECTIVE PERSONALIZED THERAPY FOR BREAST CANCER BASED ON PREDICTIONS OF CELL SIGNALING PATHWAY ACTIVATION FROM GENE EXPRESSION ANALYSIS

Current therapeutic outcomes for breast cancer underscore the complexity of treating a heterogeneous disease. Indeed, studies have shown that differences in gene expression among patients with the same subtype of breast cancer are correlated with the response to treatment. This strongly suggests that there is an urgent need to treat breast cancer with a personalized approach. Here we employed cell signaling pathway signatures predict pathway activity in subtypes of MMTV-Myc mammary tumors. We then split tumors into subsets and developed individualized combinatorial treatments for two subtypes with distinct pathway activation patterns. Elevation of the EGFR, RAS, TGFβ pathways is found in one subtype whereas these pathways are not predicted to be active in the other subtype predicted with high Myc, Stat3, and Akt pathway activity. In a proof of principle experiment, treatment of these subtypes with targeted therapies inhibited tumor growth only in the subtype of tumor where the therapy was designed to be active in. We then analyzed gene expression profiles of human breast cancer patients and patient-derived xenograft samples to predict pathway activity, and validated our approach of developing individualized treatments in mice with PDX tumors. Importantly, our combinatorial therapy resulted in tumor regression, including in PDX samples from triple negative breast cancer. Together our data is a proof-of-principle experiment that demonstrates that cell signaling pathway signature-guided treatment for breast cancer is viable.

**This part has been accepted to publish in Oncogene in Nov 2016.

3-1. Introduction

Breast cancer is the most common cancer in female patients and is responsible for approximately 23% of newly diagnosed cancers. Breast cancer has long been established as a cancer with subtypes with differences in ER and PR status, HER2 amplification status and histological grade. Based on this alone, tumors may be stratified into a number of subtypes with triple-negative breast cancer being the most aggressive subtype (Dent, Trudeau et al. 2007). Given the inability to treat these patients with hormone therapy or targeted HER2 therapy, the unfortunate reality is that only 22% of TNBC patients have a complete response to chemotherapy and a significantly worse survival rate at three years following surgery relative to non-TNBC (Liedtke, Mazouni et al. 2008). This serves to underscore the critical need to improve therapeutic options in breast cancer.

3-1-1. Heterogeneity of breast cancer

Breast cancer is known to be a heterogeneous cancer in histology and at the molecular level. In histological classification, breast cancer is comprised of two major groups: in situ carcinoma and invasive carcinoma. In situ carcinoma consists of lobular carcinoma and five subtypes of ductal carcinoma. Invasive carcinoma includes seven subtypes. Among these subtypes, infiltrating ductal carcinoma can be further split into three subgroups dependent on levels of differentiation (Malhotra, Zhao et al. 2010).

At the molecular level, breast cancer is categorized into four subtypes based on the presence of ER, PR, and HER2. HER2 subtype is HER2 positive, and the remaining HER2-negative tumors are either ER- and PR-positive, or ER- and PR-negative. Luminal A and luminal B subtypes are ER-positive and/or PR-positive. Ki67 index and expression of HER2 have been used in

distinguishing between luminal A and luminal B (Cheang, Chia et al. 2009). TNBC does not express any of these three molecules. This heterogeneity is also readily observed through gene expression profiling in which breast cancer is now routinely classified into six major intrinsic subtypes (Perou, Jeffrey et al. 1999, Perou, Sorlie et al. 2000, Sorlie, Perou et al. 2001, Herschkowitz, Simin et al. 2007): luminal A, luminal B, HER2, basal, normal-like, and claudin-low. A toal of 73% of TNBC is basal subtype (Rody, Karn et al. 2011). The characteristics of claudin-low tumors include epithelial-to-mesenchymal transition and cancer stem cell-like markers. Compared with basal subtype, claudin-low tumors have better response rate to chemotherapy (Prat, Parker et al. 2010). However, based on unsupervised clustering, six classes are unlikely to be sufficient for capturing all of the heterogeneity.

The use of gene expression pathway signature predictions (West, Blanchette et al. 2001, Bild, Yao et al. 2006) in breast cancer samples has revealed seventeen human breast cancer subtypes based on pathway activity (Gatza, Lucas et al. 2010). Indeed, a closer examination of the TNBC subtype has resulted in classification into 6 subgroups, including basal-like 1 (BL1), basal-like 2 (BL2), immunomodulatory (IM), luminal androgen receptor (LAR), mesenchymal, and mesenchymal stem-like (MSL). Genes enriched in BL1 subgroup are associated with proliferation and the cell cycle. In contrast, BL2 has high expression of growth factor receptors. Several immune signaling pathways are found in IM subgroup. LAR is enriched in hormone-associated pathways. Mesenchymal and MSL subgroups have some common pathways in cell motility and differentiation; however, MSL has enriched expression of angiogenesis genes and several metabolism pathways. In addition, MSL subgroup shares some gene expressions with claudin-low subtype (Lehmann, Bauer et al. 2011).

The heterogeneity of breast cancer is further characterized in genomic stability and cell populations. The percentages of chromosomal instability in luminal A, luminal B (HER2-negative), luminal B (HER2-positive), HER2, and basal tumors are 27.9%, 49.5%, 81.2%, 90.2%, and 76.6%, respectively (Yanagawa, Ikemot et al. 2012). In cell populations, claudin-low subtype tumors are enriched for mesenchymal tumor cells, MET-like cancer stem cells (MCSCs), and bi-lineage cancer stem cells. In contrast, basal, HER2, luminal A, and luminal B subtypes have more epithelial tumor cells and EMT-like CSCs. Luminal A subtype lacks MCSCs (Brooks, Burness et al. 2015).

3-1-2. Treatment of breast cancer and resistance

The heterogeneity of breast cancer has been applied in determining treatments. Patients with luminal A and luminal B tumors receive hormone therapy, including drugs that prevent estrogen production and block estrogen functions. Estrogen production is prevented with the use of gonadotropin-releasing hormone agonists and aromatase inhibitors. SERMs and fulvestrant bind to estrogen receptors to block estrogen functions. HER2-positive breast cancer patients are treated with HER2-targeted therapy, such as trastuzumab, pertuzumab, lapatinib, and ado-trastuzumab emtansine. Compared with other subtypes of breast cancer, TNBC tumors do not have any applicable targets for hormone therapy and HER2-targeted treatment. Currently, the main options for patients with TNBC are still chemotherapy, including single agents and combination of alkylating agents, anti-metabolites, mitotic inhibitors, antifolate drugs, and anthracyclines. The response rates to therapies as well as resistance in part explain the effects of the heterogeneity of the tumors.

The mutations in genes demonstrate that heterogeneity affects the therapeutic outcomes. BRCA1 and BRCA2 are tumor suppressor genes that are involved in DNA damage repair (Patel, Yu et al. 1998, Cortez, Wang et al. 1999). The mutations in BRCA1/2 are responsible for the inherited breast cancer (Ford, Easton et al. 1998), and 19.5% of TNBC patients have these mutations (Gonzalez-Angulo, Timms et al. 2011). Compared with patients with wild type BRCA1, patients carrying BRCA1 mutations are more sensitive to cisplatin. However, they have worse response to other treatments, such as doxorubicin and docetaxel (Byrski, Gronwald et al. 2010). Notably, p53 mutations are frequently found together with BRCA1 mutations (Schuyer and Berns 1999). These mutations contribute to the intrinsic resistance to doxorubicin (Aas, Borresen et al. 1996). Patients with normal p53 have a better pathological complete response when treated with the combination of fluorouracil, epirubicin and cyclophosphamide. In contrast, patients carrying p53 mutations are sensitive to paclitaxel treatment (Kandioler-Eckersberger, Ludwig et al. 2000). In HER2-positive subtype, PIK3CA mutations and PTEN loss lead to the resistance to trastuzumab (Nagata, Lan et al. 2004, Berns, Horlings et al. 2007). PIK3CA mutant-caused resistance can be overcome with the combination of trastuzumab and a PI3K inhibitor (Junttila, Akita et al. 2009).

Further studies on resistance of anti-HER2 targeted therapy in HER2 subtype also show that other alterations of genes that interact with target genes represent resistance mechanisms among subjects. Lapatinib, a dual inhibitor of HER2 and EGFR, causes apoptosis in trastuzumab-resistant cells. In addition, lapatinib reduces IGF-1 signaling pathway activity, which is known to block the function of trastuzumab (Lu, Zi et al. 2001, Nahta, Yuan et al. 2007). Met is involved in acquired resistance to trastuzumab by decreasing p27 (Shattuck, Miller et al. 2008). Interestingly, recombinant human erythropoietin, which is given for the side effects

of chemotherapy, decreases the response to trastuzumab by increasing PI3K pathway activity (Liang, Esteva et al. 2010).

3-1-3. Development of new therapeutic strategies

The heterogeneity of breast cancer increases the challenges of treatments. Currently, the main approaches of improving therapeutic outcomes include the identification of new targets and the development of combination therapy or other therapies. Therefore, some of these new targets are therefore utilized in the combinatorial therapy.

Several approaches have been reported to identify novel targets. The identification of genes associated with cancer vulnerability could be further used in developing new therapies. Mutations in BRCA1/2 in TNBC patients make tumors vulnerable to PARP (poly ADP ribose polymerase) inhibitors (Farmer, McCabe et al. 2005). Several phase I and II studies have shown the benefits of using PARP inhibitors alone or combined with chemotherapy in a subset of TNBC patients (Tutt, Robson et al. 2010, O'Shaughnessy, Osborne et al. 2011). In TNBC with p53 mutations, checkpoint kinase 1 (Chk1) is essential in response to DNA damage. The administration of a Chk1 inhibitor sensitizes p53-deficient TNBC PDXs to irinotecan, a topoisomerase I inhibitor (Ma, Cai et al. 2012).

The examination of known drug resistance is another approach. Alterations in the receptor tyrosine kinase signaling pathways are correlated with trastuzumab resistance, and the activation of Src is increased in cells resistant to trastuzumab. The combination of trastuzumab and saracatinib inhibits tumor growth *in vitro* and *in vivo* (Zhang, Huang et al. 2011). In addition, the analysis of gene expression alterations after drug treatment leads to drug repositioning (Lamb, Crawford et al. 2006). For instance, valproic acid, which is used in epilepsy is noted to inhibit

histone deacetylase (Gottlicher, Minucci et al. 2001). Unfortunately, the phase II clinical trials of the combination of valproic acid and chemotherapy in breast cancer were terminated (Clinical-Trials.gov number, NCT01010854). The new targets also include drug targeting the common characteristics of TNBC, such as angiogenesis. TNBC expresses higher vascular endothelial growth factor (VEGF) (Linderholm, Hellborg et al. 2009). The combination of paclitaxel and bevacizumab has increased progression-free survival for metastatic breast cancer (Miller, Wang et al. 2007), but has shown no significant improvement in overall survival (Miles, Dieras et al. 2013). In BEATRICE trial, TNBC patients receiving bevacizumab plus chemotherapy did not have a better invasive disease-free survival rate (IDFS) or disease-free survival rate. However, patients with higher VEGFR-2 expression measured prior to treatment had increased IDFS (Cameron, Brown et al. 2013). Taken together, these studies show the requirement of tumor classification.

The development of novel combination therapy is another strategy for tackling the heterogeneity of breast cancer. Novel combination therapy includes the combination of chemotherapy and targeted therapy and the combination of various target therapies. Many studies have shown that the combination of chemotherapy and HER2-targeted therapy led to better outcomes in HER2-positive breast cancer patients (Slamon, Leyland-Jones et al. 2001, Buzdar, Ibrahim et al. 2005, Romond, Perez et al. 2005). In contrast, the combination of paclitaxel and bevacizumab only increased progression-free survival, but had no benefits for overall survival (Miller, Wang et al. 2007). In the combination of various target therapies approach, the four major approaches are targeting the same target with different mechanisms, targeting upstream and downstream pathways, targeting parallel pathways, and targeting feedback loops (Dancey and Chen 2006).

3-1-3-1. Targeting the same target with different mechanisms.

One well-known example of targeting the same target with different mechanisms is the combination of trastuzumab and lapatinib. Trastuzumab is a monoclonal antibody that targets the HER2 receptor (Vogel, Cobleigh et al. 2002), and lapatinib is a small molecule tyrosine kinase inhibitor (Rusnak, Lackey et al. 2001). The combination of these two inhibitors increases the progression-free survival of trastuzumab –refractory metastatic breast cancer patients (Blackwell, Burstein et al. 2010).

3-1-3-2. Targeting upstream and downstream pathways

The PI3K/mTOR pathway is one of the downstream pathways activated by growth factor receptors, and the deregulation of these pathways, such as PIK3CA mutations, is correlated with resistance to trastuzumab and lapatinib (Berns, Horlings et al. 2007, Esteva, Yu et al. 2010, Loibl, von Minckwitz et al. 2014). The use of the dual inhibitor of PI3K and mTOR, NVP-BEZ235, restores the sensitivity of trastuzumab- and lapatinib-resistant cells to these anti-HER2 therapies (Eichhorn, Gili et al. 2008). The combination of everolimus (mTOR inhibitor), trastuzumab, and vinorelbine increases the progression-free survival of HER2-positive patients with known resistance to trastuzumab (Andre, O'Regan et al. 2014).

3-1-3-3. Targeting parallel pathways

The PI3K/mTOR and RAS/ERK pathways transduce HER2 signaling (Dittrich, Gautrey et al. 2014). The treatment of NVP-BEZ235 alone in HER2-overexpressed cell lines leads to the increase of phosphorylated ERK due to the dimerization of HER2 and HER3 (Serra, Scaltriti et al. 2011). The combination of PI3K and MEK inhibitors inhibits various gene engineered mouse models, including melanoma, and several breast cancer tumor models (Roberts, Usary et al. 2012).

3-1-3-4. Targeting feedback loops

mTOR is regulated through several mechanisms. mTORC1 could negatively inhibit the PI3K/AKT pathway though S6K1, and the inhibition of mTORC1 has increased the activation of Akt (O'Reilly, Rojo et al. 2006). NVP-BEZ235 prevents the activation of Akt by targeting PI3K and mTOR at the same time (Maira, Stauffer et al. 2008). In addition, this feedback loop is correlated with the activation of the MEK pathway after mTORC1 inhibition (Carracedo, Ma et al. 2008).

3-1-4. Models used in preclinical studies

Determining how to select models in preclinical studies is another challenge of studying the heterogeneity of breast cancer. The mutations in oncogenes or tumor suppressor genes reflect this challenge. For instance, the incidence of p53 mutations varies among subtypes of breast cancer. Up to 85% of basal and HER2-positive subtypes have p53 mutations. In contrast, only 13% of luminal A subtypes have been noted to have p53 mutations (Sorlie, Perou et al. 2001). P53 mutations are correlated with resistance to chemotherapy reagents, such as doxorubicin (Aas, Borresen et al. 1996, Geisler, Lonning et al. 2001). PIK3CA mutations cause resistance to trastuzumab (Berns, Horlings et al. 2007). Therefore, understanding the characteristics of models is important in the selection of models as well as in interpretation of results.

The following are the three main models are used in preclinical studies on breast cancer.

3-1-4-1. Cell lines

Cells lines are widely used in preclinical studies, including high-throughput screening for the identification of synthetic lethal genes and drug combination (Turner, Lord et al. 2008). It has been reported that breast cancer cell lines retain 73%-100% of the molecular characteristics of

the original tumors after being cultured for months (Wistuba, Behrens et al. 1998). However, higher frequency of copy number alterations has been noted in breast cancer cell lines (Kao, Salari et al. 2009). Notably, the microenvironment could be critical for some cell lines, such as cell lines representing HER2 subtype. These cells have various responses to trastuzumab or lapatinib depending on whether they have been cultured in a 2D or 3D environment (Weigelt, Lo et al. 2010). In addition, cell lines are considered as homogeneous populations in general (Gillet, Calcagno et al. 2011).

3-1-4-2. Transgenic mice

Genetically engineered mouse models offer opportunities to systematically evaluate the roles of oncogenes or tumor suppressors in the progression of breast cancer (Hutchinson and Muller 2000). The similarities of the gene expressions of mouse mammary tumors and human breast cancer have been noted (Herschkowitz, Simin et al. 2007). In addition, some transgenic mice share common genomic expressions with subtypes of breast cancer (Vargo-Gogola and Rosen 2007, Hollern and Andrechek 2014). For instance, tumors from BRCA1- and p53-knockout transgenic mice recaptured some characteristics of basal subtype with a BRCA1 mutation (Liu, Holstege et al. 2007). Similar to cell lines, most of tumors in transgenic mice only have one subtype and are considered as homogeneous tumors. In contrast to cell line-derived xenografts, these transgenic mice still have their own immune system.

3-1-4-3. Patient-derived xenografts (PDXs)

Among the three models, the PDX model is the one that recaptures most of the characteristics of human breast cancer. Several groups have established transplantable breast cancer PDXs and shown that PDXs retained the characteristics of their patients' tumors after serial passages (Marangoni, Vincent-Salomon et al. 2007, DeRose, Wang et al. 2011, Zhang, Claerhout et al.

2013). For instance, these PDXs have the same therapeutic response to hormone therapy or chemotherapy (Cottu, Marangoni et al. 2012, Zhang, Claerhout et al. 2013). Interestingly, estrogen supplement was found to be important in mice initially grafted with either ER-positive or ER-negative breast cancer (Iyer, Klebba et al. 2012). Similar to xenografts bearing cell lines, PDXs are an outstanding model for the preclinical assessment of responses to drugs. However, the tumors in PDXs still have the heterogeneity (Cassidy, Caldas et al. 2015).

3-1-5. The development strategy of personalized treatment for breast cancer

Some studies have demonstrated that the benefits of target therapies and combinatorial therapy in breast cancer. For instance, the combination of iniparib (PARP inhibitor) and chemotherapy has increased the overall response of TNBC patients with BRCA1/2 mutations by 20% (O'Shaughnessy, Osborne et al. 2011). However, the remaining 80% of TNBC patients that lack BRCA1/2 mutations are therefore without targeted therapy for their cancers.

When developing targeted therapy for TNBC, it has been shown that the examination of known drug resistance mechanisms as well as the common characteristics of TNBC tumors needs to be considered in addition to defining the subset of patients that will benefit from proposed treatments (Cameron, Brown et al. 2013, Bear, Tang et al. 2015, Bertucci, Fekih et al. 2016). Closer examination of the resistance mechanisms to targeted therapy suggests that cross-talk between targets and pathways varies in both cell lines and patients (Nahta, Yuan et al. 2005, Berns, Horlings et al. 2007, Xia, Husain et al. 2007, Shattuck, Miller et al. 2008). Taken together, these studies suggest that the development of therapeutic options needs to consider the interaction of targets, signaling pathways and appropriate selection of experimental model systems for success.

To address the requirement for the development of therapies targeted to TNBC, we have hypothesized that the activation of cell signaling pathways could stratify subjects into groups where the development of personalized combinatorial therapy would be effective. Here we have sought to test this hypothesis in a proof-of-principle experiment. Initially, we tested this hypothesis in mammary tumors from MMTV-Myc transgenic mice where we used gene expression and pathway signatures to guide therapy selection (Figure 3.1). We then tested this approach in breast cancer patient-derived xenograft models (Figure 3.2). Through this approach, we could take advantage of both transgenic mouse models and patient-derived xenografts, the former having an innate immune system and heterogeneous tumors and the latter one recapturing the characteristics of human breast cancer. Taken together, our data demonstrate that the development of individualized therapy using pathway signatures is a viable therapeutic strategy for triple-negative breast cancer.

3-2. Results

3-2-1. Use of cell signaling pathway signatures to design individualized therapies for subtypes of breast cancer in a mouse model system.

With the advent of genomic characterization of breast cancer, the individual nature of each tumor has become apparent and underscores the need for individualized treatment. To test the hypothesis that gene expression patterns could be used to direct breast cancer therapy we started by comparing tumor subtypes from the MMTV-Myc transgenic tumor model. Tumors in this model are spontaneous, minimizing the background effects associated with use of human tumor cell lines. MMTV-Myc mice developed tumors with papillary (Figure 3.3A) and epithelial to mesenchymal transition (EMT) histological characteristics (Figure 3.3B). Gene expression from MMTV-Myc papillary and EMT tumors revealed clear expression differences at the fold change level (Figure 3.3C). With these differences in gene expression, we assessed pathway signatures in the various major subtypes of MMTV-Myc tumors. This used previously defined training data and bioinformatic methods to predict whether each of the individual pathways were active in the Myc induced tumor samples. The activity (blue for low probability of pathway activity to red for a high probability of pathway activity) was then assessed in each of the Myc induced tumor subtypes. The probability of pathway activation is presented in a heatmap and revealed that each tumor subtype had a characteristic pattern of predicted signaling pathway activation (Figure 3.3D). Similar to the differences observed in histology and gene expression fold change, EMT and papillary tumors have distinct pathway activation patterns. The papillary tumors were noted to have an elevation in predicted AKT, Myc and Stat3 pathway activity (shown in red) while the EMT tumors had a high probability of Ras, EGFR and TGFβ pathway activity. Consistent with these predictions of pathway activation,

Myc, activation of Stat3, AKT, and TGFβ, and phosphorylated EGFR differences were noted between these tumor types by Western blot (Figure 3.3E). In addition, the predicted Ras pathway activation in EMT tumors correlated with a high percentage of activating mutations in Kras relative to tumors with low predicted Ras pathway activity (Figure 3.4). To use these pathway predictions to derive a targeted treatment plan, characteristic pathway activation patterns unique to a tumor subtype were determined (Figure 3.3F).

Based on predictions of cell signaling pathway activity we predicted specific therapeutic opportunities for two subtypes of breast cancer. To prove the principle that this approach could be used to direct therapy, we then sought to test whether these therapies were effective and specific. Based on the gene expression signatures we selected therapeutic compounds to specifically treat EMT and papillary tumors. When selecting compounds, key factors included drugability of pathways, FDA approval or entry into clinical trials, efficacy, toxicity and known mechanisms of action (Figure 3.5). Given that we sought to use a combinatorial approach, we used low dosages for each compound. These selection criteria resulted in the identification of drugs targeting Myc, Akt and Stat3 for papillary tumors and EGFR, Ras and TGFβ inhibitors for EMT tumors (Figure 3.3F). Drugs to target these pathways included WP1066 which inhibits phosphorylation of Stat3 (Iwamaru, Szymanski et al. 2007) and miltefosine, which inhibits phosphorylation of AKT (Bhatt, Bhende et al. 2010). Due to the difficulty of targeting Myc we used VX680 in a synthetic lethal approach, selectively inhibiting aurora B kinase in cells with high Myc expression (Yang, Liu et al. 2010). From the FDA-approved anti-EGFR inhibitors, we chose afatinib based on its efficacy and its multi-target characteristic mechanism of action (Li, Ambrogio et al. 2008). Targeted therapies for Ras are unavailable and therefore we searched inhibitors of upstream and downstream targets

of the Ras pathway, selecting a MEK inhibitor (Trametinib) (Yamaguchi, Kakefuda et al. 2011). We also selected SB505124 for inhibition of TGFβ receptors, ALK4 and ALK5 (DaCosta Byfield, Major et al. 2004, Tang, Wu et al. 2009). Together, pathway signatures guided targeted inhibitor selection for two subtypes of Myc induced breast cancer in a mouse model system.

3-2-2. Efficacy and specificity of papillary-specific combinatorial treatment in mice

In a proof of principle experiment to validate the approach of developing therapeutic options based on predicted cell signaling pathway activity, we tested the papillary-specific combinatorial treatment. Using a combination of inhibitors for the Myc (VX680), Stat3 (WP1066), and Akt (miltefosine) pathways, we initiated safety trials in control FVB/NJ female mice. Dosage was based on efficacy in published studies and we used the lowest dosage possible. Individually, or in combination, we noted no significant health issues with body weight changes of less than 15% (Figure 3.7-3.9) or organs (Figure 3.10 and Table 3.1). To test the utility of the combination therapy, we began by assessing the efficacy of the individual drugs in the therapeutic regimen. The scheme for drug treatment (Figure 3.6A), illustrates our approach where viably frozen papillary tumors were implanted into the mammary gland of 6-8 week old female mice. Once these tumors reached 6mm in the largest dimension, single agent therapy for three weeks was initiated. This revealed that tumors grew slightly more slowly with VX680 treatment relative to vehicle treated controls (Figure 3.6B). However, tumors treated with either miltefosine (Figure 3.6C) or WP1066 (Figure 3.6D) did not have obvious differences in growth compared to controls receiving vehicle alone.

To then test the personalized combination therapy, the combination of these three drugs was given to mice bearing papillary tumors. As shown in Figure 3.6E, growth of established

papillary tumors was arrested or these tumors grew significantly more slowly after treatment with the papillary-specific combination. The alterations to tumor growth were highly significant ($p=0.0001$). The specificity of this papillary combination therapy was then validated in mice implanted with EMT tumors, which were not predicted to respond to this targeted therapy. Treatment of EMT tumors with the papillary treatment demonstrated that these tumors were not responsive to this therapy (Figure 3.6F), with only minor effects on tumor growth being observed. These results demonstrate that we were able to use cell signaling pathway signatures to design a specific and effective therapy for a subtype of breast cancer.

To evaluate changes in gene expression in the tumors following treatment, we placed tumors with vehicle alone or with the combination therapy on microarray. We performed unsupervised hierarchical clustering on the gene expression data (Figure 3.6G and Figure 3.11). Given the minor differences we also analyzed changes in probability of pathways with treatment. Interesting, drug treated tumors were observed to have increased predicted EGFR and RAS pathway activation using the gene expression signatures (Figure 3.6H and 3.6I) ($p=0.07$ and $p=0.06$, respectively). The increase in RAS pathway activity in drug-treated tumors was validated using immunohistochemical staining (Figure 3.6J), where we observed an increase in phospho-ERK staining in drug treated tumor samples ($p=0.05$). Notably, significant heterogeneity was observed in phospho-Erk staining (Figure 3.6H, right panel, top and bottom).

Given the excellent response of the papillary tumors to the low dose combination therapy, we sought to increase the dose to a level that would result in a reduction in the tumor burden. Accordingly, we increased the dose of VX680 from 50 mg/kg to 60 mg/kg and administered the new combinatorial therapy to mice implanted with papillary tumors. As expected, with an increased dosage the tumor burden was reduced and average tumor size dropped from 216

mm^3 to 15.75 mm^3 after ten days of treatment (Figure 3.12A). Despite this initial reduction in tumor size, the tumors began to grow again by the end of the treatment regimen. To explore the differences in proliferation and apoptosis we examined the tumors through BrdU and TUNEL stainings (Figure 3.12B). As expected, samples treated with vehicle alone had consistent elevation of BrdU at 7, 14 and 21 days after initiation of treatment. Conversely, tumors in the treatment arm had a significant reduction in BrdU positive cells at each measured time point, with a slight increase at day 21 (Figure 3.12B and 3.12C). In addition, there were only slightly more cells undergoing apoptosis in the combination drug treatment samples relative to vehicle alone (Figure 3.12B and 3.12D). Together, these data support the premise of designing therapy based on gene expression patterns.

3-2-3. Efficacy and specificity of EMT-specific combinatorial treatment in mice

To ensure that the strategy of using gene expression to direct therapy would be effective in other breast cancer subtypes, we next tested the EMT specific combinatorial treatment. This treatment consisted of inhibitors of EGFR (afatinib), RAS (trametinib), and TGFβ (SB505124) pathways. Mice with EMT tumors implanted into the mammary gland of 6-8 week old mice were allowed to grow until tumors reached 6 mm in diameter, at which point the EMT specific drugs were administered (Figure 3.13A). None of the single agent therapies had a dramatic effect in tumor growth and health (Figure 3.13B-D and Figure 3.14). The drop in tumor volume later in the treatment course noted in Figure 3.13B-D was due to removal of mice from the study as they reached endpoint. However, the combination of these three drugs significantly slowed EMT tumor growth (Figure 3.13E) without significant effects of health (Figure 3.15). The drop in the tumor curve in the vehicle control was due to removal of individual mice being removed from treatment as they reached endpoint. Importantly, papillary tumors treated with the EMT treat-

ment did not show a significant response (Figure 3.13F). Taken together, these data demonstrate the utility of using gene expression to direct precision medicine in a proof of principle mouse experiment.

3-2-4. Individualized combinatorial treatment in patient-derived breast cancer xenografts.

To extend the method of using gene expression signatures to direct therapy we sought to test this approach in human breast cancer, using PDX. Here we focused on developing personalized therapy for triple negative breast cancer given that this subtype of breast cancer is associated with poor outcome and lacks effective targeted treatment. To first uncover potential therapies, we combined seven publicly available datasets of human breast cancer with one PDX gene expression dataset (Figure 3.16). After predicting PAM50 subtypes, we selected basal breast cancers for further study. Using cell signaling pathway signatures, we then predicted activity for key pathways in both basal breast cancer samples and basal PDX samples. After predicting pathway activity, the resulting probabilities of pathway activation were then used in a clustering analysis (Figure 3.17A). This separated the basal breast cancer samples into several subgroups. PDX samples, denoted with the black lines between the heatmap and the dendrogram, were noted to be interspersed with several of the basal breast cancer subtypes. Interestingly, this analysis revealed that some basal breast cancers were elevated for EGFR, Ras and the TFGβ pathways. For the two indicated PDX lines, we noted that there were clear differences in these signaling pathways (Figure 3.17B), with BCM2147 having high EGFR, RAS, and TGF-beta pathways activation than BCM3887. The prediction of pathway activity was validated by examining levels of phosphorylation of ERK1/2 protein using immunohistochemical staining (Figure 3.17C) and through western blotting (Figure 3.17D). Combined EGFR, RAS, and TGFβ inhibi-

tors were tested in SCID mice for safety and no adverse effects were noted. As bio-informatically predicted, mice implanted with PDX line BCM2147 and treated with the combinatorial therapy were noted to have a significant reduction in tumor volume relative to vehicle controls, ranging from 30.6% to 63%, in the first 14 days of treatment (Figure 3.17E-G). Of note, after 27 days of treatment, the average decrease in tumor volume was 20.9%. Inhibition of EGFR and Ras pathways was confirmed by decreased phosphorylation of Erk1/2 (Figure 3.17I). To establish specificity of this treatment, mice implanted with PDX BCM3887 were treated with the same combination of drugs, which was not predicted to be as effective as in BCM2147 (Figure 3.17B). This combinatorial treatment only has limited tumor growth inhibition effects in this PDX (Figure 3.17H). Taken together, these data demonstrate that the use of gene expression signatures can be used to specifically and effectively design a personalized therapy.

3-3. Discussion

One of the primary challenges in breast cancer treatment is tumor heterogeneity. In addition, response to targeted therapies varies in subtypes of breast cancer. For instance, HER2+ve patients are recognized to have a varied response to anti-HER2 therapy. Indeed, a poor response to trastuzumab was observed in PTEN-deficient HER2+ve patients (Nagata, Lan et al. 2004). Resistance to trastuzumab is also known to be associated with expression of EGFR or HER3 *in vitro* (Narayan, Wilken et al. 2009). In TNBC, heterogeneity and drug resistance are compounded by having few targeted therapies, instead relying upon chemotherapy with limited therapeutic efficacy. Currently, the major strategy to address the need of treating TNBC is to increase the sensitivity of chemotherapy by combining it with targeted therapy. For instance, BRCA1/2 mutation patients who failed to chemotherapy were treated with olaparib (a PARP inhibitor), resulting in 22-41% objective response rate (Tutt, Robson et al. 2010). Nevertheless, several clinical trials suggest that further assessment is required in the combination of bevacizumab (anti-vascular endothelial growth factor antibody) and chemotherapy to determine the benefits in subtypes of breast cancer (Cameron, Brown et al. 2013, Bear, Tang et al. 2015). Together these data indicate that developing personalized combinatorial treatment for subtypes of breast cancer will have the greatest efficacy and that this approach is urgently required in TNBC.

Here we have used genomic signatures to predict signaling pathway activation patterns that were used to guide individualized treatment of breast cancer, with a focus on the proof of concept experiments and TNBC. In our initial proof of concept experiments, we selected two subtypes of MMTV-Myc transgenic tumors with distinct cell signaling pathway activities. The mammary tumors in this model not only are heterogeneous in subtypes of tumors (Andrechek,

Cardiff et al. 2009) but have clear similarities to human breast cancer (Hollern and Andrechek 2014). Thus, this approach has the potential to bridge between preclinical studies and clinical trials.

In the experimental criteria for combinational therapy to target subtypes of breast cancer, we took advantage of current approaches, including therapy for combination of different pathways, targeting upstream and downstream of the identified pathways and gene-expression based strategies. Importantly, we sought to include FDA-approved drugs, drugs with multiple targets, and potentially repurposed therapies using connectivity map (Lamb, Crawford et al. 2006). However, using connectivity map, the majority of targets were anti-inflammatory agents and antibiotics. In our papillary-specific combinatorial treatment, we targeted Myc, Stat3 and AKT.
The Myc pathway was targeted using VX680. Based on the synthetic lethal approach of using PARP inhibitor in PTEN-deficient cells (Farmer, McCabe et al. 2005), VX680 selectively kills cells with high Myc expression through inhibiting aurora B kinase activity (Yang, Liu et al. 2010). For the Stat3 pathway, WP1066 was selected since it inhibits both Stat3 as well Janus Kinase 2 (JAK2) upstream of Stat3 (Iwamaru, Szymanski et al. 2007). Lastly, Miltefosine is an Akt inhibitor that has been approved by FDA for treatment of Leishmaniasis. In our EMT-specific combinatorial therapeutic strategy, we targeted EGFR, Ras, and TGFβ pathways. The dependence and crosstalk of EGFR and Ras have been observed, and the synergistic effects of combining EGFR inhibitor and MEK inhibitors have been observed *in vitro* and *in vivo* (Li, Ambrogio et al. 2008, Sun, Hobor et al. 2014). In addition, HER2 expression is associated with the resistance to EGFR inhibitor (Wang, Narasanna et al. 2006). Thus, we elected to
use afatinib which targets both wild type and mutant EGFR, HER2 and is currently used for EGFR pathway inhibition (Li, Ambrogio et al. 2008). Given the Ras activity and the inability to

target Ras, we used trametinib to target MEK downstream of Ras. The concept of cotargeting the same pathway at both upstream and downstream nodes led to an en-couraging result in a phase III trial where melanoma patients received dabrafenib (BRAF inhibitor) and trametinib (Grob, Amonkar et al. 2015). Importantly in human TNBC, expression of these targets is increased in the residue breast cancer after chemotherapy (Balko, Giltnane et al. 2014).

Our proof of principle individualized treatment for transgenic mouse tumors demonstrated that we were able to inhibit tumor growth effectively with specificity and safety. Importantly, this was also true in basal PDXs. In the transgenic mouse tumors, we noted no reduction of tumor size in either papillary or EMT specific combinatorial treatments. One possible reason for the lack of tumor regression is that with the innate characteristics of mouse tumor cells, the growth of these tumors are significantly faster than those from human cancer cell lines and the derived xenografts, in which most of the drugs are tested for determining doses. Based on this assumption, we increased the VX680 dose in the papillary-specific combination and observed tumor regression. An additional possibility is that the intratumor heterogeneity in papillary tumors results in a population selection effect during treatment. Similar to intratumor heterogeneity noted in human cancers (Yates, Gerstung et al. 2015, Hoefflin, Lahrmann et al. 2016), we also noted sub populations in treated tumors in proliferation and pERK expression (Figure 3.6J and Figure 3.12B-C). Gene expression differences after the vehicle or combinatorial treatment largely split samples based on treatment. However, one drug-treated tumor was noted to cluster with vehicle treated tumors (Figure 3.6G). Compared to the other drug-treated tumors, this tumor grew significantly more quickly, in line with the vehicle treated controls. In addition, we examined whether tumors had compensatory changes in pathway activity following treatment. Given that the EGFR and Ras pathways have a strong tendency to be increased after

drug treatment, we examined phospho-Erk1/2 protein expression in drug-treated tumors and noted a significant increase. Considering that the increase of activated Erk was observed after the short-term treatment in mice implanted with mouse tumors, it is possible that the apparent activation of Erk could be caused by population selection rather than induction due to acquired resistance. Tumor populations with increased phospho-Erk1/2 would then be observed due to transcriptional changes after combinatorial treatments, mutations in the Ras pathway (Emery, Vijayendran et al. 2009), and the crosstalk between the Ras and Akt pathways through S6 (Carracedo, Ma et al. 2008) and Akt (Zimmermann and Moelling 1999). In addition, it has been reported that treatment of MEK inhibitors alone led to activation of Akt (Turke, Song et al. 2012). Therefore, it is plausible that the drug-induced selection pressure in papillary tumors would increase activated Erk1/2. Despite this selection pressure on the papillary tumors and activation of pathways present in the EMT subtype, we did not note EMT histological characteristics in the papillary treated tumors. This finding also raises the possibility that repeated biopsies will be required to continue to refine the optimal treatment for an individual tumor.

Translating the mouse studies to human breast cancer was done with the mouse EMT-specific treatment of the PDX line BCM2147. While we decreased the dose of afatinib in the PDX system and decreased dosing frequency of SB501524 in the PDX model due to toxicity concerns, the comparison is still instructive. Despite the reduction in dosage in the PDX model, the same combinatorial treatment that inhibited EMT tumor growth in mice resulted in tumors that were reduced by at least 30% in volume in the BCM 2147 model after two weeks. Together, these data convincingly demonstrate that cell signaling pathway-guided therapeutic strategies are able to inhibit tumor growth.

In summary, we have demonstrated proof-of-principle experiments where individualized treatments for breast cancer were developed based on cell signaling pathway activity patterns derived from gene expression microarray data. The systematic analysis of targets and pathways combined with current drug treatment regimens is a method with strong potential to improve therapeutic outcomes in cancer. However, it is critical that other genomic factors should be taken into consideration in selections of targets and available drugs. For instance, both MET amplification and mutations in EGFR are correlated with resistance to EGFR inhibitors (Riely, Pao et al. 2006, Bean, Brennan et al. 2007), suggesting that copy number and sequencing data are critical to consider. Taken together, in the future our approach could be combined with an examination of the alterations in individual tumors in order to use a comprehensive assessment in the process of developing and modifying treatment options.

CHAPTER 4

STAT3 REGULATES TUMOR LATENCY AND GROWTH RATE BUT NOT METASTASIS IN MYC INDUCED BREAST CANCER

Alterations in Myc expression are noted in basal breast cancer. As a transcription factor and potential drug target, it is crucial to characterize the interaction of Myc with other genes. In this study, we focused on the interaction of Myc and Stat3 signaling pathways, potential therapeutic targets important in metastasis. We found that deletion of Stat3 in the mammary glands of MMTV-Myc mice unexpectedly resulted in increased and earlier hyperplasia and expedited tumorigenesis. Conversely, Myc tumors lacking Stat3 grew slowly with alterations in the resulting histological subtypes, including a dramatic increase in EMT-like tumors. We also observed that these tumors have impaired angiogenesis and a slight decrease in lung metastases. During normal mammary function, loss of Stat3 in Myc transgenic dams resulted in lethality of pups due to the lactation deficiencies. Together, the literature and our current research demonstrate that Stat3 can function as an oncogene or as a tumor repressor depending on the oncogene driver. Interestingly, in primary breast cancer patients with high Myc pathway activity, low expression of activated Stat3 is related to poor survival, suggesting careful consideration be given to clinical inhibition of Stat3 dependent upon the other genetic mutations driving tumor growth, development and progression.

**This part was published. Jhan JR and Andrechek ER. Stat3 accelerates Myc induced tumor formation while reducing growth rate in a mouse model of breast cancer. Oncotarget. 2016. doi: 10.18632/oncotarget.11667

4-1. Introduction

The identification of new targets, including hormone receptors and HER2, improves the therapeutic outcomes of some populations of breast cancer patients. More biomarkers and targets have been studied for TNBC patients still receiving traditional chemotherapy or patients developing a resistance to current treatment regimens. However, not all of these targets are druggable due to their intrinsic properties, such as the complexity of the structures and location. For instance, many transcription factors are located inside the nucleus and do not have enzymatic activity for direct targeting (Yan and Higgins 2013). In addition, studies of drug resistance suggest that interactions of genes or targets should be taken into consideration. To address these issues, in this chapter we focus on the interactions of c-Myc (herein termed Myc) and Stat3 in a breast cancer transgenic mouse model. The alteration of c-Myc expression has been noted in breast cancer patients, especially in basal-like-subtype patients (Perou, Sorlie et al. 2000, Sorlie, Perou et al. 2001). Considering that Myc is an undruggable transcription factor and regulates the expression of many genes, dissecting the interactions of Myc and other genes in transgenic mice will lead to a better understanding of these interactions as well as offer opportunities to target Myc efficiently. In this study, we focused on one of the transcription factors that regulate the mRNA level of Myc, Stat3 (Kiuchi, Nakajima et al. 1999). Stat3 is also important in mammary gland involution. However, the effects of a lack of Stat3 in Myc-driven breast cancer are still unclear. Through transgenic models, we observed the consequence of the loss of Stat3 in Myc-driven tumorigenesis, progression, and metastasis.

4-2. Overview of Myc

4-2-1. Myc in breast cancer

Te altered regulation of Myc is associated with tumorigenesis, metastasis, and survival in many cancers, including leukemia, breast cancer, colon cancer, liver cancer, and ovarian cancer (Figure 4.1). Among breast cancer patients, Myc amplification is noted in 15.7% of cases, and correlated with some prognostic factors, such as lymph node metastasis and tumor grades (Deming, Nass et al. 2000). In Myc mRNA expression, 22% of breast cancer patients have 3.2-19-fold higher expression compared with normal breast tissue (Bieche, Laurendeau et al. 1999); in Myc protein expression, 45% of cases have overexpression(Naidu, Wahab et al. 2002). Among the subtypes of breast cancer, elevated Myc expression has been found in basal breast cancer, the most aggressive molecular subtype (Perou, Sorlie et al. 2000, Sorlie, Perou et al. 2001).

4-2-2. Myc functions in physiological conditions and cancer

Myc is a pleiotropic transcription factor involved in different physiological conditions, including the cell cycle and proliferation, apoptosis, ribosome biogenesis, protein synthesis, development, stem cells, and miRNA expression. Through its helix-loop-helix leucine zipper domain, Myc protein can bind to DNA and also form dimerization with other proteins, such as Myc-associated factor X (Max) and Myc-interacting zinc finger protein-1 (Miz1), to regulate the expressions of other genes.

4-2-2-1. Cell cycle, apoptosis, and proliferation

The cell cycle is tightly regulated, and Myc is known to be involved in the G1-S progression of the cell cycle. Stimulated by mitogens, Myc increases the expression of cyclin D and CDK4, and the formation of the cyclin D-CDK4 complex. The complex phosphorylates RB proteins and then causes the release of E2Fs from the RB-E2Fs complex. These E2Fs induce the transcription of cyclin E, and the assembled cyclin E-CDK2 complex enhances the phosphorylation of RB. Once more E2Fs are released, the expression of E2F target genes are increased, which promotes cell-cycle entry into the S phase (Heikkila, Schwab et al. 1987, Mateyak, Obaya et al. 1999, Hipfner and Cohen 2004). The downregulation of Myc expression causes cell-cycle arrest or abnormal cell-cycle progression *in vitro* (Heikkila, Schwab et al. 1987, Hanson, Shichiri et al. 1994, Alexandrow, Kawabata et al. 1995, Wang, Liu et al. 2005). However, the absence of the stimulation of mitogens in cells with constitutively activated Myc leads to apoptosis (Evan, Wyllie et al. 1992). In addition, Myc is required for apoptosis induced by some stimulations, such as TNF-alpha (Janicke, Lee et al. 1994), radiation-caused DNA damage (Rupnow, Murtha et al. 1998), and chemotherapy (Dong, Naito et al. 1997).

4-2-2-2. Stem cells and development

Myc is also required in different development processes. Together with Oct4, Sox2, and Klf4, Myc is responsible for stem cell reprogramming, including maintaining self-renewal and pluripotency ability (Takahashi and Yamanaka 2006, Wernig, Meissner et al. 2007). Later, it was reported that Myc is not required for inducing pluripotent stem cells in mouse and human fibroblasts (Nakagawa, Koyanagi et al. 2008). The depletion of Myc causes dormancy in mouse embryonic stem cells (Scognamiglio, Cabezas-Wallscheid et al. 2016); however, the loss of Myc leads to embryonic lethality in mice (Davis, Wims et al. 1993). The lethality is known to be as-

sociated with retarded growth and defective development in hematopoiesis and vasculogenesis (Davis, Wims et al. 1993, Baudino, McKay et al. 2002). Indeed, Myc mRNA expression varies among organs in mouse embryos. For instance, Myc is highly expressed in the thymus during gestation (Schmid, Schulz et al. 1989). The conditional deletion of Myc in the endothelial cells of mouse embryos also shows that Myc is essential for angiogenesis (He, Hu et al. 2008). In contrast, the overexpression of Myc leads to increased VEGF-A expression and impaired vessel remodeling (Kokai, Voss et al. 2009).

4-2-2-3. Mammary gland development

Myc plays important roles in multiple development stages in the mammary gland, including pregnancy, lactation, and involution. During pregnancy, Myc mRNA expression is increased from day 6 to 12.5 (Blakely, Sintasath et al. 2005). In WAPiCre-Myc$^{Flox/Flox}$ mice, the proliferation of alveolar cells is delayed during pregnancy, and the production of milk were reduced during lactation (Stoelzle, Schwarb et al. 2009). The aberrant Myc expression from days 12.5 to 15.5 of pregnancy found in MMTV-Myc mice causes the precocious lactation and involution. Studies have shown that Myc is involved in apoptosis during involution in MMTV-Myc mice (Blakely, Sintasath et al. 2005) as well as in conditional deletion of Socs3 in mice (Sutherland, Vaillant et al. 2006). Consistent with these findings, the expression of the Myc pathway is low before lactation and high in involution (Andrechek, Mori et al. 2008).

4-2-2-4. Transformation, tumorigenesis, and genomic instability

As an oncogene, Myc is able to transform some types of cells into tumor cells (Stone, de Lange et al. 1987, Eilers, Picard et al. 1989). However, this transformation can be reversible after the withdrawal of Myc (Eilers, Picard et al. 1989). In contrast, most normal cells require Myc and another oncogene to be transformed (D'Cruz, Gunther et al. 2001). For instance, studies

show that collaboration between Myc and Ras is required for transformation (Land, Parada et al. 1983, Leone, DeGregori et al. 1997, Sears, Leone et al. 1999). Ras can enhance the stability of Myc through inhibition of the degradation of the Myc protein (Sears, Leone et al. 1999). In addition, studies have reported that Myc drives tumorigenesis in transgenic models (Leder, Pattengale et al. 1986, Harris, Burns et al. 1988). The genomic instability caused by Myc is known to be associated with tumorigenesis and transformation (Felsher and Bishop 1999, Vafa, Wade et al. 2002). The overexpression of Myc might cause the acceleration of the G1/S phase and abolish the G1/S checkpoint (Felsher and Bishop 1999).

4-2-3. Regulation of Myc

From the embryos to adult stages, Myc is known to be tightly controlled in terms of mRNA and protein levels as well as in location. However, in human cancers, Myc expression is dysregulated via amplification (Beroukhim, Mermel et al. 2010), chromosomal translocation (Taub, Kirsch et al. 1982), single nucleotide polymorphism (Wright, Brown et al. 2010), and increased protein stability (Takeda, Noguchi et al. 1997). Some genes or proteins have been reported to regulate the transcription and translation of Myc. For instance, Fan and colleagues found that the histone demethylase JMJD1A increases transcription of Myc mRNA and attenuates the degradation of the Myc protein (Fan, Peng et al. 2016).

4-2-3-1. Transcriptional and post-transcriptional regulators

To activate or repress the transcription of Myc, transcription factors bind to the promotor of Myc directly and/or occupy the promoter region (Wierstra and Alves 2008). The stability of Myc mRNA is determined primarily by the 5’ UTR and exon 1, and 3’ UTR regions. Without the exon 1 region, Myc mRNA becomes more stable (Rabbitts, Forster et al. 1985). 3’UTR and

the coding region determinant (CRD), which is located in the carboxyl-terminal of the coding region are also related to the instability of Myc mRNA (Wisdom and Lee 1991). Truncation or deletion in these regions increases the half-life of Myc-mRNA (Jones and Cole 1987, Aghib, Bishop et al. 1990, Herrick and Ross 1994). In addition, CRD-binding protein (CRD-BP) protects Myc mRNA from being degraded by an endonuclease attack (Bernstein, Herrick et al. 1992), especially in the translational pausing of Myc mRNA translation (Lemm and Ross 2002). Similar to the role of CRD-BP, the RNA-binding protein IGFII mRNA binding protein 1 (IGF2BP1) also collaborates with proteins to protect Myc mRNA in translation (Weidensdorfer, Stohr et al. 2009). Moreover, several pathways including Hedgehog, WNT, Notch, and JAK-STAT3 increase the transcription of Myc, and TGFbeta signaling blocks the transcription (Kress, Sabo et al. 2015). In addition, miRNAs have been reported to regulate Myc mRNA expression (Kim, Kuwano et al. 2009, Sachdeva, Zhu et al. 2009).

4-2-3-2. Translational and post-translational regulators

The translation control of Myc mRNA is directed by the MAPK (Mitogen-activated protein kinase)/HNRPK, mTORC1/S6K1, and MAPK/FOXO3A pathways (Kress, Sabo et al. 2015). Under normal conditions, the half-life of Myc protein is about 30 minute (Ramsay, Evan et al. 1984). The stability of Myc protein is determined by post-translational modifications. Phosphorylation on residues of Myc protein causes stabilization or degradation via the ubiquitination/proteasome pathway. MAPK can phosphorylate serine 62 (S62) residue to stabilize Myc (Seth, Gonzalez et al. 1992). Once Myc is phosphorylated at S62, the residue of threonine 58 (T58) can be phosphorylated by glycogen synthase kinase-3 (GSK3) (Lutterbach and Hann 1994). Subsequently, S62 can be dephosphorylated by protein phosphatase 2A (PP2A) (Yeh, Cunningham et al. 2004), and F-box and WD repeat domain-containing 7 (FBW7) or S-phase

kinase-associated protein 2 (SKP2) triggers ubiquitination (Kim, Herbst et al. 2003, Welcker and Clurman 2008). Notably, Ras can stabilize Myc protein by activating the MAPK pathway to phosphorylate S62, and prevent the degradation of Myc protein by inhibiting AKT through GSK3 (Sears, Nuckolls et al. 2000). The T58A mutation accumulates Myc protein and increases the transformation potential (Bahram, von der Lehr et al. 2000, Wang, Cunningham et al. 2011). Interestingly, the T58I mutation frequently found in lymphoma also impedes the phosphorylation of S62 and decreases the transformation ability of Myc (Chang, Claassen et al. 2000). Studies on mutations at other residues, such as S71A/S81A, suggest that the phosphorylation of these residues blocks transformation (Wasylishen, Chan-Seng-Yue et al. 2013). In addition, it has been reported that T58 can be glycosylated, and the consequent effects need to be further studied (Chou and Hart 2001, Kamemura, Hayes et al. 2002).

4-2-4. Regulation of Myc target genes and non-coding RNAs (ncRNAs)

About 15% of human genes are transcriptionally regulated by Myc (Li, Van Calcar et al. 2003), and these genes are known to be involved in diverse biological processes (Dang, O'Donnell et al. 2006), such as cell growth (Schmidt 1999), the cell cycle (Hanson, Shichiri et al. 1994, Menssen and Hermeking 2002), apoptosis (Hoffman and Liebermann 2008), DNA replication and transcription (Gomez-Roman, Grandori et al. 2003), and metabolism (Dang 1999). As a transcription factor, Myc forms a heterodimer with Max using its basic helix-loop-helix leucine zipper domain. This dimer binds to the consensus sequence of the E box CACGTG, and activates transcription (Blackwood and Eisenman 1991). This dimerization is essential for transformation induced by Myc (Amati, Brooks et al. 1993). However, Max can also form homodimers or heterodimers with other proteins, including Mad and Mnt, to suppress transcription (Ayer, Kretzner

et al. 1993, Hurlin, Queva et al. 1997). In addition, Myc can repress the transcription of its target genes by binding to Miz-1) (Claassen and Hann 1999), or sequestering other transcription factors, such as specificity protein 1 (Sp1) (Gartel, Ye et al. 2001). Furthermore, it has been reported that Myc-induced mRNA cap methylation increases the transcription and translation of Myc target genes (Cowling and Cole 2010).

Myc also regulates the expression of ncRNAs directly and indirectly. Myc triggers the expression of the miR-17-92 cluster as well as represses the expression of many miRNAs in lymphoma (Chang, Yu et al. 2008). Notably, some of miRNAs regulated by Myc decreases the expression of E2F1, another Myc target gene (O'Donnell, Wentzel et al. 2005). In addition, Myc regulates the expression of 5S ribosomal RNAs and transfers RNAs indirectly by activating RNA polymerase III (Gomez-Roman, Grandori et al. 2003).

4-2-5. Transgenic mouse models of Myc-induced tumors

Deregulated Myc expression has been found in many human cancers. Considering the embryonic lethality noticed in Myc knockout mice (Davis, Wims et al. 1993) and the complexity of Myc functions, transgenic mouse models with tissue-specific Myc expression are widely used in studying the roles of Myc in different stages of tumor development. These transgenic mice represent certain types of cancers, including MMTV-Myc (mammary tumors) (Stewart, Pattengale et al. 1984), Eμ-Myc (lymphoma) (Harris, Burns et al. 1988), and probasin-Myc (prostate cancer) (Ellwood-Yen, Graeber et al. 2003). Later, Myc expression in mice could be controlled in some models using the Tet-On/ Tet-Off system (D'Cruz, Gunther et al. 2001, Gunther, Belka et al. 2002). A lack of constitutively overexpression of Myc in mice causes tumor regression (D'Cruz, Gunther et al. 2001), and this regression can be interrupted with the re-

activation of Myc expression or through a Myc-independent mechanism (Boxer, Jang et al. 2004).

A causative role for Myc in breast cancer is demonstrated in Myc transgenic mice using MMTV (Stewart, Pattengale et al. 1984) and WAP promoters (Schoenenberger, Andres et al. 1988). Both of these models spontaneously develop mammary adenocarcinoma. The expression of Myc varies among MMTV-Myc strains (Stewart, Pattengale et al. 1984), and the onset of some tumors in WAP-Myc mice occurs 2 months after Myc is overexpressed (Schoenenberger, Andres et al. 1988). Later, MMTV-Myc T58A transgenic mice were found to recapture the heterogeneity of human breast cancer in histology (Andrechek, Cardiff et al. 2009). The overexpression of Myc in the mammary gland results in tumors after a long latency; however, the tumors have not been noted as highly metastatic (Yuwanita, Barnes et al. 2015). In addition, crossing MMTV-Myc strains with other transgenic mice results in accelerated tumorigenesis. For instance, the latency of mammary tumors in mice carrying MMTV-Myc and MMTV-Ras is shortened (Sinn, Muller et al. 1987). Similar results have been found in bitransgenic MMTV-Myc/ WAP-Bcl-2 (Jager, Herzer et al. 1997) and MMTV-Myc/ p53 null mice (McCormack, Weaver et al. 1998).

4-2-6. Drugs targeting Myc

The prevalence of Myc deregulation in many cancers leads to the development of treatments targeting Myc. The majority of Myc deregulation in human cancers is amplification and overexpression; however, Myc is essential for diverse physiological functions and the half-life of Myc mRNA and protein is short (Dani, Blanchard et al. 1984, Hann and Eisenman 1984). It is challenging to target Myc efficiently without seriously impeding normal biological functions se-

riously. The approaches for developing Myc-targeted therapy include (1) targeting Myc directly by inhibiting Myc expression, and targeting the genes and proteins involved in Myc transactivation, and (2) targeting Myc indirectly using synthetic lethal methods or inhibiting other members in the same pathway.

The first approach is to targeting Myc directly. The stabilization of the G-quadruplex structure in the Myc promoter results in the repression of Myc transcription *in vitro* (Brooks and Hurley 2010). Omomyc is a domain mutant form of Myc with mutations in regions that are important in the dimerization of Myc and other proteins; thus, it inhibits Myc-dependent transactivation (Soucek, Jucker et al. 2002). 10058-F4 is a small molecular inhibitor that hinders the binding of the Myc/Max dimers that bind to DNA (Huang, Cheng et al. 2006).

The second approach is to targeting Myc indirectly. Targeting cell cycle kinases is an example of the application of the synthetic lethal ideas in targeting Myc. In breast cancer cell lines, cells with high Myc expression are much more sensitive to CDK1 inhibition (Kang, Sergio et al. 2014). VX-680, an aurora-B kinase inhibitor, selectively kills cells with Myc overexpression (Yang, Liu et al. 2010). Several genes have been identified with synthetic lethal interactions with Myc using the high-throughput siRNA screening (Kessler, Kahle et al. 2012, Toyoshima, Howie et al. 2012). Notably, the BET bromodomain, which is targeted by JQ1, regulates Myc-driven transcription as well as the transcription of Myc (Delmore, Issa et al. 2011, Mertz, Conery et al. 2011).

4-3. Overview of Stat3

4-3-1. Stat3 in breast cancer

In normal cells, the phosphorylation and activation of Stat3 is transient. Persistent activation of Stat3 has been observed in various types of cancer, including breast cancer (Watson and Miller 1995, Bromberg 2002). However, the roles of Stat3 in breast cancer are ambiguous. The increased activation of Stat3 is correlated with an incomplete response to chemotherapy (Diaz, Minton et al. 2006). In contrast, the expression level of phosphorylated Stat3 in the nucleus is associated with the overall survival in node-negative breast cancer patients (Dolled-Filhart, Camp et al. 2003, Berishaj, Gao et al. 2007). Abundant Stat3 mRNA expression is also correlated with smaller tumor size (Aleskandarany, Agarwal et al. 2016). In addition, the activated Stat3 is essential for the growth and maintenance of breast cancer stem-like cells (Zhou, Wulfkuhle et al. 2007, Marotta, Almendro et al. 2011).

4-3-2. Stat3 functions in physiological conditions and cancer

Similar to other members of the STAT family, Stat3 is a transcription factor that regulates the expression of diverse genes, such as apoptosis (Fukada, Hibi et al. 1996), differentiation (Snyder, Huang et al. 2008), and wound healing (Dauer, Ferraro et al. 2005). Stat3 is also important in the early stage of embryonic development, and the knockout of Stat3 leads to embryonic lethality (Takeda, Noguchi et al. 1997). In addition, Stat3 induces programmed cell death (PCD) during mammary gland involution (Chapman, Lourenco et al. 1999). Instead of relying on caspase cascades, this kind of PCD is lysosomal-dependent (Kreuzaler, Staniszewska et al. 2011). The mammary-specific deletion of Stat3 significantly delays involution in BLG-Cre/Stat3$^{Fl/-}$ (Chapman, Lourenco et al. 1999) and WAP-Cre/Stat3$^{Fl/Fl}$ mice (Humphreys, Bierie et al. 2002).

Studies have shown that the constitutive activation of Stat3 and somatic mutations are important in transformation (Bromberg, Wrzeszczynska et al. 1999), tumorigenesis (Dechow, Pedranzini et al. 2004), apoptosis (Gritsko, Williams et al. 2006), angiogenesis (Niu, Wright et al. 2002), and immune evasion (Yu, Kortylewski et al. 2007). Stat3 inhibits apoptosis by increasing the expression of the anti-apoptotic proteins, including Bcl-xL (Catlett-Falcone, Landowski et al. 1999), Mcl-1 (Epling-Burnette, Liu et al. 2001), and survivin (Aoki, Feldman et al. 2003). Stat3 promotes angiogenesis by increasing the transcription of VEGF and also mediates v-Src-induced VEGF expression (Niu, Wright et al. 2002). In immune evasion, constitutive activation of Stat3 inhibits the expression of pro-inflammatory mediators and elevates the expression of immuno-suppressive factors (Wang, Niu et al. 2004, Kortylewski, Kujawski et al. 2005). In tumor-initiating stem cells, VEGF upregulates the expression of Myc and Sox2 via Stat3 activation (Zhao, Pan et al. 2015).

4-3-3. Activation and regulation of Stat3

The stimulation of cytokines and tyrosine kinases leads to the transient activation of Stat3 through phosphorylation. The activated Stat3 is then translocated into the nucleus, and binds to DNA to regulate the expression of its target genes (Ihle 2001). IL-6 is a well-studied cytokine involved in this process (Heinrich, Behrmann et al. 1998). Followed by the binding of IL-6 to the IL-6 receptor, gp130 proteins form complexes with IL-6 receptors. The cytokine-activated tyrosine kinase JAK phosphorylates gp130, and induces the Y705 phosphorylation of Stat3. In addition, some serine/threonine kinases, such as MAPK, can phosphorylate the serine 727 residue of Stat3 to modulate Stat3 transcription activity (Yokogami, Wakisaka et al. 2000). Stat3 activation can also be mediated by receptor tyrosine kinases or non-receptor tyrosine kinases. Growth fac-

tors activate the phosphorylation of Stat3 directly by binding to growth factor receptors, such as EGFR (Park, Schaefer et al. 1996), and Src mediates Stat3 activation and transformation (Turkson, Bowman et al. 1998).

In normal cells, the activation and deactivation of Stat3 is tightly controlled. The negative regulators of Stat3 include tyrosine phosphatases, protein inhibitors of activated STATs (PIAS), and suppressors of cytokine signaling (SOCS) proteins. CD45 deceases the expression of activated Stat3 by dephosphorylating JAKs (Irie-Sasaki, Sasaki et al. 2001). PIAS3 hampers the transcription of Stat3-targeted genes by blocking the binding of Stat3 to DNA (Chung, Liao et al. 1997). SOCS regulates the phosphorylation of Stat3 by binding to JAKs or inducing proteasomal degradation (Alexander and Hilton 2004). Studies have found that several mechanisms contribute to the constitutive activation of Stat3 in cancer. First, increased stimuli: the mutations in EGFR increases IL-6 expression in lung adenocarcinoma (Gao, Mark et al. 2007). Second, somatic mutations of Stat3: the three nucleotide mutations of Stat3 that cause the persistent activation of Stat3 have been identified in hepatocellular carcinoma (Pilati, Amessou et al. 2011). Third, positive feedback: Stat3 increases the expression of shingsosine-1-phosphate receptor-1 (S1PR1), and increases S1PR1-activated Stat3 as well as leads to persistent Stat3 activation (Lee, Deng et al. 2010). Finally, deficient negative regulators of Stat3. Hypermethylation in the SOCS3 promoter causes the transcriptional silencing of SOCS3 and constitutive activation of Stat3 in lung cancer (He, You et al. 2003).

4-3-4. Treatments targeting Stat3

Stat3 is an attractive target for cancer therapy because of the persistent activation of Stat3 in various types of cancer. Several approaches have been developed for targeting Stat3 directly or indirectly. The phosphorylation of Stat3 is decreased by using a Stat inhibitor, OPB-31121

(Hayakawa, Sugimoto et al. 2013). In addition, Stat3 is directly inhibited by targeting certain domains of Stat3, completing with the dominant-negative form of Stat3, or using oligonucleotides. The SH2 domain of Stat3 is required for Stat3 activation. PpYLKTK hinders the dimerization of Stat3 and reduces the transactivation ability of Stat3 (Turkson, Ryan et al. 2001). Some platinum complexes, such as CPA-7, blocks the DNA-binding ability of Stat3 in colon cancer (Turkson, Zhang et al. 2004). ST3-H2A2 inhibits the Stat3 N-terminal domain and increases the transcription of Stat3-regulated proapoptotic genes (Timofeeva, Tarasova et al. 2013). Stat3beta lacking the transactivation domain of Stat3 induces apoptosis in cells and in xenografts (Niu, Heller et al. 1999). The Stat3 decoy, a 15 bp double-stranded oligonucleotide, blocks Stat3-mediated transactivation by binding to the *cis*-elements of Stat3 (Leong, Andrews et al. 2003). This inhibitor decreased Stat3-regulated gene expression in patients with head and neck squamous cell carcinoma in a phase 0 clinical trial (ClinicalTrials.gov number, NCT00696176) (Sen, Thomas et al. 2012). On the other hand, strategies for targeting Stat3 indirectly involve inhibiting a different upstream component of Stat3 activation or inducing the negative regulators of Stat3. KDl1 attenuates EGF-mediated Stat3 activation (Buerger, Nagel-Wolfrum et al. 2003). AG490 and WP1066 are JAK inhibitors that represses the phosphorylation of Stat3 (Ferrajoli, Faderl et al. 2007). Dasatinib inhibits the phosphorylation of Src and Stat3 in synovial sarcoma cells (Michels, Trautmann et al. 2013). Trichostatin A represses the activation of Stat3 by increasing the expression of SOCS3 (Xiong, Du et al. 2012).

4-3-5. Effects of loss of Stat3 in transgenic mouse models

The versatile characteristics of Stat3 have been further studied in transgenic mouse models. The absence of Stat3 caused embryonic lethality at embryonic days 6.5 (E6.5)-7.5 (Takeda, Noguchi et al. 1997). In T cells, the deletion of Stat3 suppressed IL6-stimulated T cell prolifera-

tion (Takeda, Kaisho et al. 1998). In the mammary gland, Stat3 deficiently resulted in the delayed involution (Chapman, Lourenco et al. 1999, Humphreys, Bierie et al. 2002). When one of the cytokines activating Stat3 in mice, leukemia inhibitory factor, was deleted in mice, delayed involution and absence of the Stat3 activation were observed (Kritikou, Sharkey et al. 2003). In Neu induced tumors, Stat3 was noted to regulate the metastatic progression of breast cancer. This is associated with the decreased expression of Stat3-targeted genes in angiogenesis (Ranger, Levy et al. 2009). Impaired immune responses in MMTV-PyVmT (polyomavirus middle T antigen) tumors without Stat3 led to defective metastases (Jones, Broz et al. 2016). Notably, the Stat3-deficient tumor onset was delayed only in PyVmT tumors, not in Neu ones. This suggests that Stat3 could have different effects depending on the oncogenic drivers.

Given the known functions of Stat3 and widespread effects of Myc in breast cancer, it is clear that the interactions of these two oncogenes should be examined *in vivo*. As mentioned previously, Stat3 might have distinct impacts on various oncogene-driven tumors. Additionally, studies have shown that Myc and Stat3 regulate each other in cases. Therefore, here we investigate the roles of Stat3 in Myc-induced mammary tumors in MMTV-Myc mice with the conditional knockout of Stat3.

4-4. Results

4-4-1. Stat3 has diverse functions in MMTV-Myc and MMTV-Neu tumors

To investigate the role of Stat3 in different oncogene-driven tumors, we compared gene expression profiles of MMTV-Myc and MMTV-Neu tumors. First, significant up-regulated and down-regulated genes from Stat3 pathway activation (Dauer, Ferraro et al. 2005) were isolated. Gene expression from Myc and Neu mediated tumors were then filtered to this list of Stat3 genes and were then used for unsupervised clustering. As shown in Figure 4.2A, MMTV-Neu tumors, and the various subtypes of Myc induced tumors were clustered into their histological groups. Analysis of the Stat3 genes enriched in MMTV-Neu tumors revealed that some of these genes are associated with metastasis. Indeed, patients with high expression of these genes are more susceptible to metastasis relative to patients with lower levels of these genes (Figure 4.2B). In contrast, the Stat3 regulated genes enriched in papillary tumors are not able to stratify patients for metastasis effects (data not shown). This result indicates that Stat3 might have different effects in MMTV-Myc tumors relative to Neu induced tumors. To test the role of the Stat3 genes in a predictive manner, we used the Stat3 pathway signature to test for activation in subtypes of MMTV-Myc tumors. Using the Stat3 signature (Dauer, Ferraro et al. 2005, Gatza, Lucas et al. 2010) in a binary regression approach (Bild, Yao et al. 2006), we predicted Stat3 activity in the Myc induced tumors. Compared to other subtypes, the majority of papillary tumors have elevated Stat3 pathway probability (Figure 4.2C). To explore the relation of Stat3 with Myc and knowing that Stat3 regulation functions through the active phosphorylated form, we analyzed effects of co-expression of phosphoStat3 and Myc in human breast cancer. In patients where we predicted high Myc pathway activity phosphoStat3 is correlated with overall survival (Figure 4.2D). Taken together, these data suggest the hypothesis that Stat3 has various

roles in MMTV-Myc tumors and that these roles are different from those previously observed in MMTV-Neu tumors.

4-4-2. Roles of STAT3 in physiological functions

To study roles of Stat3 in MMTV-Myc tumors, we interbred MMTV-Myc, MMTV-Cre, and $Stat3^{Fl/Fl}$ mice to generate Stat3 conditional knockout mice in MMTV-Myc background ($Stat3^{Fl/Fl}$ MMTV-Cre MMTV-Myc; Myc Stat3 CKO). We noticed that pups from the Myc Stat3 CKO dams were smaller than usual or died before being weaned. These pups were rescued by using other dams to foster them, demonstrating that lethality was due to defects in the dams. To study effects of Stat3 in normal development functions where Myc was overexpressed, we monitored the first litters of Myc Stat3 CKO, Stat3 CKO, and Myc dams. The size of litters was normalized to 6 by the end of the day after delivery and pup weights were tracked (Figure 4.3A). For the first and second litter of each group we found that there was a significant reduction in average weight from the Myc transgenic dams lacking Stat3. For the first litter, control Myc transgenic dams reared pups with an average weight of 3.7g 5 days postpartum. There was a significant reduction in the Myc transgenics lacking Stat3 to 3.4g. In the second litter, this difference was more pronounced with a reduction to 2.4g in the Myc transgenic Stat3 conditional knockout dams. Indeed, some of the pups from Myc Stat3 CKO dams did not have any visible milk spots on postpartum days 1-5. In the third litter of this group, several pups from Myc Stat3 CKO dams died before day 5. These data showed that deletion of Stat3 in dams is associated with the lower pup body weight, and the presence of the
Myc transgene exacerbates this defect and suggested that Stat3 might have other roles in normal mammary gland development.

To examine the role of Stat3 in Myc transgenic mammary glands, we compared morphology changes in 10- and 20-week-old virgin mice using whole mount staining and histology (Figure 4.3B). At both 10 and 20 weeks, the Myc transgenics had more side branches than their Stat3 CKO counterparts. Interestingly, the Myc Stat3 CKO mice had progressed to hyperplasia by 20 weeks of development. The histology of these various strains was consistent with the whole mounts. Taken together, these results suggest that loss of Stat3 in dams influences body weight of their pups, and expedites hyperplasia in the transgenic Myc background.

4-4-3. Loss of STAT3 alters tumor onset, tumor growth and histology

Given the hyperplastic phenotype in the Myc Stat3 CKO mice, we investigated if loss of Stat3 in MMTV-Myc mice accelerated tumor formation. Consistent with the mammary gland histological findings, Myc Stat3 CKO mice developed mammary tumor significantly more quickly than Myc transgenics ($p<0.001$) (Figure 4.4A). Median tumor onsets are 294 days in Myc Stat3 CKO mice and 360 days in Myc mice. Interestingly, we noticed that once tumors were palpable in the Myc Stat3 CKO mice, the majority of tumors grew relatively slowly compared to the Myc control tumors (Figure 4.4B). Measuring the time from initial palpation to 2500 mm^3 in Myc, and Myc Stat3 CKO mice revealed an average of 36 and 109 days respectively (Figure 4.4C). Consistent with this, Ki67 staining results support that tumors in Myc mice proliferate faster than those in Myc Stat3 CKO mice (Figure 4.4D and 4.4E, $p=0.04$).

While the delay in growth rate was substantial with loss of Stat3, we noted a several tumors that appeared to grow at the same rate as the Myc control tumors. Given the previous ob-

servation that tumors with MMTV-Cre directed excision could select against tumor progenitors with Cre expression (White, Junor et al. 2004), we examine tumors from Myc Stat3 CKO mice for excision. Using PCR on primary tumors to test for Stat3 excision revealed a number of tumors with and without excision (Figure 4.5A). Indeed, of the 38 tumors examined, 10 lacked Stat3 excision (Figure 4.5B). Tracked back to tumor growth of Myc Stat3 CKO mice with these tumors, mice with non-excised Stat3 in tumors have faster tumor growth compared to other mice with Stat3-excised tumors (Figure 4.5C). At the same time, protein expression of Stat3 from tumors with Stat3 excision was tested, confirming the knockout (Figure 4.5D). While there is a weak signal in the excised tumor samples, it is important to note that the MMTV-Cre transgene only directs expression to the mammary epithelial cells and that there are a number of additional cell types in a tumor. As a further confirmation of functional excision, we performed immunohistochemical staining of phosphorylated Stat3 (Tyrosine 705) to detect the active form of Stat3. As shown in Figure 4.5E, tumors in Myc and unexcised-Stat3 tumors in Myc Stat3 CKO mice had strong pStat3 signals. Importantly, Stat3-excised tumors in Myc Stat3 CKO mice did not have detectable pStat3.

Given the alterations to growth rate of the tumor and the selective pressure to maintain Stat3 expression, we hypothesized that loss of Stat3 may result in alterations to the histology of the tumors. Examining the tumors histologically we noted changes in histology of these tumors (Figure 4.6A). Notably, for the strain we used, 40% of MMTV-Myc tumors typically have a papillary pattern (Figure 4.6A and B). With the loss of Stat3, this was reduced to 20.5%. In addition, MMTV-Myc tumors frequently developed a squamous pathology, readily detected through the accumulation of keratin pearls. Interestingly, this subtype was not detected in tumors lacking Stat3 (Figure 4.6A). Moreover, the EMT tumors that were detected at a low frequency in

the Myc transgenics (2.7%) were significantly enriched (15.4%) after loss of Stat3 (Figure 4.6A and C). In addition, we noted an increase in myoepitheliomas after loss of Stat3 in these tumors (Figure 4.6A and D). Together these results indicate that loss of Stat3 resulted in significant histological alterations to the Myc induced tumors in addition to the acceleration of tumor initiation and decreased tumor growth rate.

4-4-4. STAT3 ablation affects angiogenesis and inflammation

With the increase of the EMT subtype and given the previously identified role of Stat3 in breast cancer metastasis (Ranger, Levy et al. 2009), we investigated how loss of Stat3 affected metastasis in the MMTV-Myc strain. Surprisingly, we noted that there was not a significant difference in tumor bearing mice with pulmonary metastasis when mice reached the endpoint of 2500 mm^3 (Figure 4.7A). In addition, we noted no differences in the size or number of metastatic lesions in the lung. While there were no significant differences, it is important to consider that the alterations to growth rate in the Myc Stat3 CKO mice resulted in tumors that were in the mouse for over twice the length of time of MMTV-Myc controls and it is thus possible that Stat3 does impact metastasis.

To support this idea, we first examined the impact of Stat3 loss on tumor vasculature. Based on results of CD31 staining, we noticed that tumors with Stat3 excision have less vessels than those with endogenous Stat3 (Figure 4.7B). After quantification, tumors lacking Stat3 were noted to be trending towards lower CD31-positive signals than those with Stat3 (Figure 4.7C). Next, we examined if tumors without Stat3 in the Myc transgenic background had altered inflammation. Presence of macrophages was tested through F4/80 staining. As predicted, tumors in MMTV-Myc mice have more macrophages than those in Myc Stat3 CKO mice (Figure

4.7D and 4.7E). Taken together, these results suggest that Stat3 affects angiogenesis and is involved in inflammation in tumors.

4-5. Discussion

The heterogeneity of breast cancer has been well characterized at the gene expression level, leading to the development of numerous classes of breast cancer (Perou, Sorlie et al. 2000, Sorlie, Perou et al. 2001). The heterogeneity is also reflected in the cell signaling pathways that are activated in tumor samples in both human breast cancer and mouse models (Andrechek, Cardiff et al. 2009, Gatza, Lucas et al. 2010, Hollern and Andrechek 2014). Given the potential for activation of other signaling pathways to compensate when one pathway is targeted (D'Cruz, Gunther et al. 2001), and for the ability of pathways to be involved in evolution of drug resistance (Yakes, Chinratanalab et al. 2002), it is therefore critical to characterize gene interactions in tumor development and progression. Here we have used a bioinformatics method to identify and focus on two transcription factors, Myc and Stat3. The proteins encoded by these genes have been found to be associated with the resistance to both endocrine therapy (Miller, Balko et al. 2011) and chemotherapy (Gritsko, Williams et al. 2006). In addition, their interaction has been noted in tumor-initiating cells resistant to chemotherapy (Zhao, Pan et al. 2015).

To understand the importance of the Myc / Stat3 interaction, we generated a mammary specific knockout of Stat3 in MMTV-Myc transgenic mice. Unexpectedly, we noted mammary gland effects that were apparent during lactation. Pups nursed by a Myc Stat3 CKO dam grew abnormally slowly or died after litter sizes were standardized and litters contained several different genotypes. Growth of these pups was similar to other pups after being fostered by dams of other genotypes. While Stat3 is known to initiate involution after weaning (Philp, Burdon et al. 1996), where deletion of Stat3 in the mammary gland resulted delayed involution, we were surprised to note the pup death. Epithelial apoptosis was decreased in BLG-Cre-Stat3 CKO mice (Chapman, Lourenco et al. 1999) and involution was delayed for 3 days in WAP-Cre-

Stat3 CKO mice (Humphreys, Bierie et al. 2002). On the other hand, mice lacking Socs3, a negative regulator of Stat3, have been found with precocious involution due to increased apoptosis with elevated expression of Myc and Stat3 (Sutherland, Vaillant et al. 2006). Similarly, overexpression of Myc resulted in accelerated lactation, and earlier onset of involution during pregnancy through activation of Stat3 (Blakely, Sintasath et al. 2005). However, in our study, there was no dramatic change in morphology at day 17.5 of pregnancy among Myc, Stat3 CKO, and Myc Stat3 CKO mice. Premature involution also caused pup death in MMTV-Myc mice (Blakely, Sintasath et al. 2005); however, we did not observe this phenomenon in the MMTV-Myc strain that we employed. These results suggest that deletion of Stat3 together with Myc overexpression leads to more severe impaired remodeling of mammary gland.

Interestingly, compared to wild-type MMTV-Myc mice, loss of Stat3 increased the formation of hyperplastic areas in the mammary glands, accelerated tumorigenesis, and slowed tumor growth. MMTV-Myc mice were initially reported to develop adenocarcinoma spontaneously (Stewart, Pattengale et al. 1984), and further studies revealed that additional mutations, such as Kras, were accumulated in Myc-driven tumors (D'Cruz, Gunther et al. 2001). Interestingly, the overexpression of the activated form of Stat3 transformed fibroblasts and resulted in development of mammary tumor in mice (Dechow, Pedranzini et al. 2004). Stat3 has also been shown to sensitize cells to DNA damage (Barry, Townsend et al. 2010). Thus, it is plausible that Stat3 activates DNA repair pathways to repair DNA damage caused by Myc, thereby delaying tumor onset. Without Stat3, these tumorigenic cells are able to continuously grow, resulting in the accelerated tumor detection that we described. Similarly, overexpression of the anti-apoptotic gene Bcl-2 in WAP-Myc mice reduced apoptotic cells and expedited tumorigenesis (Jager, Herzer et al. 1997). During proliferation, Myc is known to

shorten G1 phase and accelerate the cell cycle (Facchini and Penn 1998), and Stat3 could be activated after stimulation of growth factor through JAK2. Expression of dominant-negative Stat3 or treatment of a JAK2/Stat3 inhibitor in breast cancer cell lines inhibited cell growth (Li and Shaw 2002). Consistent with these findings, these tumors in the Myc Stat3 CKO mice grew more slowly than the controls.

Another important characteristic of tumor progression regulated by Myc and Stat3 is metastasis and angiogenesis. While Myc has been shown to be essential in angiogenesis (Baudino, McKay et al. 2002), MMTV-Myc mice metastasize at a low frequency (Yuwanita, Barnes et al. 2015). Activated Stat3 regulates key factors in angiogenesis, including VEGF and HIF-1α (Hypoxia-Inducible Factor) (Niu, Wright et al. 2002). Indeed, HER2 activation increased expression of VEGF and HIF-1α through pathways mediated by Stat3 (Xu, Briggs et al. 2005). In agreement with this, ablation of Stat3 in MMTV-Neu mice has been reported to impair angiogenesis and reduce metastasis (Ranger, Levy et al. 2009). Here we demonstrated that deletion of Stat3 in MMTV-Myc mice slightly decreased the percentage of mice with lung metastasis, and was associated with a reduction in CD31-positive cells. Notably, these tumors took a two-fold longer period of time after detection to reach the end point, suggesting that the metastatic effects were more significant than measured. These results indicate that loss of Stat3 in Myc-driven tumors leads to defective angiogenesis. In addition, solid tumors require angiogenesis factors to grow beyond 2 mm (Folkman 1974) and this was consistent with the tumor growth curve in Myc Stat3 CKO mice.

In contrast to the Neu Stat3 CKO results, we noted that loss of Stat3 in Myc background only shared some effects on tumor development and progression (Ranger, Levy et al. 2009). In contrast to the Myc results, loss of Stat3 did not affect tumor onset of Neu induced tumors, and

led to significantly reduced metastasis. This is consistent with genes enriched in the Stat3 pathway in Neu induced tumors being correlated with distant metastasis in human breast cancer patients (Figure 4.2B). In another highly metastatic mammary tumor model, PyMT, ablation of Stat3 also abrogated metastasis (Chang, Bournazou et al. 2013). These data showed that interaction of Stat3 with other oncogenes led to various consequent effects. More recent studies support the theory that Stat3 acts as an oncogene as well as a tumor suppressor in oncogene-driven tumors. Constitutive activated Stat3 blocked the transformation of mouse embryonic fibroblast triggered by Myc, but did not suppress transformation driven by Harvey rat sarcoma viral oncogene homolog (Hras) (Ecker, Simma et al. 2009). Moreover, lack of Stat3 in Kras induced lung adenocarcinoma accelerated tumorigenesis (Grabner, Moll et al. 2016). Herein we reported that knockout Stat3 in Myc-driven mammary tumor also caused early tumorigenesis.

In summary, Stat3 acts as both an oncogene or a tumor suppressor dependent upon the oncogenic driver and tumor stage. While Stat3 CKO alone did not develop tumors, Stat3 loss in Myc transgenic mice accelerated tumor onset relative to Myc transgenic controls. Surprisingly, we showed that breast cancer patients with low Stat3 by IHC and high Myc pathway activation have poor survival. These findings suggest that strategically targeting Stat3 in breast cancer should be done in careful consideration of other oncogenes when developing personalized treatment.

CHAPTER 5

FUTURE DIRECTIONS

The pathway-guided personalized treatment has led to the inhibition of tumor growth in a mouse mammary tumor model and tumor regression in human breast cancer-derived xenografts. These encouraging results show that it is practical to tackle the inter-tumor heterogeneity challenges. In addition, the continued uses of these mouse models could lead to the evaluation of new therapy agents and regimens as well as reveal the potential problems. However, more studies will be needed to modify this approach to fit more samples and derive better therapeutic outcomes.

Additional genomics data of subjects will be required for the development of tailored treatment. For instance, most of EMT tumors have high RAS pathway activation regardless of KRAS mutations. Concerning mutually exclusive mutations of genes in the same pathway and crosstalk between pathways, the possible compensation pathways or genes after treatment in tumors with various mutations might lead to distinct transcriptomic changes. In addition, it has been proposed that alterations of the genes involved in DNA damage responses has been proposed to cause the amplification in certain chromosome regions in luminal subtype. These data could be compared with alterations found in patients before and after chemotherapy. These results could be applied in the rationalization of the combination of chemotherapy and targeted therapy and then facilitate the transition of preclinical findings to clinical trials.

Additional characteristics of targets or drugs used in the development of personalized treatment could enhance therapeutic effects. In the pilot tests, only some two-drug combinations had synergistic effects on tumor growth. This could indicate the existence of some common targets and crosstalk. In addition, it could be due to the impacts of genes/targets on tumor growth. Numerous studies have shown that the weight of oncogenes and tumor suppressors in tumor development varies in cancers. With this understanding, the evaluation of the benefits of adding these repurposed FDA-approved drugs in the combinatorial treatments could be more complete.

On the other hand, stromal effects and the tumor microenvironment also contribute to the sensitivity to treatment, especially for those targets involved in inflammation or that have paracrine functions. The role of Stat3 in cancer immunosurveillance has been reported. In Chapter 4, I found that the deletion of Stat3 in the Myc-induced tumor accelerated tumorigenesis as well as delayed tumor growth. It is plausible that Stat3 in the surrounding regions relieves the consequent effects caused by targeting Stat3 in tumors. Further studies will be needed to address this concern.

APPENDIX

Table 3.1. The values of ALT, AST, and creatinine in papillary tumor mice with drug or vehicle treatment. The value marked with an asterisk represents the value is higher than normal range.

Treatment	ALT (U/L)	AST (U/L)	Creatinine (mg/dL)
No	94*	430*	0.2
	121*	477*	0.2
	140*	524*	0.2
Vehicle_VX-680	105*	369*	0.2
	52	198	0.2
	98*	302*	0.2
VX-680	75	230	0.2
	100*	204	0.2
	54	140	0.2
Vehicle_Miltefosine	116*	307*	0.2
	144*	347*	0.2
	142*	455*	0.2
Miltefosine	108*	254	0.2
	102*	299*	0.2
	56	226	0.2
No	83	302*	0.2
	132*	365*	0.2
	114*	370*	0.2
Vehicle_WP1066	152*	464*	0.2
	117*	375*	0.2
	28	190	0.2
WP1066	124*	390*	0.2
	275*	803*	0.2
	106*	289	0.2
Vehicle_Miltefosine plus VX-680	104*	318*	0.2
	42	932*	0.2
	75	234	0.2
Miltefosine plus VX-680	45	202	0.2
	61	230	0.2
	62	210	0.2
No	138*	315*	NA
	100*	169	NA
	82*	225	NA
Vehicle_VX-680 plus WP1066	115*	803*	NA
	199*	373*	NA
	12	192	NA
VX-680 plus WP1066	11	148	NA
	80*	213	NA
	78*	155	NA

Table 3.1. (Cont'd)

Treatment	ALT (U/L)	AST (U/L)	Creatinine (mg/dL)
No	100*	345*	NA
	158*	392*	NA
	144*	232	NA
Vehicle_Miltefosine plus WP1066	64	183	NA
	80*	164	NA
	93*	227	NA
Miltefosine plus WP1066	240*	347*	NA
	82*	247	NA
	197*	352*	NA
Vehicle_Miltefosine	116*	307*	NA
	144*	347*	NA
	142*	455*	NA

Figure 2.1. Isolation of EMT cell lines and the relative application.

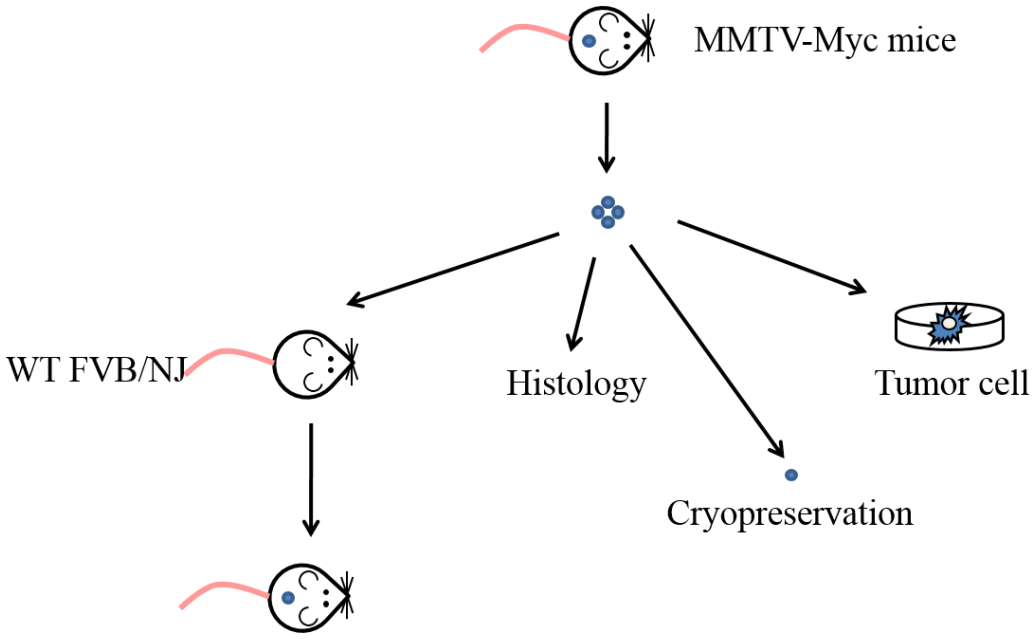

The original tumors with mixed histology were from MMTV-Myc mice. After the histology phenotype was confirmed, the frozen tumors were implanted back into WT FVB/NJ mice. Once the tumor grew consistently, the tumors were harvested and cells were isolated. After the cell lines were established, these cells were injected back to WT FVB/NJ mice to check if the tumors are EMT or not.

Figure 3.1. Overview of development of subtype-specific combinatorial treatments in MMTV-Myc mouse model.

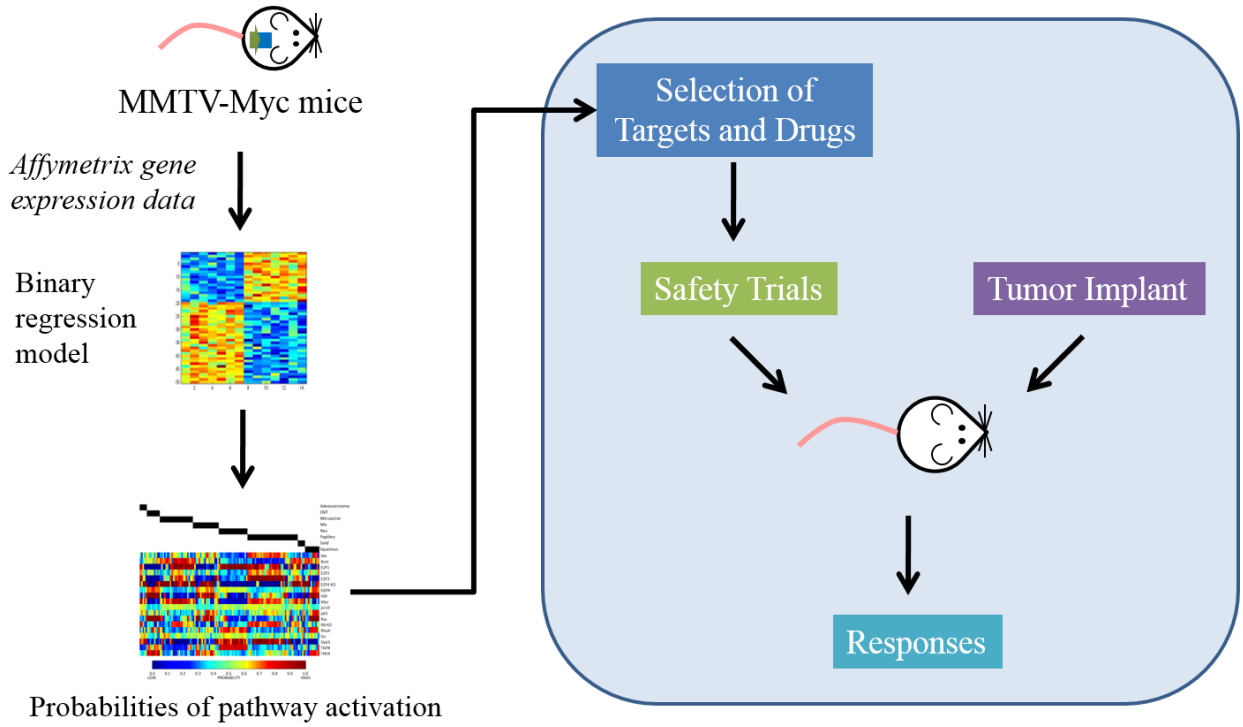

The RNA microarray data from tumors obtained from MMTV-Myc mice were analyzed to generate the probabilities of pathway activations. Based on the pathway activation patterns, targets and drugs were selected. The pilot test of the safety trials was performed in wild-type FVB/NJ, and the safety and efficacy trials were tested in wild-type FVB/NJ female mice implanted with one subtype of tumors from MMTV-Myc mice.

Figure 3.2. Overview of development of individualized combinatorial treatments in patient-derived xenograft model.

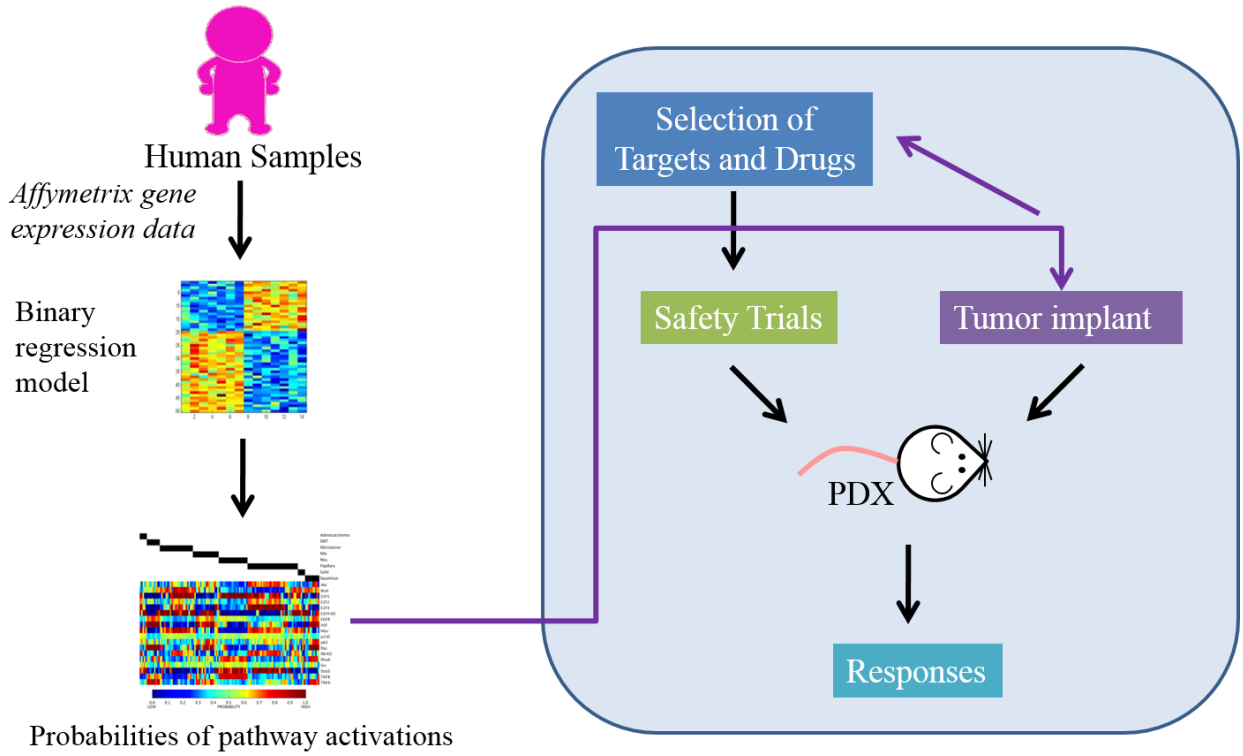

The RNA microarray data from human breast cancer and patient-derived xenografts were analyzed to generate the probabilities of pathway activations. The selection of targets and drugs were based on the availability and characteristics of patient-derived xenografts and pathway activation patterns. The pilot test of the safety trials was performed in wild-type FVB/NJ, and the safety and efficacy trials were tested in SCID/Beige female mice implanted with the tumor from one patient-derived xenograft line.

Figure 3.3. Designing breast cancer therapy based on gene expression patterns.

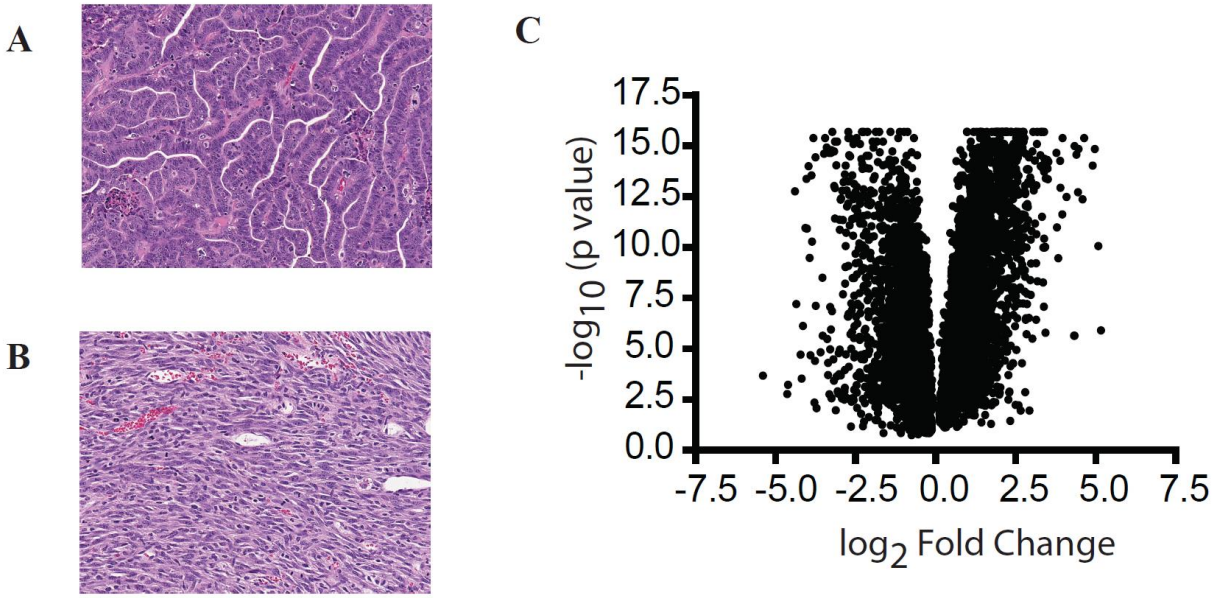

Histology of two major subtypes of MMTV-Myc tumors includes
both (A) papillary and (B) EMT. (C) Comparison of these two subtypes for gene expression differences in a volcano plot reveals significant differences in fold change.

Figure 3.3. (Cont'd)

D

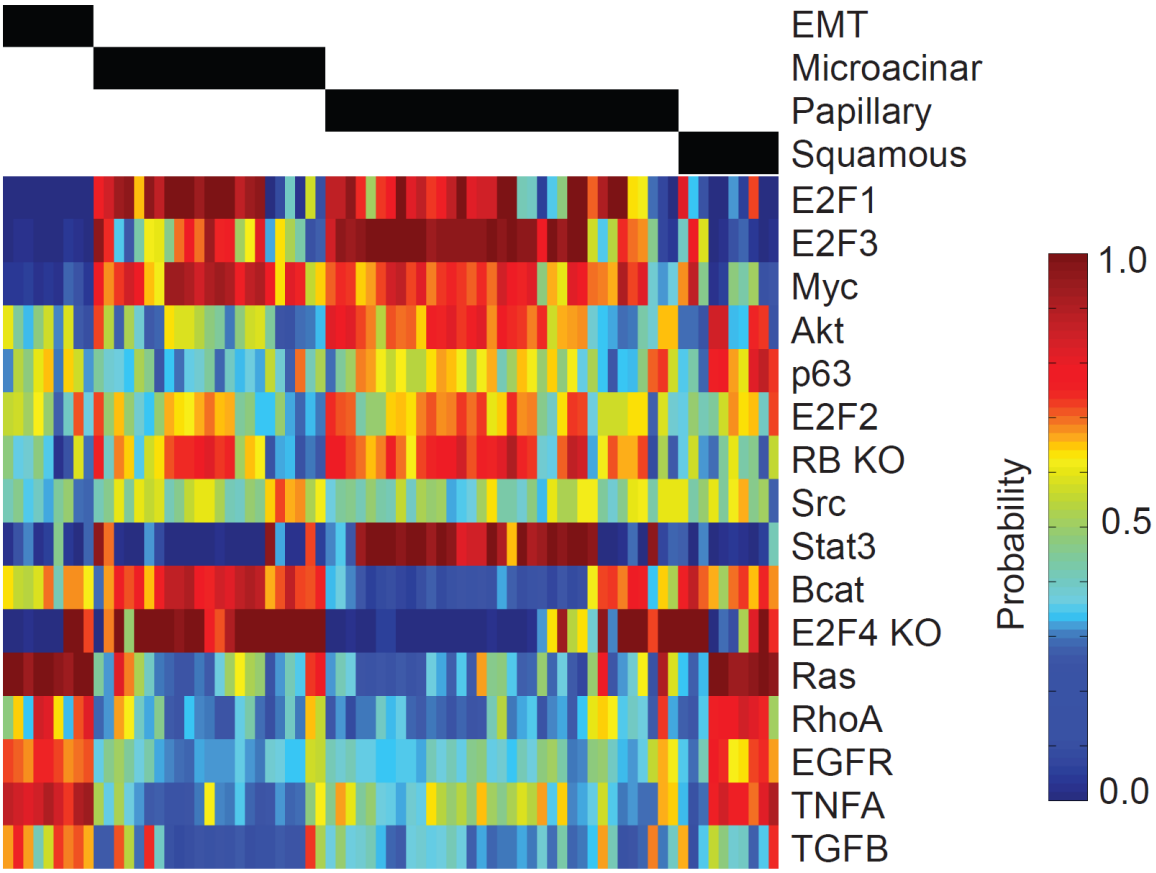

(D) Probability of pathway activation prediction in major subtypes of MMTV-Myc tumors demonstrates differences in signaling pathways. The black bars on the top show identity of the subtypes. In the heatmap, each column represents one tumor sample and each row represents a cell signaling pathway (identified at the right). The color of position in the heatmap indicates the probability of the activity of the cell signaling pathway in comparison to the training data for each pathway, and the color map represents the corresponding value of probability. For example, in the first row for the EMT samples at the left, there is a very low probability of E2F1 activation. However, to the right of those samples there is a high probability that E2F1 is active in the papillary samples.

Figure 3.3. (Cont'd)

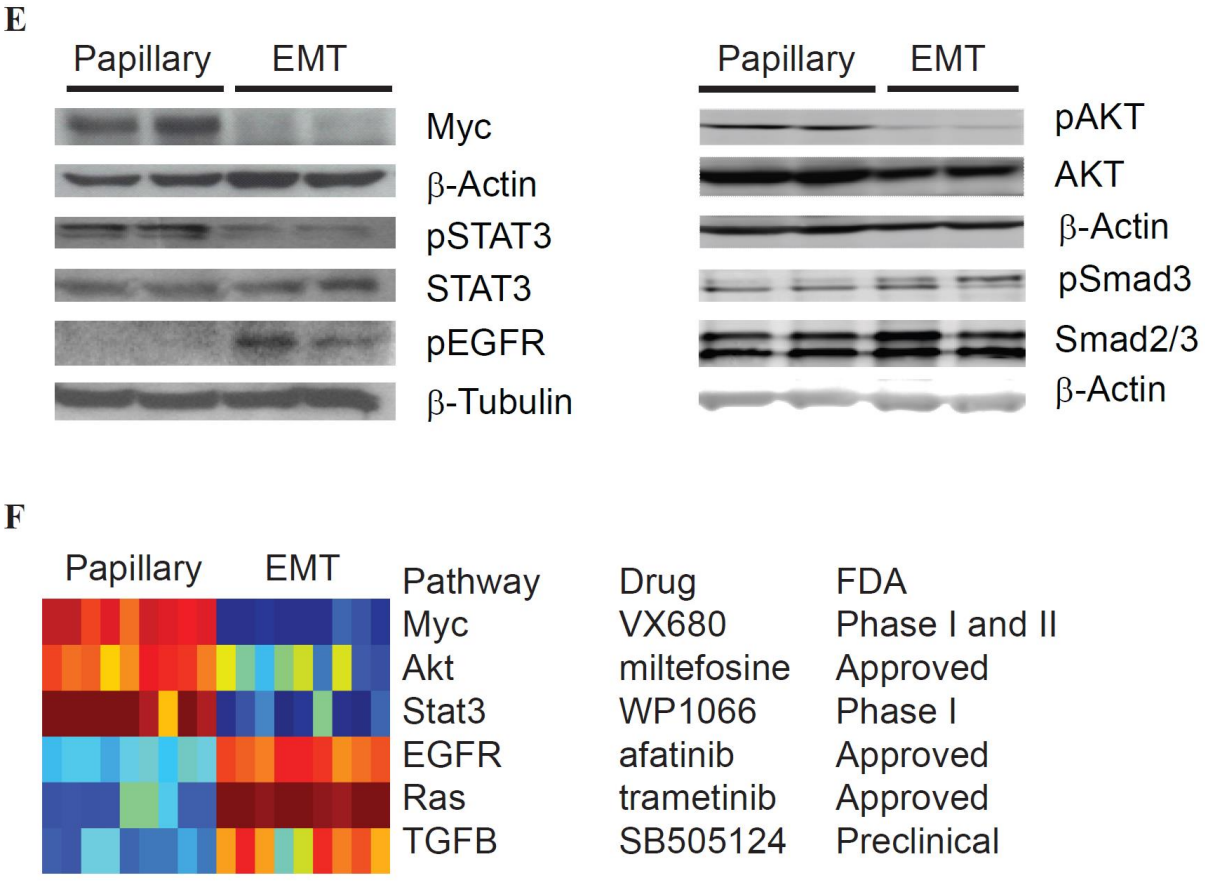

Western blots for the indicated pathways validate the probability of pathway activation in EMT and papillary subtypes (E). Extracting pathways with major differences in papillary and EMT tumors reveals the extent of the predicted difference. Compounds targeting these pathways and their FDA approval status are also shown (F).

Figure 3.4. Kras mutations in EMT and papillary tumors.

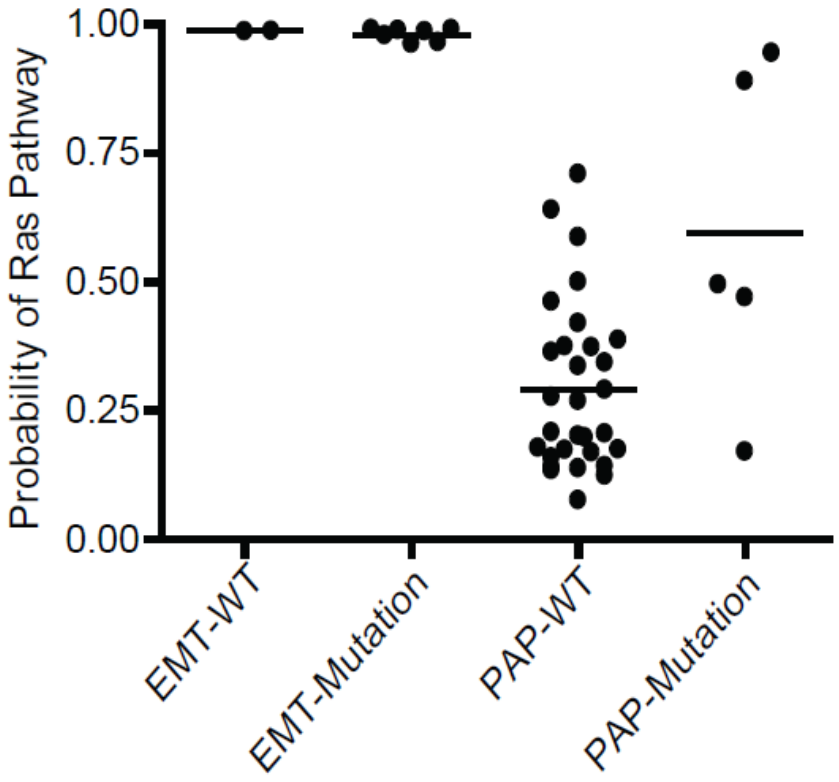

The probability of Ras pathway activation was plotted for tumors where Kras was sequenced across codon 12, 13, and 61. EMT tumors with a wild type Kras (EMT-WT) and a mutation in Kras (EMT-mutation) were both noted to have elevated predicted activity for Kras. The EMT-WT samples were also sequenced for Braf where activating mutations were noted. The EMT samples were compared to papillary with wild type Kras (Pap-WT) and papillary with activating mutations in Kras (Pap-mutation). This revealed a significant correlation of Kras activity with activating mutations in Kras.

Figure 3.5. Strategy of development of subtype-specific combinatorial therapies.

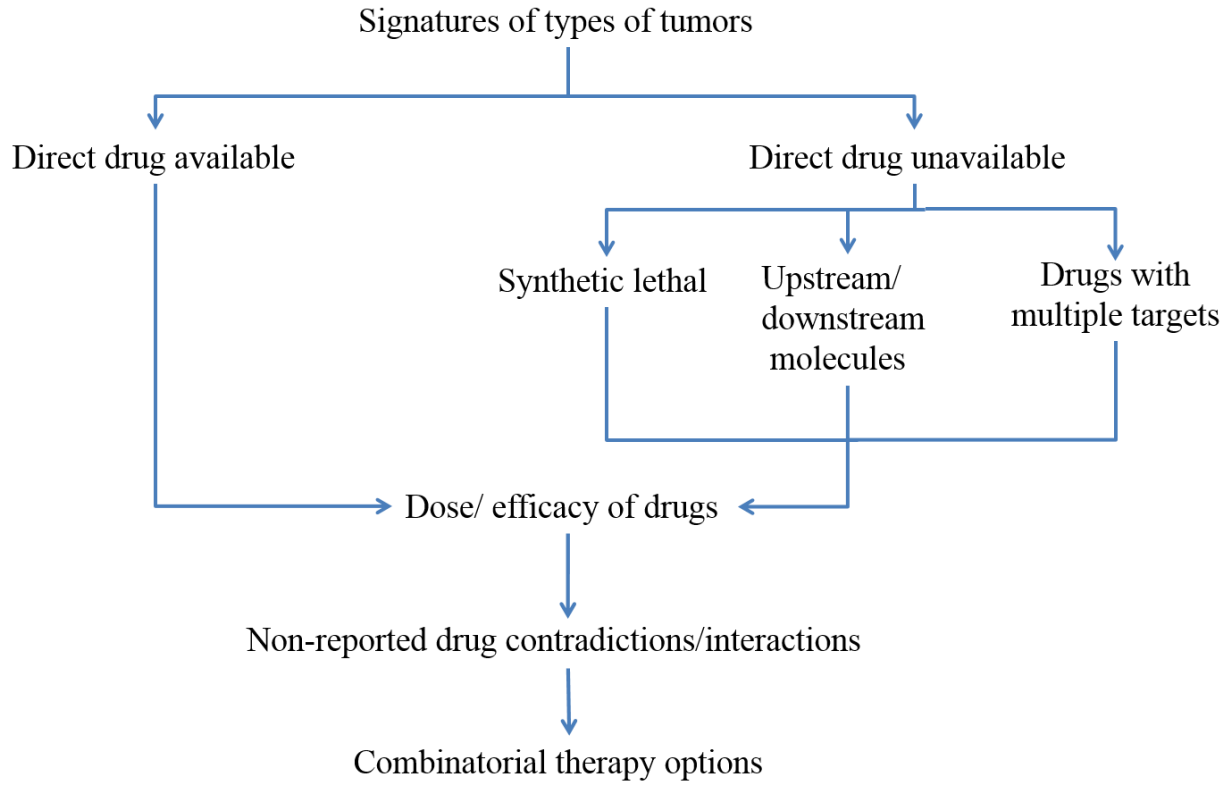

Based on the availability of drugs targeting pathways directly, pathways were split into two groups. For the pathways with available direct targeted drugs, the dose and efficacy of drugs were compared with each other. In addition, FDA-approved status is another important factor. Drug contradictions and interactions were also considered. Finally, the combinatorial therapy options were formed and modified according to the characteristics of drugs. However, if drugs targeting pathway directly are not available, the three major solutions include 1) drugs targeting pathways through synthetic lethal, 2) drugs targeting upstream or downstream of pathways, and 3) drugs with multiple targets. When comparing the dose and efficacy of drugs, these solutions would be used again in ranking the priority of drugs. After generation of a list of drugs, the same selection process which was used in the "direct drug available" group was taken.

Figure 3.6. Papillary-specific combinatorial treatment in mice implanted with papillary or EMT tumors.

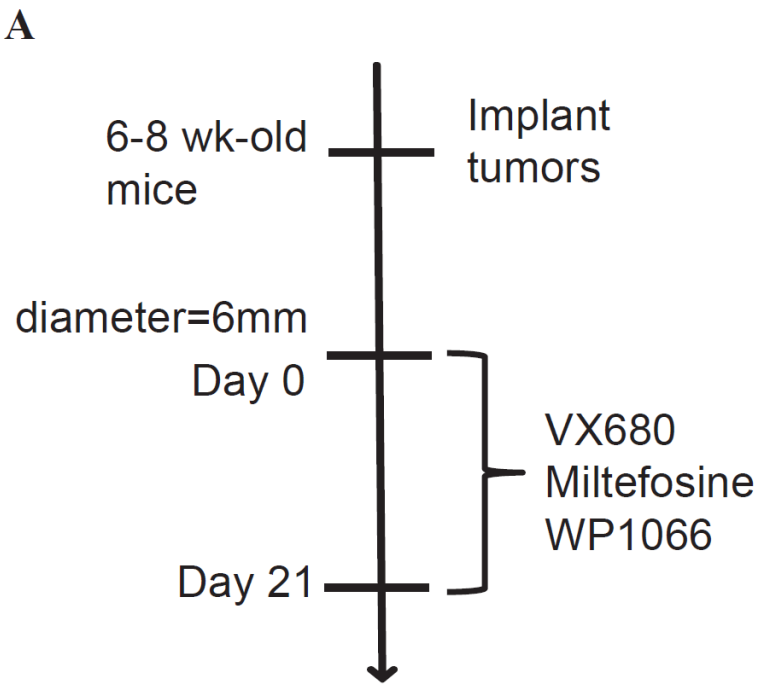

The trial design to test the therapeutic regimens for papillary tumors is shown (A). Each drug in the papillary-specific combinatorial treatment was given individually to mice orthotopically implanted with papillary tumors for 21 days.

Figure 3.6. (Cont'd)

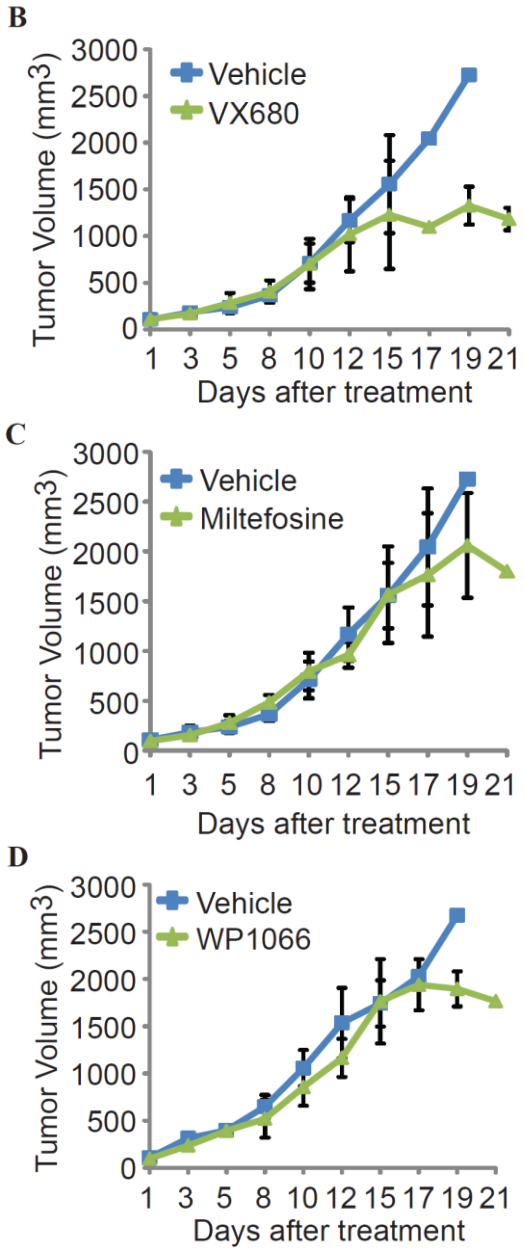

Effects of tumor growth rate are shown for the (B) Aurora B kinase inhibitor (VX680 50 mg/kg, 6 days per week, intraperitoneal injection (i.p.)), (C) Akt inhibitor (miltefosine 50 mg/kg, 5 days per week, i.p.), and (D) Stat3 inhibitor (WP1066 20mg/kg, 5 days per week, i.p.), n=3 in each group.

Figure 3.6. (Cont'd)

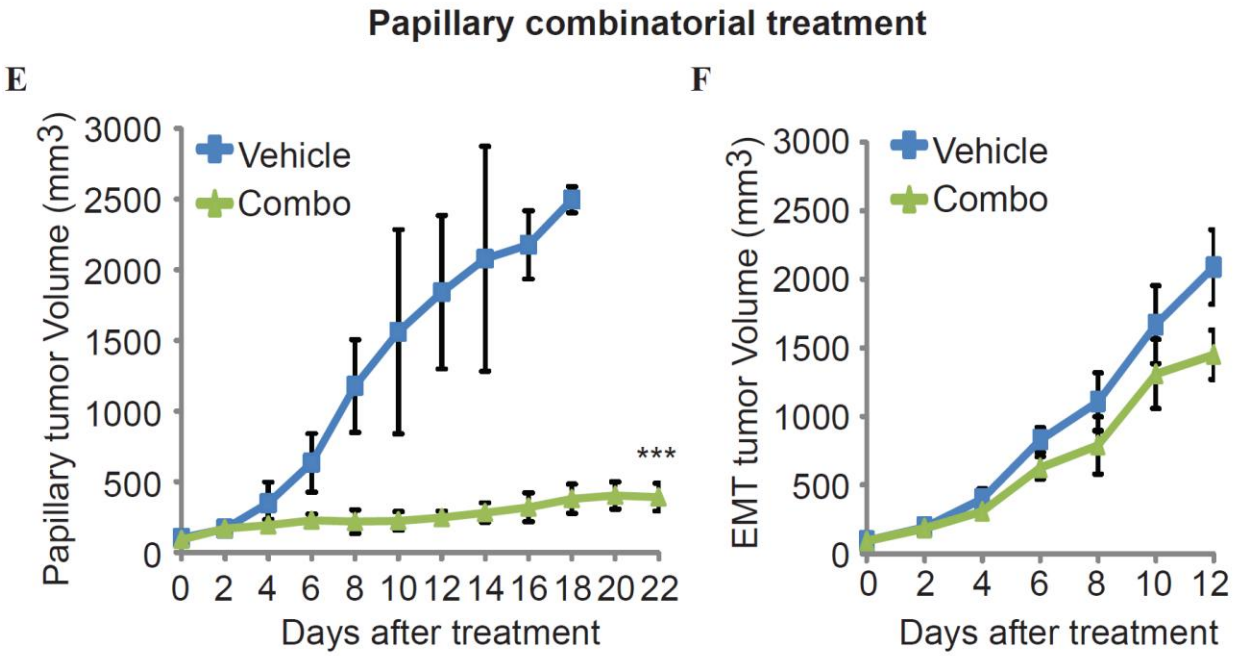

(E) Effect on tumor growth in mice orthotopically implanted with papillary tumors receiving the papillary-specific three-drug combinatorial therapeutic composed of the same dose and dosage regimen of each drug used in panels B-D for 21 days is shown. p= 0.001, n=6 in each group. (F) Specificity of the papillary-specific combinatorial treatment was tested in mice implanted with EMT-subtype tumors for 12 days (n=4 in each group).

Figure 3.6. (Cont'd)

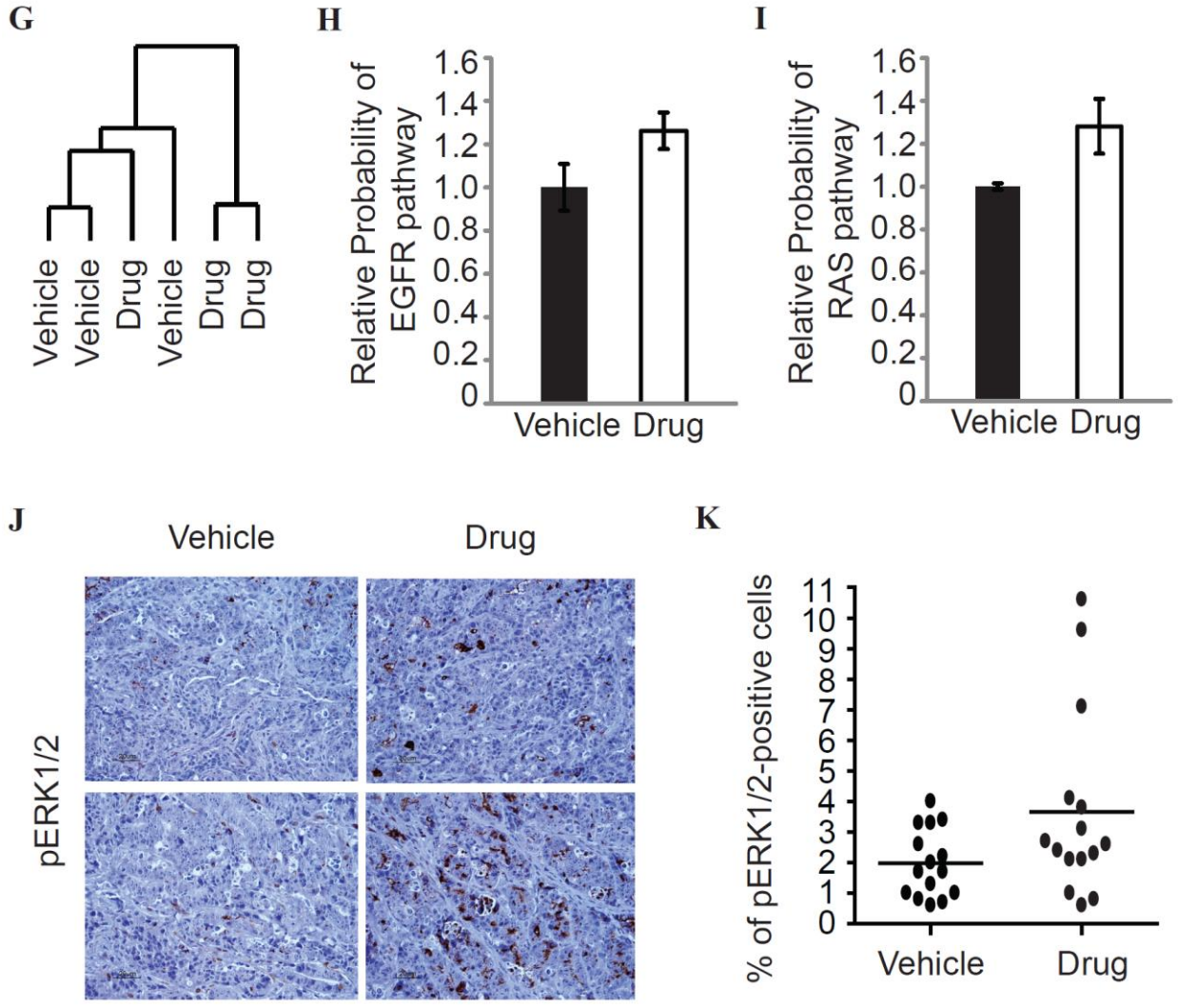

(G) Comparison of gene expression between mice in vehicle-treated group versus those in the combinatorial therapeutic-treated group after 21-day treatment using unsupervised hierarchical clustering. The dendrogram is shown and n=3 in each group. (H) Relative probability of EGFR pathway activation in mice treated with vehicle or the combinatorial treatment for 21 days was calculated from the gene expression data, with the same methods as shown in Figure 1D, p=0.07. (I) Relative probability of RAS pathway activation in mice treated with vehicle or the combinatorial treatment for 21 days was also calculated using the genomic signature method, p=0.06. (J) Immunohistochemical staining of pERK1/2 in mice implanted with papillary tumors receiving vehicle or the combinatorial therapeutic for 21 days is shown. Representative images are shown for each treatment arm. (K) Quantification of pERK1/2-positive cells was completed with n=5 for each of the three samples. p=0.05. All data are mean ± S.D. Statistical analysis were performed with two-tailed Student's t test. *p<0.05, **p<0.01, and ***p<0.001.

Figure 3.7. Percentage of body weight changes in papillary tumor mice receiving single-drug or vehicle treatment.

A

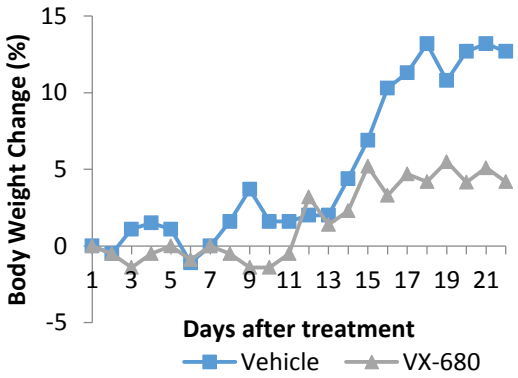

B

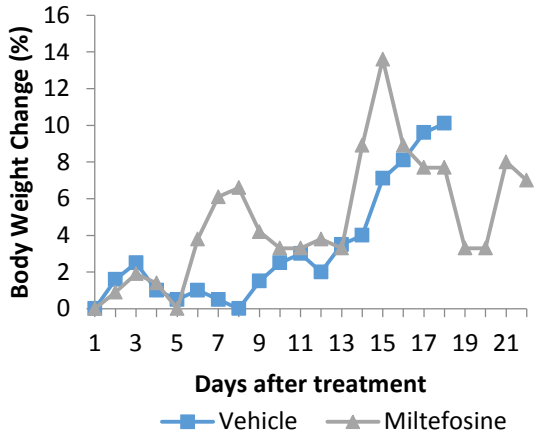

C

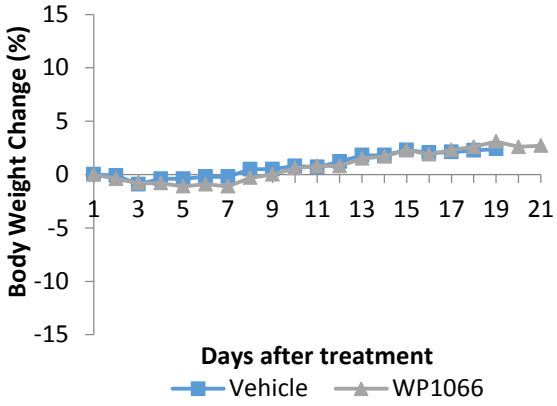

To test for side-effects associated with single-drug treatments mice receiving treatment were assessed for changes to body weight. Body weight changes in mice with papillary tumors that received vehicle control or drug treatment were recorded as a percentage of the weight of the mice at the start of the trial with a 6mm tumor. This revealed no significant differences. Data presents median. N=3 in each group.

Figure 3.8. Percentage of body weight changes in papillary tumor mice receiving two-drug combinatorial or vehicle treatment.

A

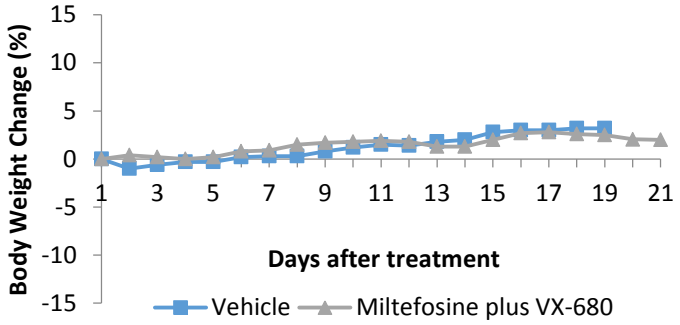

B

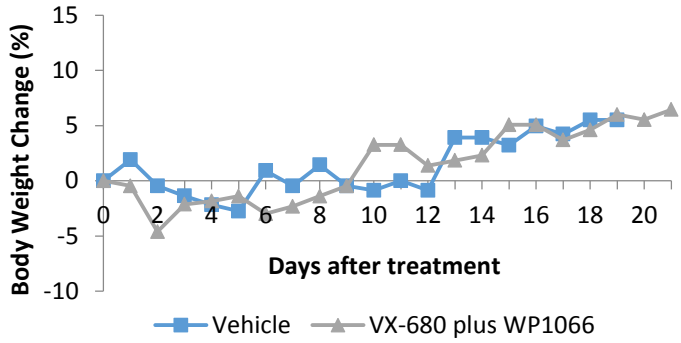

C

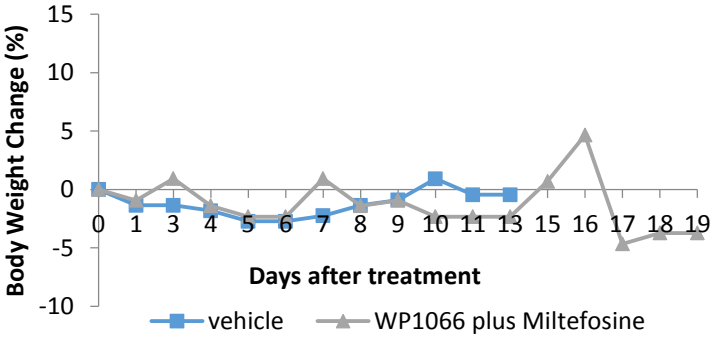

To test for side-effects associated with single-drug treatments mice receiving treatment were assessed for changes to body weight. Body weight changes in mice with papillary tumors that received vehicle control or drug treatment were recorded as a percentage of the weight of the mice at the start of the trial with a 6mm tumor. This revealed no significant differences. Data presents median. N=3 in each group.

Figure 3.9. Body weight change (shown in %) of mice received papillary-specific combinatorial treatment.

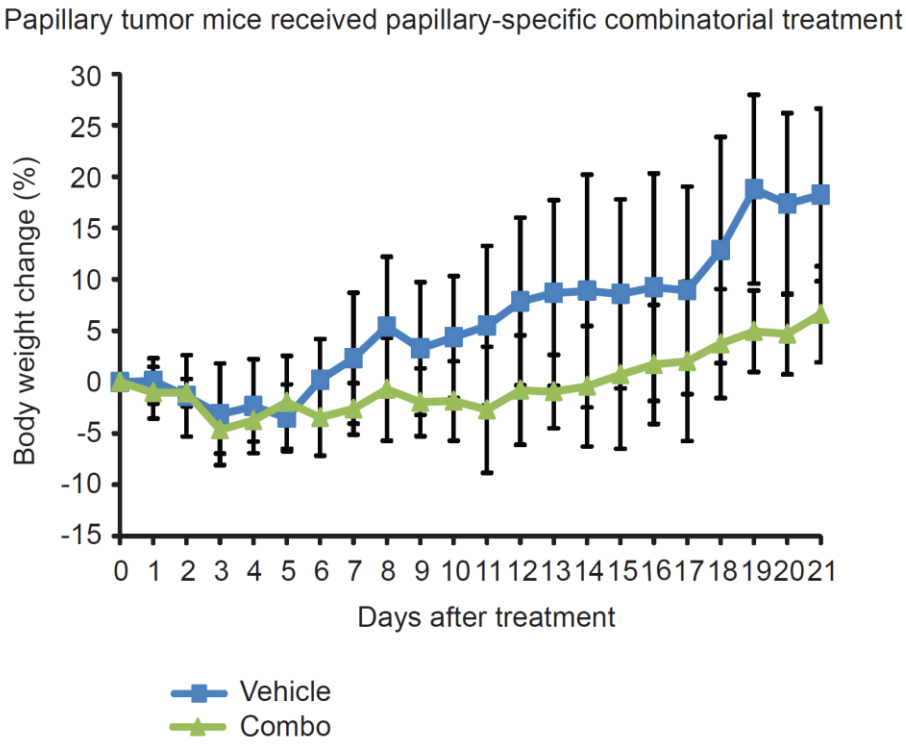

To test for side-effects associated with combinatorial treatment mice receiving treatment were assessed for changes to body weight. Body weight changes in mice with papillary tumors that received vehicle control or papillary-specific treatment were recorded as a percentage of the weight of the mice at the start of the trial with a 6mm tumor. For each group, n=6. This revealed no significant differences. All data are mean ± S.D.

Figure 3.10. Health condition of papillary tumor mice.

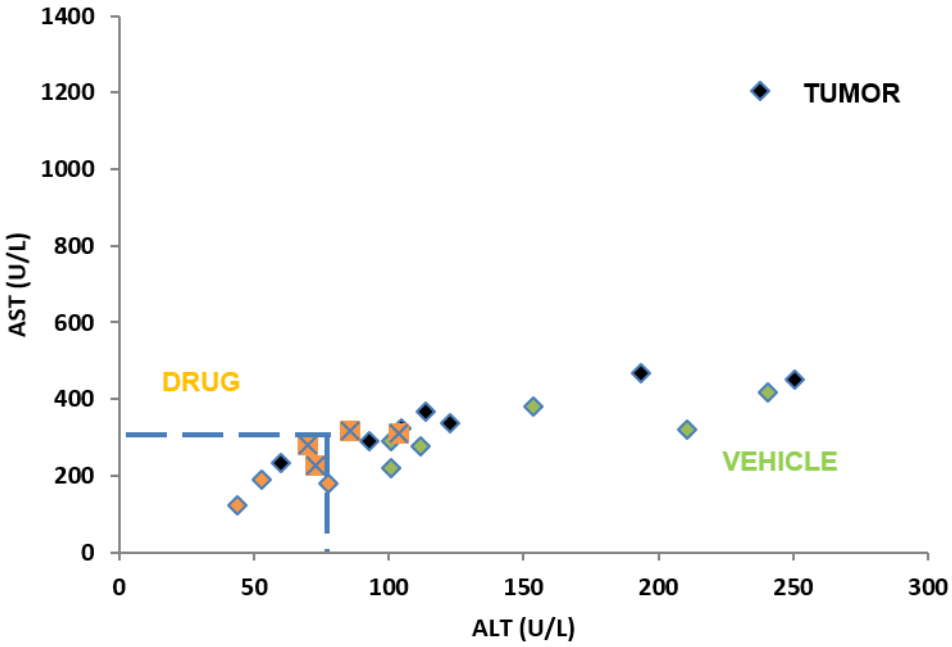

The health effects of the papillary-specific treatment in papillary tumor mice were shown using AST and ALT labels. Blood samples were collected after 21-day treatment. The black dots represent tumor only, the green dots represent vehicle-treated tumors, and the orange dots represent drug-treated tumors. The dash lines are the cut-off levels of AST and ALT. The value above the line indicates abnormal.

Figure 3.11. Heatmap of gene expression data from papillary tumors after vehicle or papillary-specific combinatorial treatment.

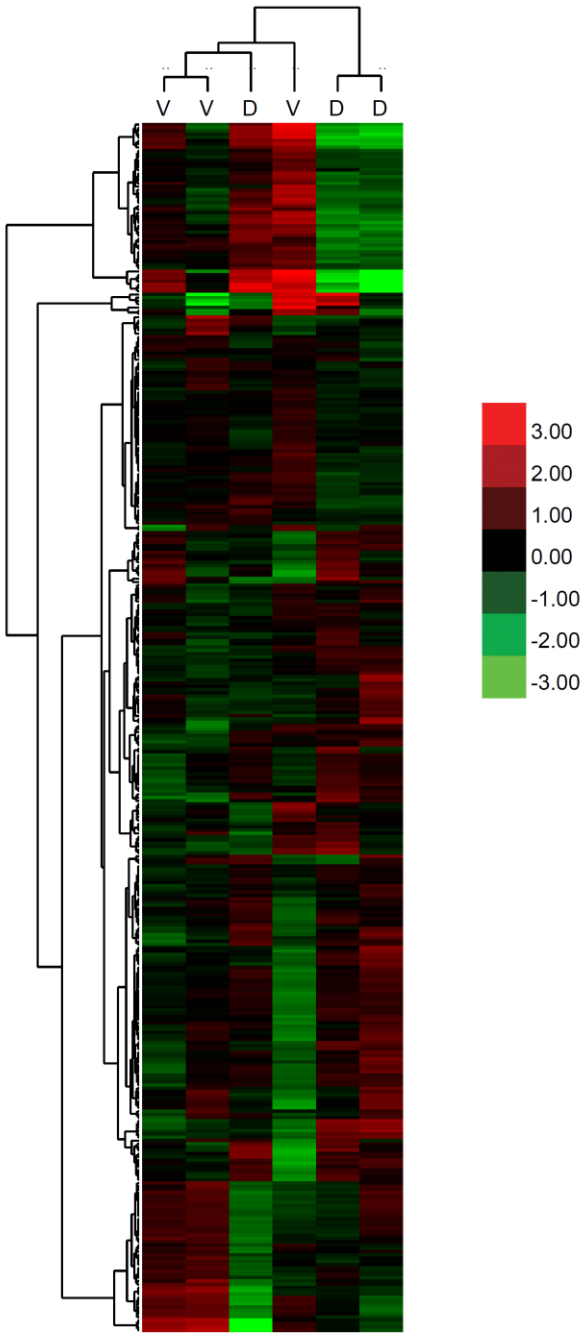

Unsupervised heretical clustering of papillary tumors after treatment with vehicle control or combinatorial treatment specific for papillary tumors. N=3 in each group. V represents Vehicle-treated mice, and D represents Drug-treated mice. The colorbar indicated the differences in gene expression.

Figure 3.12. Increased dose of VX680 in the papillary-specific combinatorial treatment.

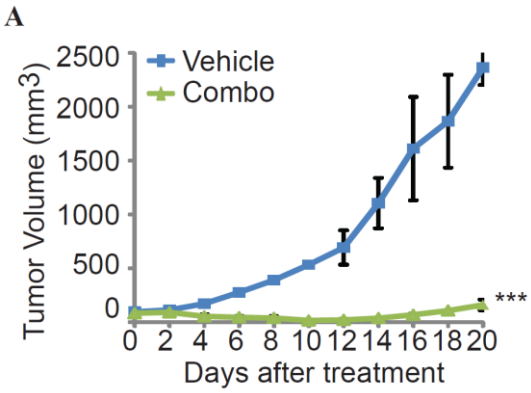

The dose of VX680 in the papillary-specific combinatorial treatment was increased from 50 mg/kg to 60 mg/kg. This modified combinatorial treatment consists of 60 mg/kg VX680, 50 mg/kg miltefosine, 20 mg/kg WP1066, and the same dosage regimen and administration route for each drug as was described in Figure 2. The effect of this modified papillary-specific combinatorial therapeutic strategy in mice implanted with papillary tumors is shown. The tumor growth rate demonstrated tumor regression (A). ***p=0.004, n=3 in the vehicle-treated group and n=4 in the drug-treated group.

Figure 3.12. (Cont'd)

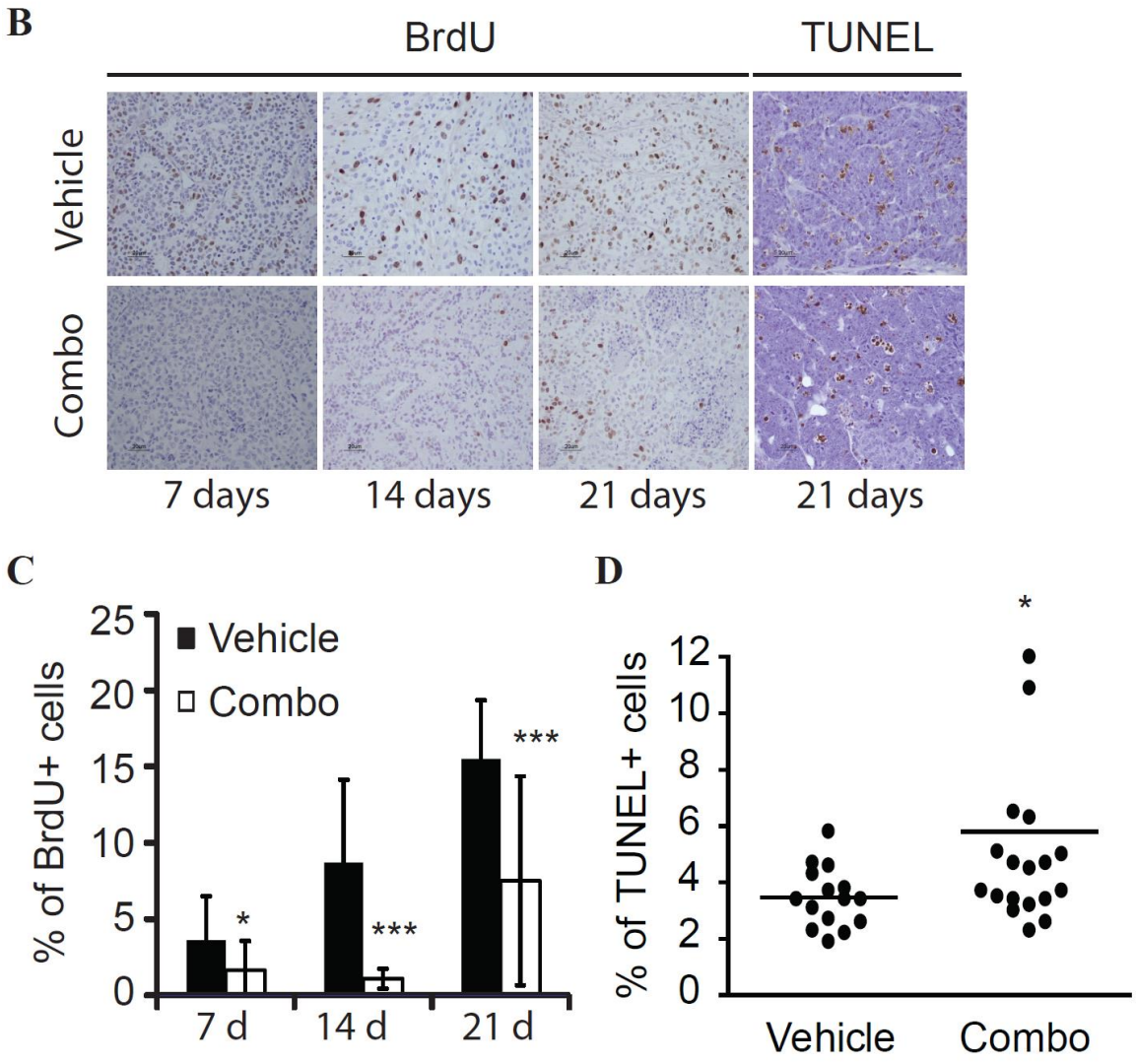

(B) Effects of this modified therapeutic strategy on proliferation and apoptosis in mice implanted with papillary tumors is shown. BrdU staining for mice after 7, 14, and 21 days of treatment, and TUNEL staining for mice after 21 days of treatment is depicted, scale bar = 20 um. (C) Quantification of BrdU staining in vehicle- or drug-treated mice implanted with papillary tumors. Number of mice that received the 7, 14, and 21 day treatment are 4, 3, and 4. 3 to 5 representative sections were examined for each tumor, *p=0.03, and ***p=0.003. Data is shown as mean± S.D. (D) Quantification of TUNEL staining in vehicle- or drug-treated mice implanted with papillary tumors receiving 21 days of treatment is shown with n=3 in the vehicle-treated group and n=4 in the drug-treated group. 5 sections per tumor were used for quantification. *p=0.02. All data were analyzed by two-tailed Student's t test.

Figure 3.13. EMT-specific combinatorial treatment in mice implanted with EMT or papillary tumors.

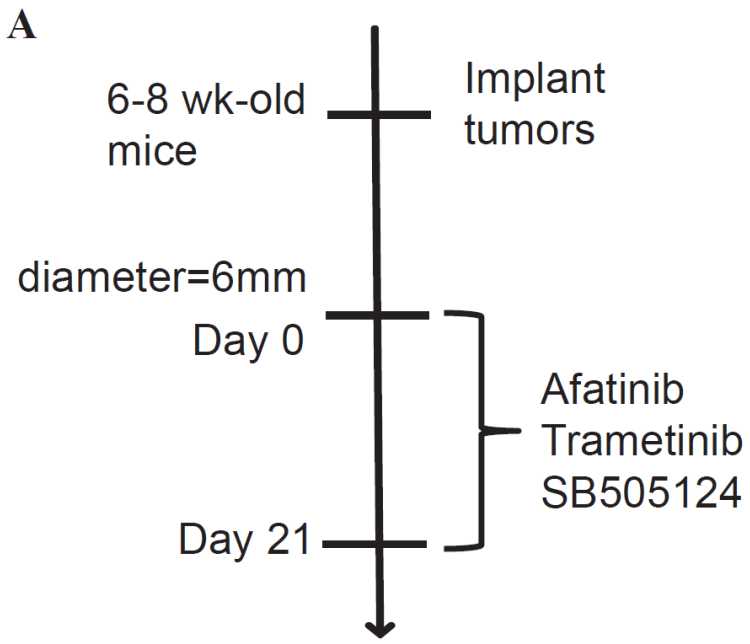

The design to test the therapeutic regimens for EMT tumors is shown (A). Each drug in the EMT-specific combinatorial treatment was given individually to mice orthotopically implanted with EMT tumors for 21 days.

Figure 3.13. (Cont'd)

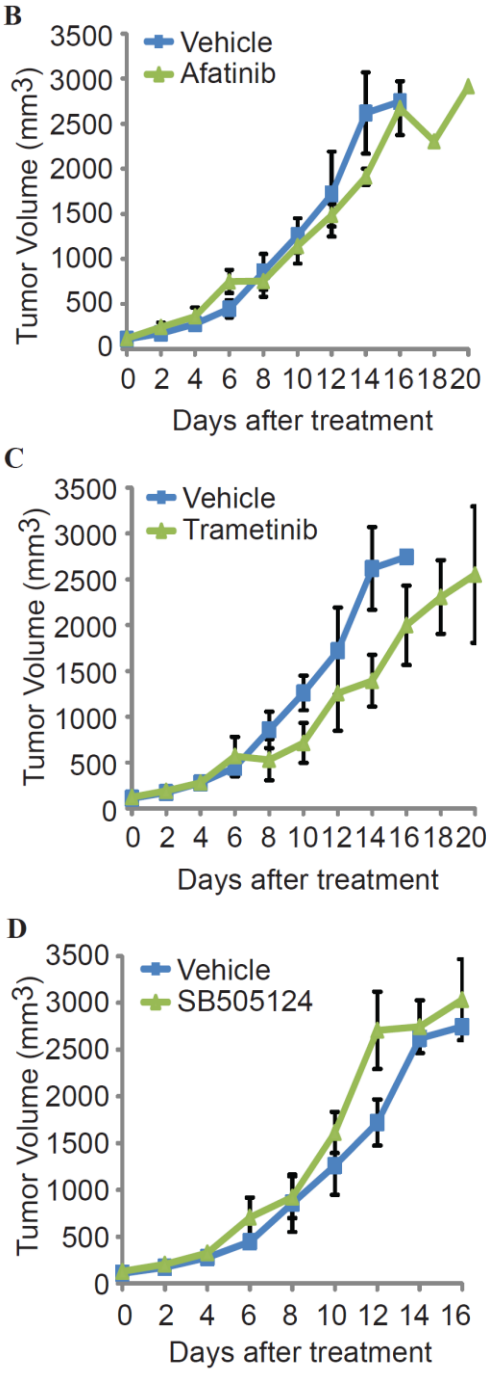

Effects of tumor growth rate are shown for (B) EGFR inhibitor alone (afatinib 15 mg/kg daily, oral), (C) MEK inhibitor alone (trametinib 1 mg/kg daily, oral), and (D) TGF-beta inhibitor alone (SB505124 10mg/kg daily, oral). n=4 for each group receiving each drug treatment.

Figure 3.13. (Cont'd)

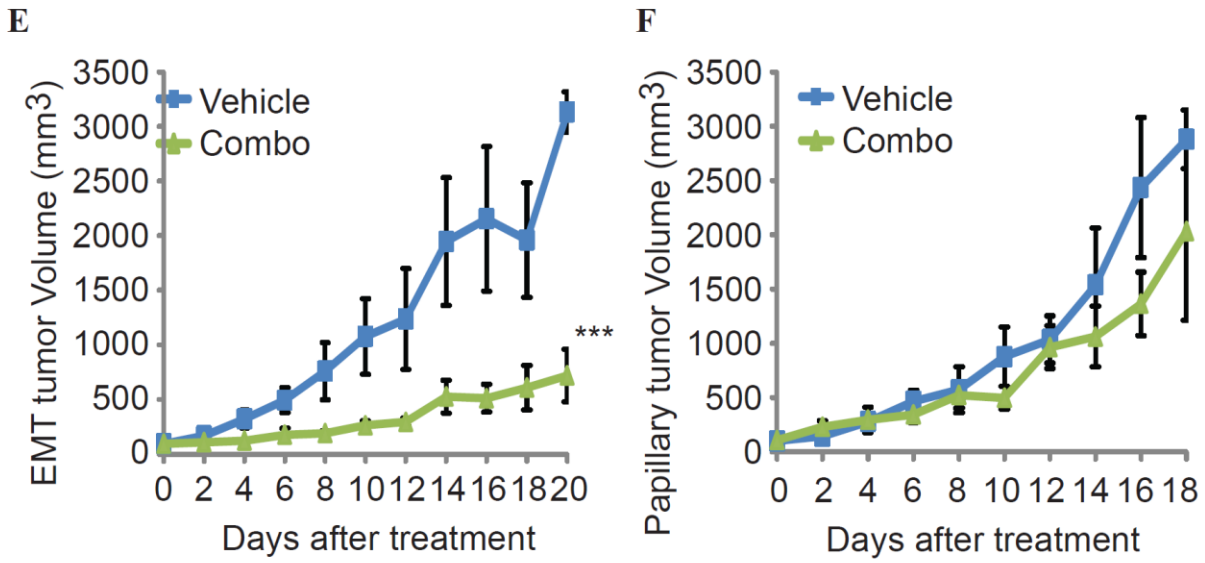

(E) Effects on tumor growth in mice orthotopically implanted with EMT tumors receiving the EMT-specific combinatorial therapeutic composed of the same dose and dosage regimen of each drug used in B-D for 21 days. p=0.008, n=5 for both vehicle and drug treated groups. (F) Specificity of the EMT-specific combinatorial treatment was tested in mice implanted with papillary subtype tumors for 21 days (n= 4 for each group). All data are mean ± S.D, and statistical analysis was performed with two-tailed Student's t-test.

Figure 3.14. Percentage of body weight changes in papillary tumor mice receiving revised papillary-specific combinatorial treatment.

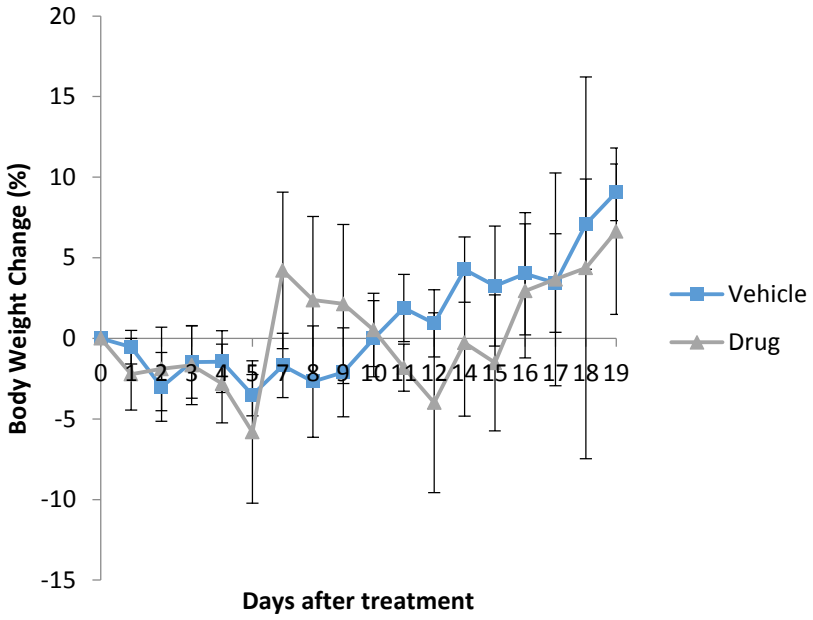

Compared to the original papillary-specific treatment, the dose of VX-680 was increased from 50 mg/kg to 60 mg/kg in this combinatorial treatment. N=4-6 in each group. All data are mean ± S.D.

Figure 3.15. Body weight change (shown in %) of mice received EMT-specific combinatorial treatment.

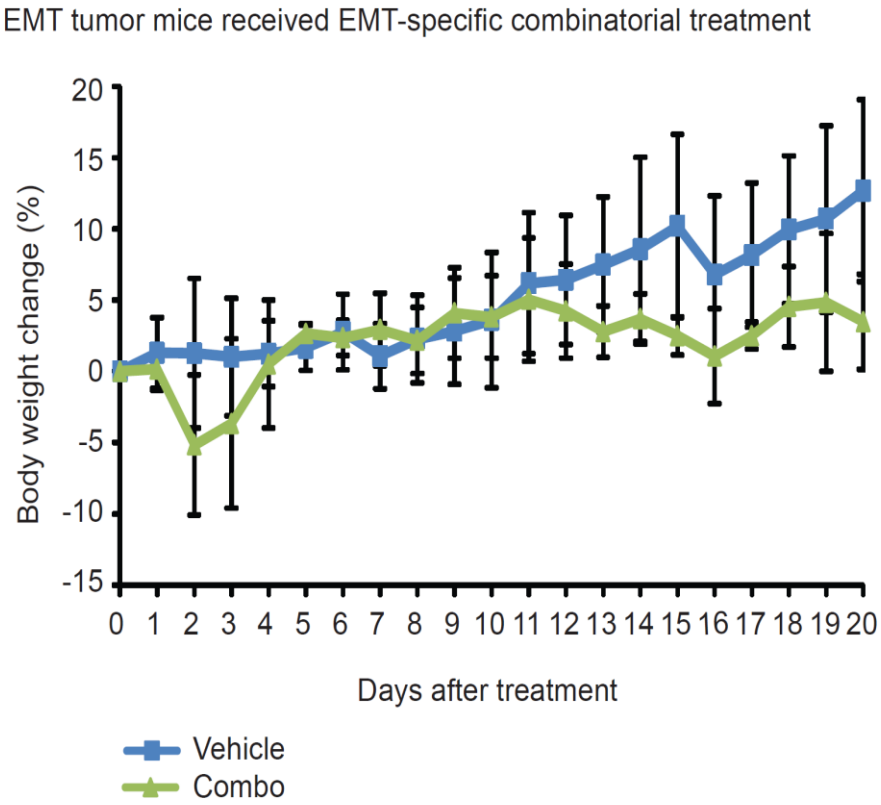

To test for side-effects associated with combinatorial treatment mice receiving treatment were assessed for changes to body weight. Body weight changes in mice with EMT tumors that received vehicle control or EMT-specific treatment were recorded as a percentage of the weight of the mice at the start of the trial with a 6mm tumor. For each group, n=5. This revealed no significant differences. All data are mean ± S.D.

Figure 3.16. Unsupervised clustering of pathway activation patterns of human breast cancer and patient-derived xenografts (PDXs).

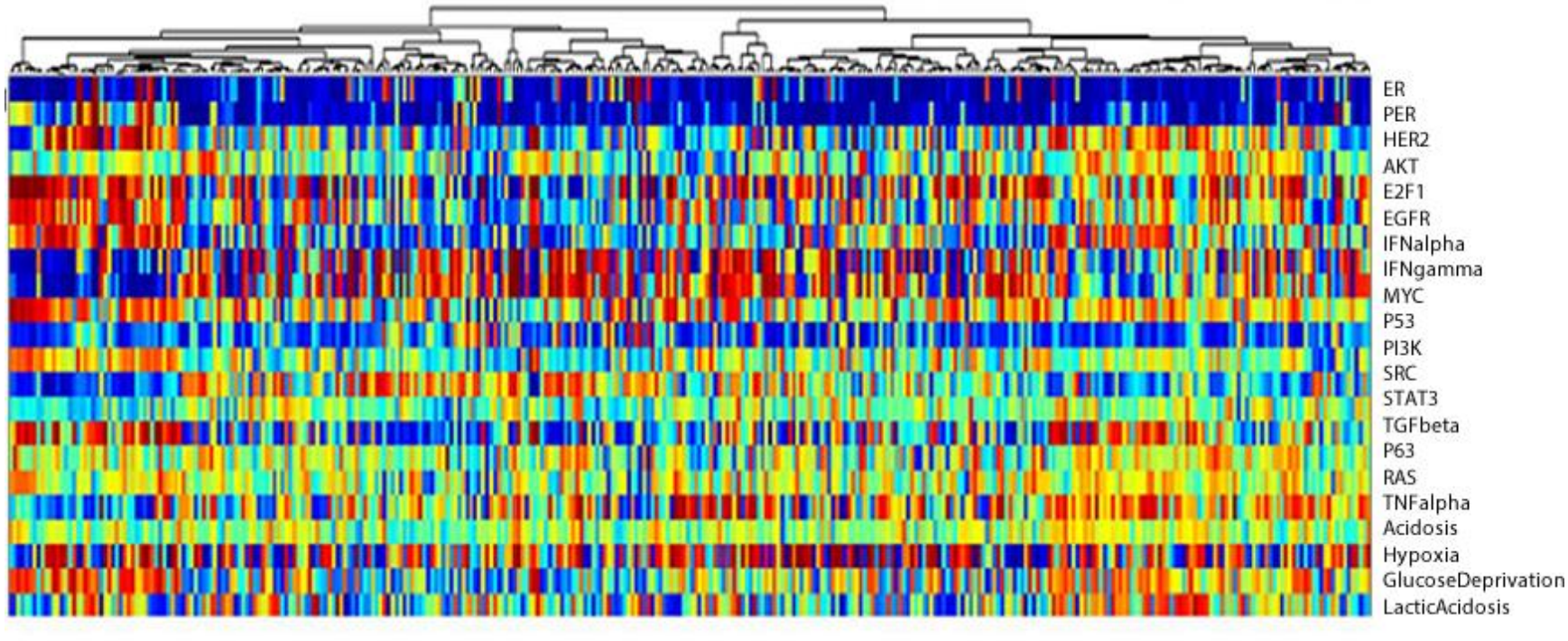

Seven human breast cancer microarray data and one human PDXs dataset were merged and the batch effects were removed. Only basal or TNBC subtype samples are shown.

Figure 3.17. Individualized combinatorial treatment in patient-derived breast cancer xenografts.

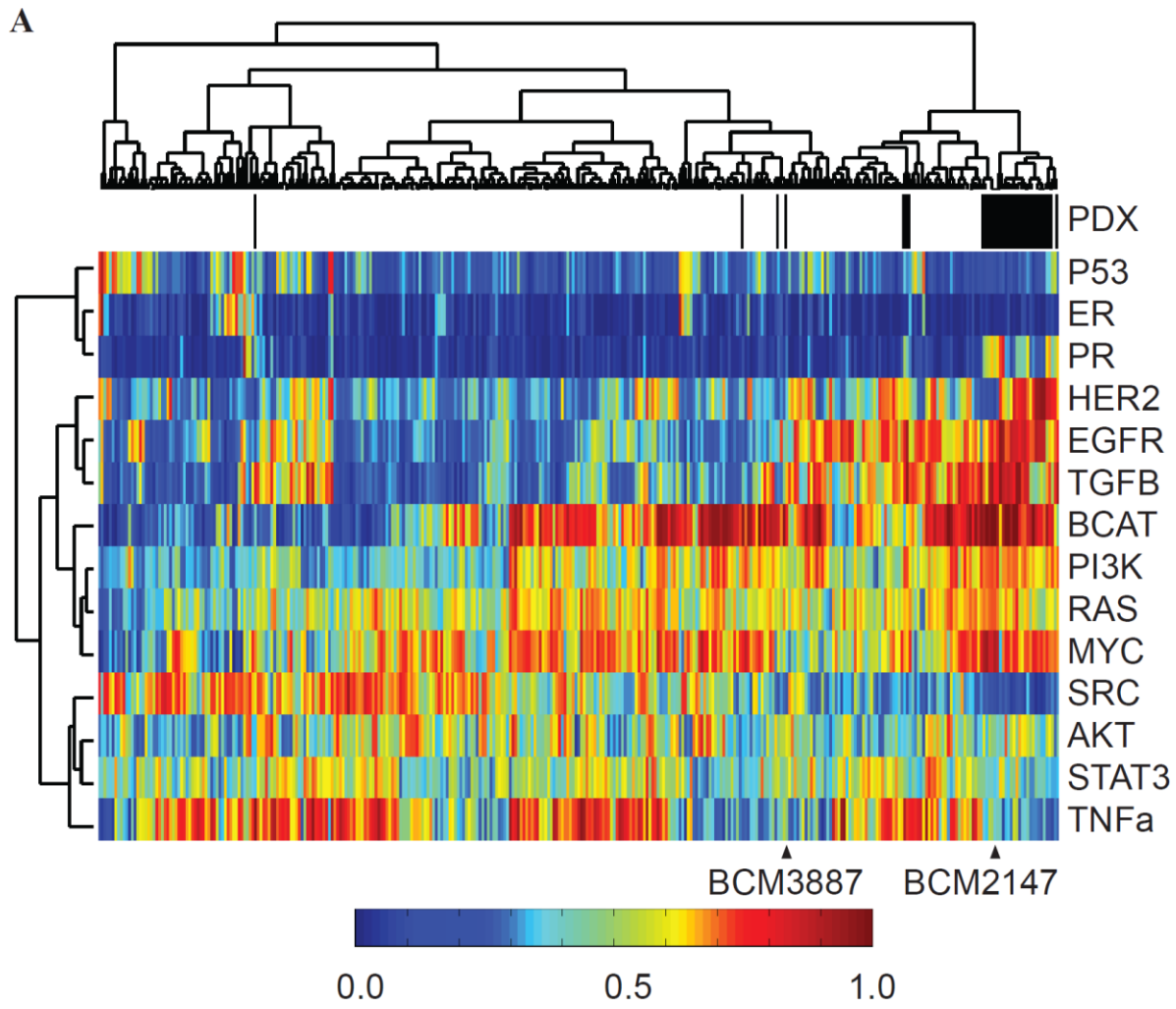

(A) Probability of cell signaling pathway activation was calculated for breast cancer samples and PDX lines. The resulting probabilities were used in an unsupervised clustering analysis to determine which PDX samples most closely represented the basal breast cancer samples from patients. The horizontal and vertical dendrograms show hierarchical clustering of samples and pathways, respectively. The black bars between the upper dendrogram and the heatmap identify samples from patient-derived xenografts and the white regions between the black bars identify breast cancer samples. The two patient-derived xenografts used in this study are marked with black triangles below the heatmap. The color map shows the probability of pathway activation with blue being a low probability of a pathway being active and red representing a high probability of a pathway being active.

Figure 3.17. (Cont'd)

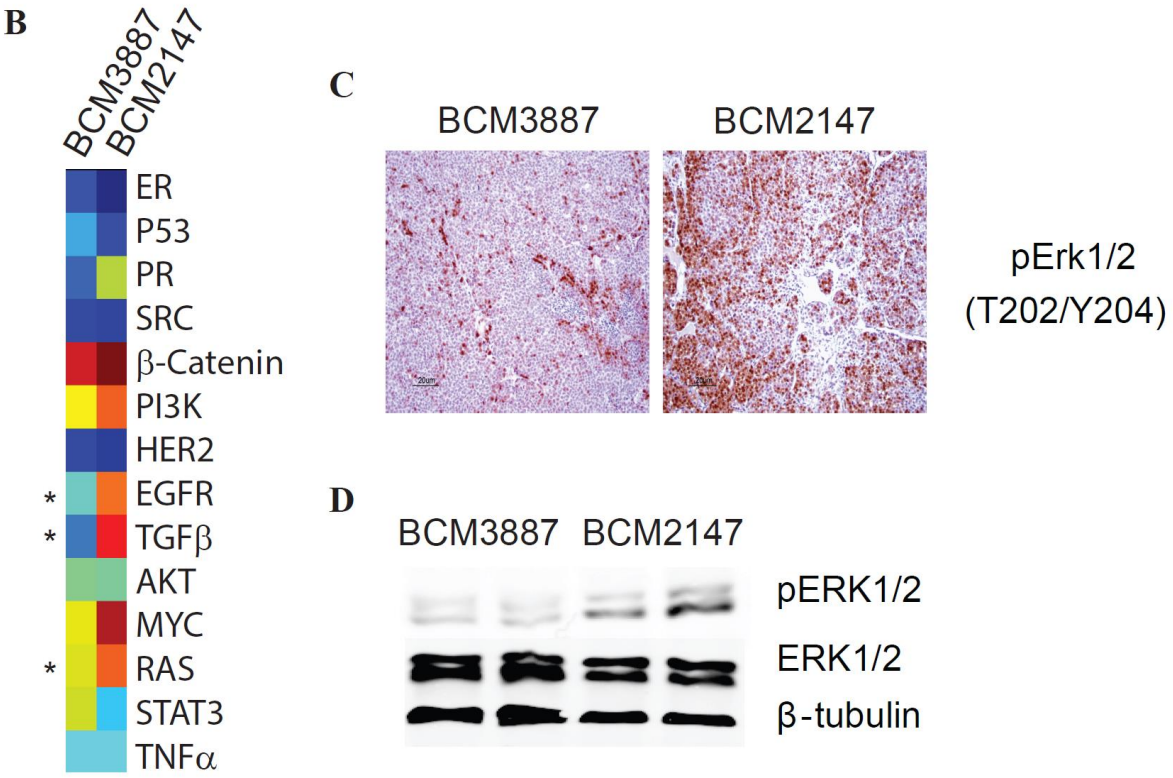

(B) In order to highlight the probability of pathway activation in the patient-derived xenografts samples selected for further study (labeled with triangles in (A)), the probability of pathway activation is shown. (C) Immunohistological staining and (D) Western blots of phospho-Erk1/2 in patient-derived xenografts confirm the predictions and are shown with each lane representing one tumor sample after growth in a mouse. Scale bar= 20 um

Figure 3.17. (Cont'd)

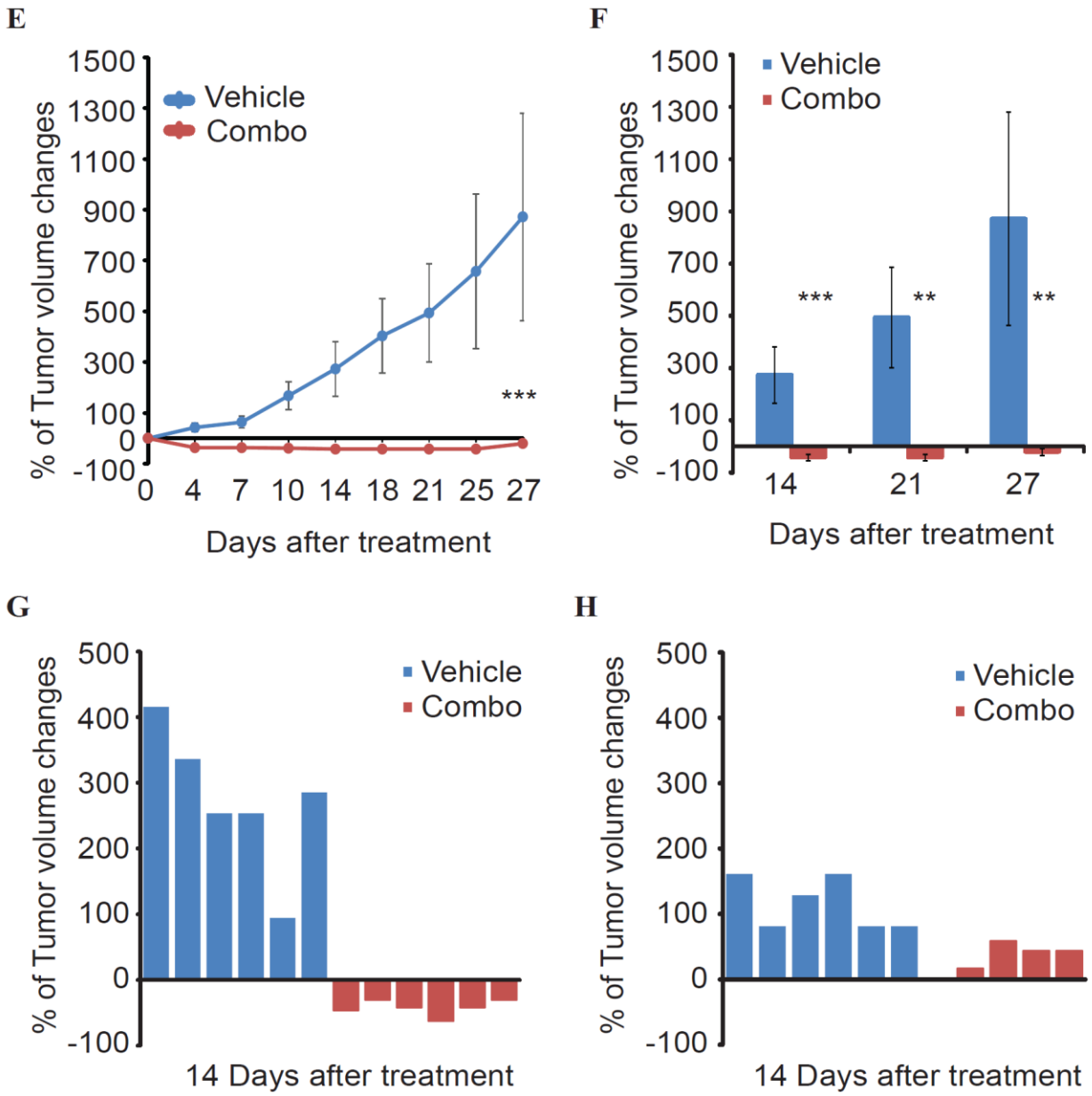

(E) Percentage change in tumor volume is depicted after the combinatorial treatment (12.5 mg/kg afatinib daily, 1 mg/kg trametinib daily, and 10 mg/kg SB505124 for 4 days per week) was given via oral gavage to mice orthotopically implanted with patient-derived xenograft BCM2147 (n=6 for each group). ***p=0.002. (F) The bar plot shows tumor volume change as a percentage in mice implanted with patient-derived xenograft BCM2147 after 14, 21, and 27 days of treatment. **p<0.05 and ***p<0.001. (G-H) Waterfall plots of percentage change in tumor volume after 14 days of treatment in mice orthotopically implanted with patient-derived

xenograft BCM2147 (G) and BCM3887 (H). Numbers of mice used in vehicle-treated BCM2147 or BCM3887, drug-treated BCM2147, and drug-treated BCM3887 are 6, 6, and 5 respectively.

Figure 3.17. (Cont'd)

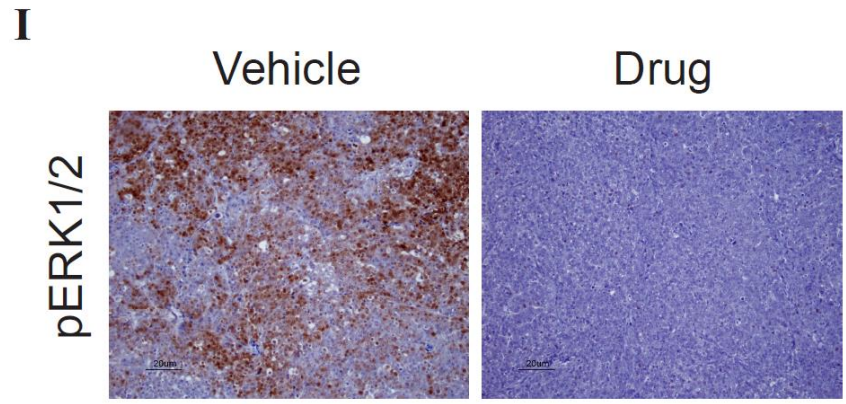

(I) Immunohistochemical staining of phospho-Erk1/2 in patient-derived xenografts BCM2147 receiving 21 days of drug or vehicle treatment. Scale bar= 20 um. All data are mean± S.D., and analyzed by two-tailed Student's t-test.

Figure 4.1. Alteration frequency of Myc in cancers.

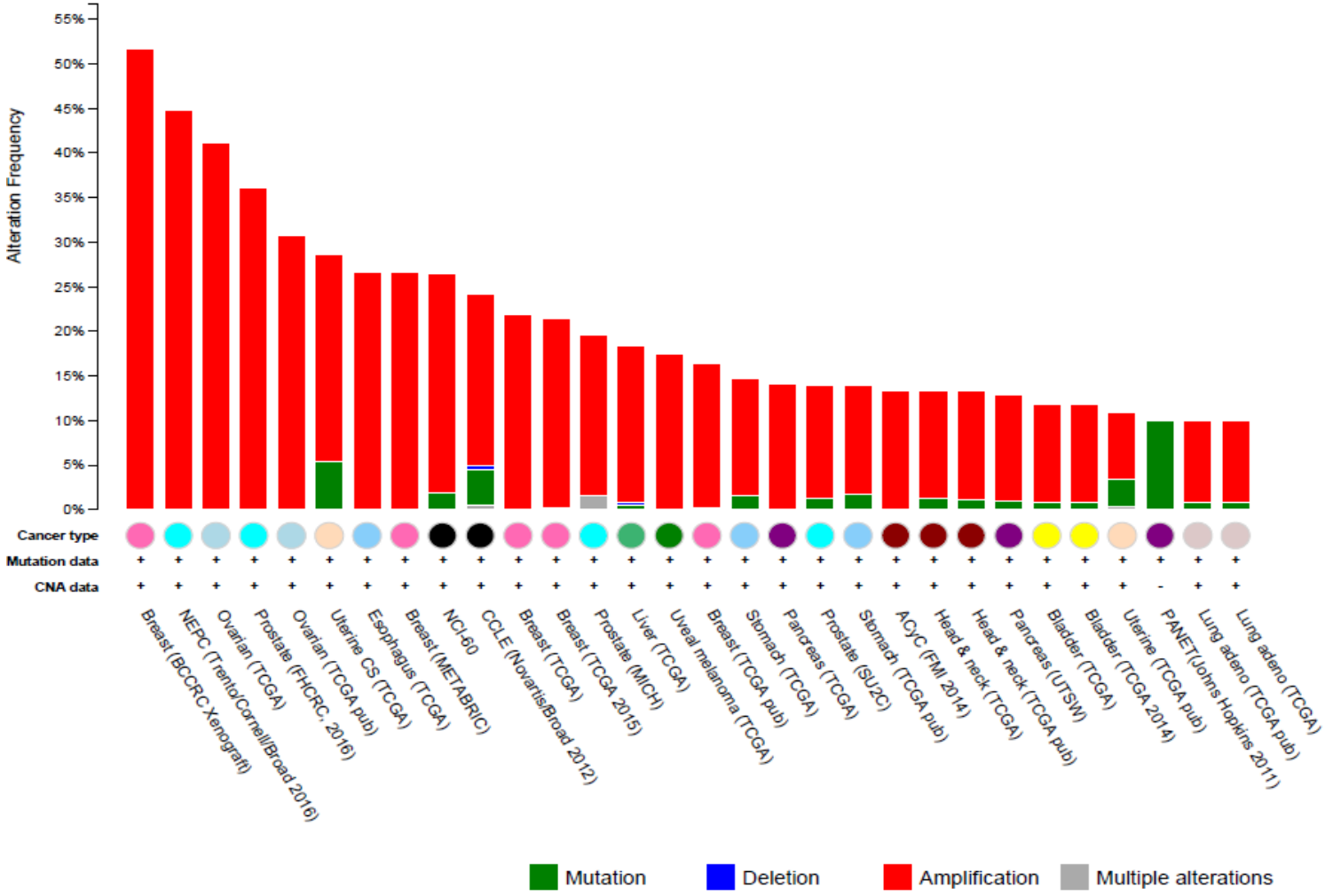

Only datasets have at least 10% of samples with alteration of Myc are shown. This figure is made according to the available data on cBioportal data website (http://www.cbioportal.org/) on Oct 3, 2016.

Figure 4.2. Stat3 has diverse functions in MMTV-Myc and MMTV-Neu tumors.

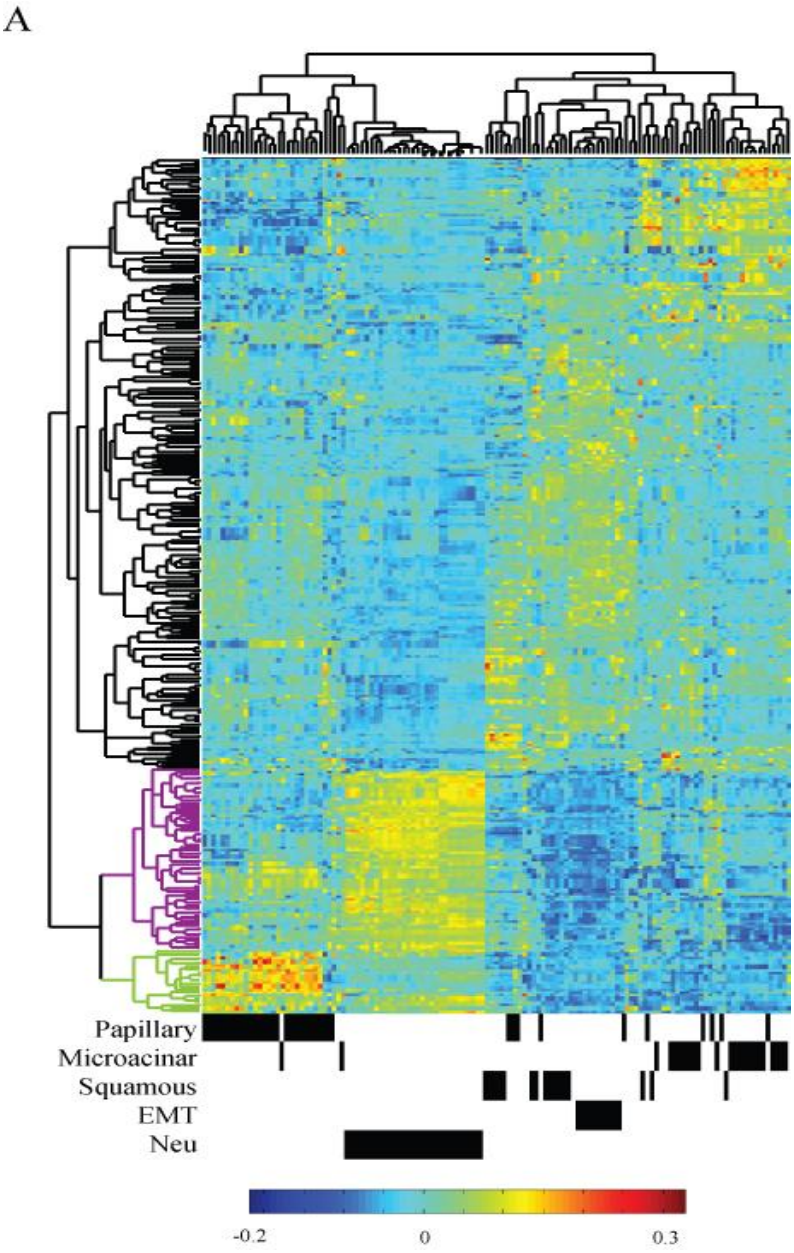

(A) Unsupervised clustering of the top up and down-regulated genes from the Stat3 pathway in MMTV-Myc and MMTV-Neu tumors. The dendrogram on the top shows the relationship among the individual tumors. The annotated information for histological subtypes of MMTV-Myc tumors and MMTV-Neu is shown at the bottom where a black bar represents a tumor sample. The vertical dendrogram represents clusters of genes. Black clusters represent genes downregulated by Stat3 activation. Purple and green clusters include genes up-regulated by Stat3 activation in MMTV-Neu tumor and in Myc papillary subtype tumors respectively.

Figure 4.2. (Cont'd)

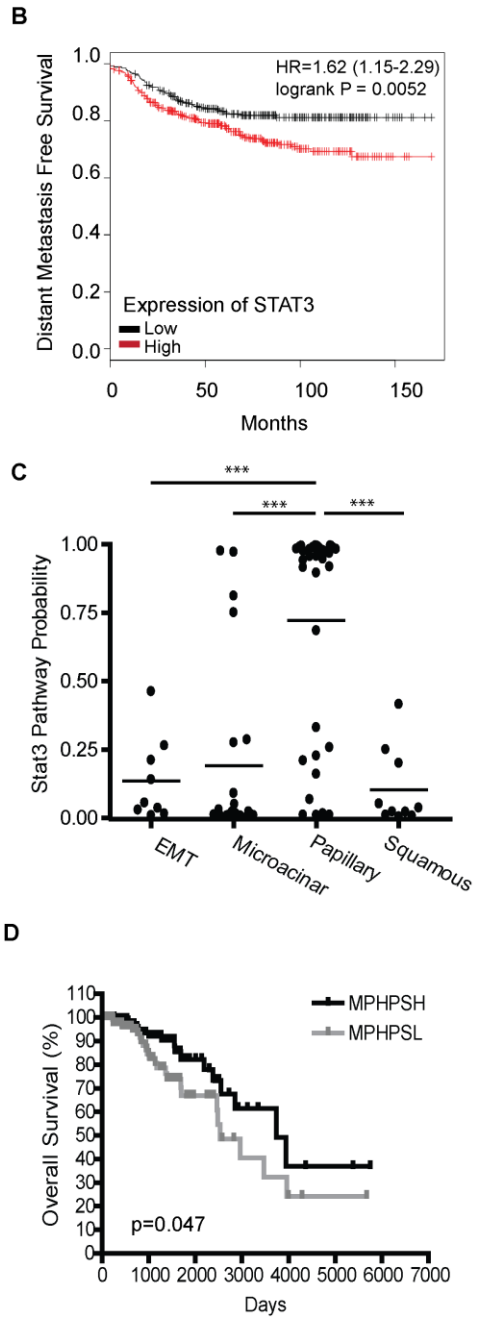

(B) A Kaplan-Meier plot demonstrates distant metastasis free survival in human breast cancer patients with clustered genes that are upregulated in the Stat3 pathway signature (shown in purple in panel A) in MMTV-Neu tumors. HR=1.62 (1.15-2.29) and logrank P = 0.0052. (C) Probability of Stat3 pathway activation in subtypes of MMTV-Myc tumors. ***p<0.001, two-tailed Student's t test. (D) A Kaplan-Meier plot showed overall survival of patients with high (MPHPSH) or low level of phosphorylated Stat3 (MPHPSL) in samples with high Myc pathway activity probability (p=0.047).

Figure 4.3. Physiological effect of STAT3 loss on mammary function.

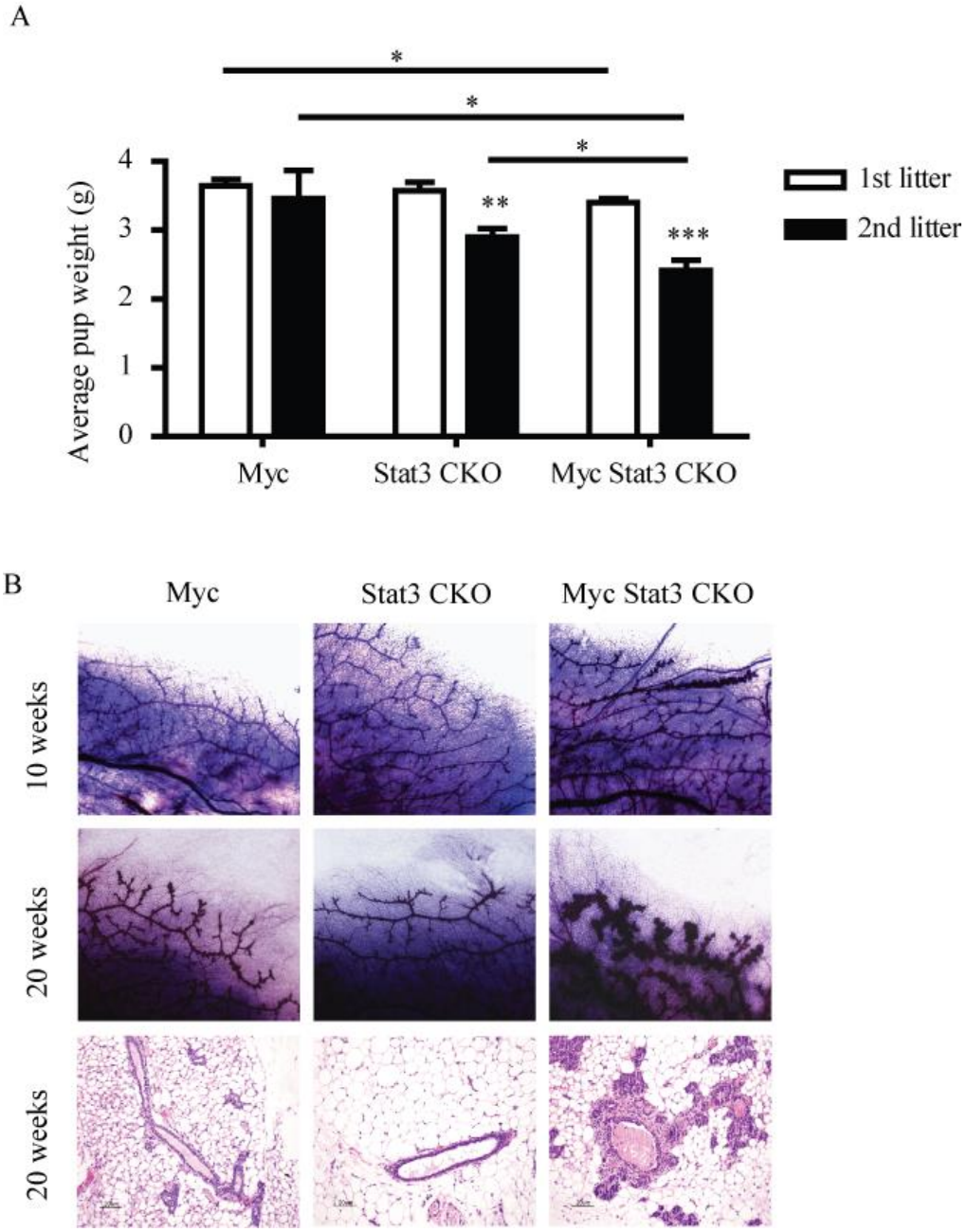

(A) Effects of STAT3 loss on the body weight of pups nursed by different genotypes of dams including MMTV-Myc, Stat3 CKO and Myc Stat3 CKO. The litter size was normalized to six pups one day post-partum. The average body weights of the first and second litter pups on Day 5 are shown with an n of at least six per group. Data were analyzed by two-tailed t-test. * $p<0.05$; ** $p<0.01$; *** $p<0.001$. (B) Whole mount staining (top and middle rows) in 10- and 20-week-old virgin mice as well as hematoxylin and eosin staining (bottom row) of mammary glands in 20-week-old virgin mice are shown. Representative images were chosen for each.

Figure 4.4. Loss of STAT3 alters tumor onset and tumor growth.

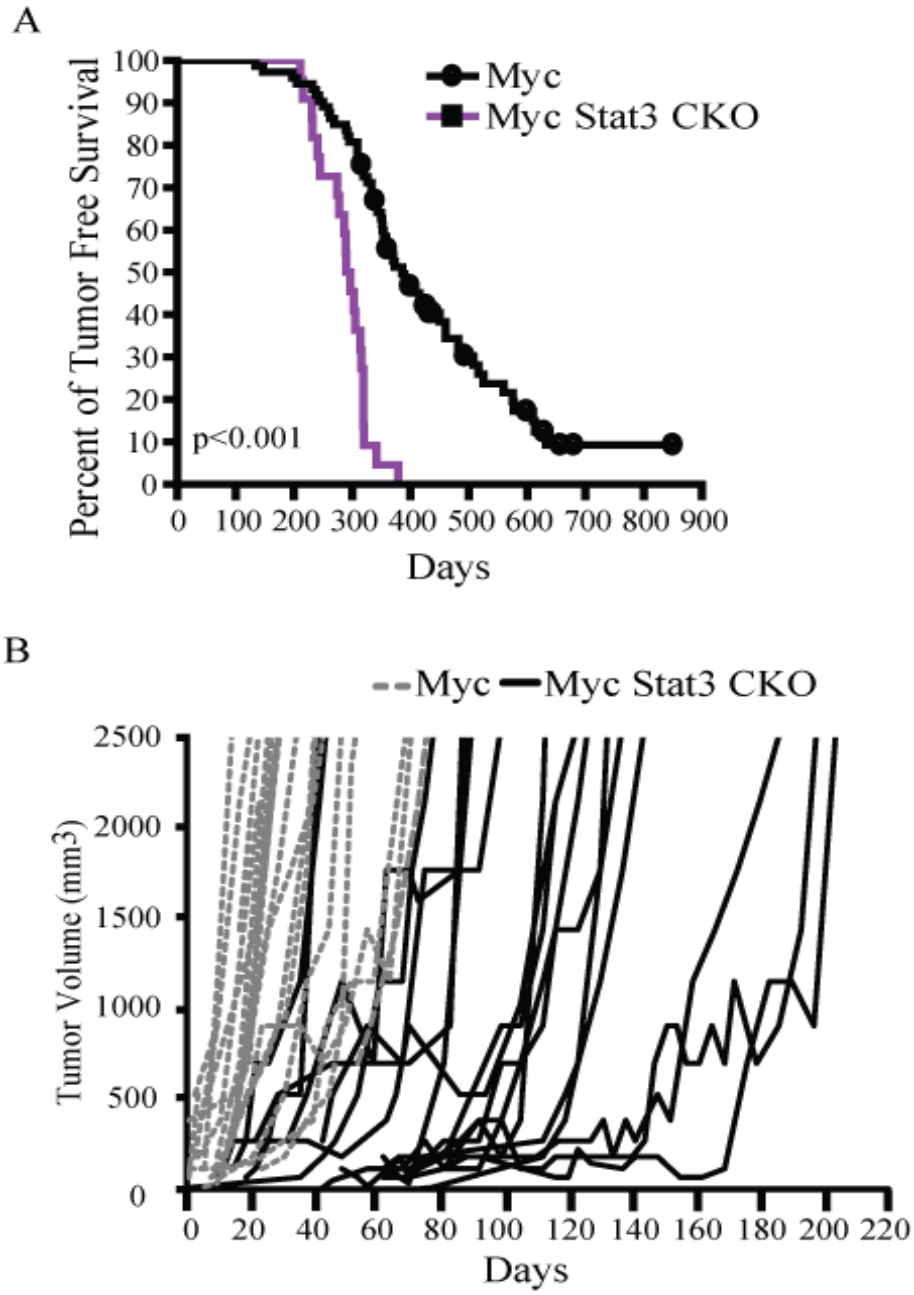

(A) A Kaplan-Meier plot of tumor-free survival for MMTV-Myc (n=73) and Myc Stat3 CKO (n=22). (B) Tumor growth curves are shown for individual tumors. MMTV-Myc mice are shown with dashed lines (n=20). Myc Stat3 CKO mice are shown with solid black lines (n=18).

Figure 4.4. (Cont'd)

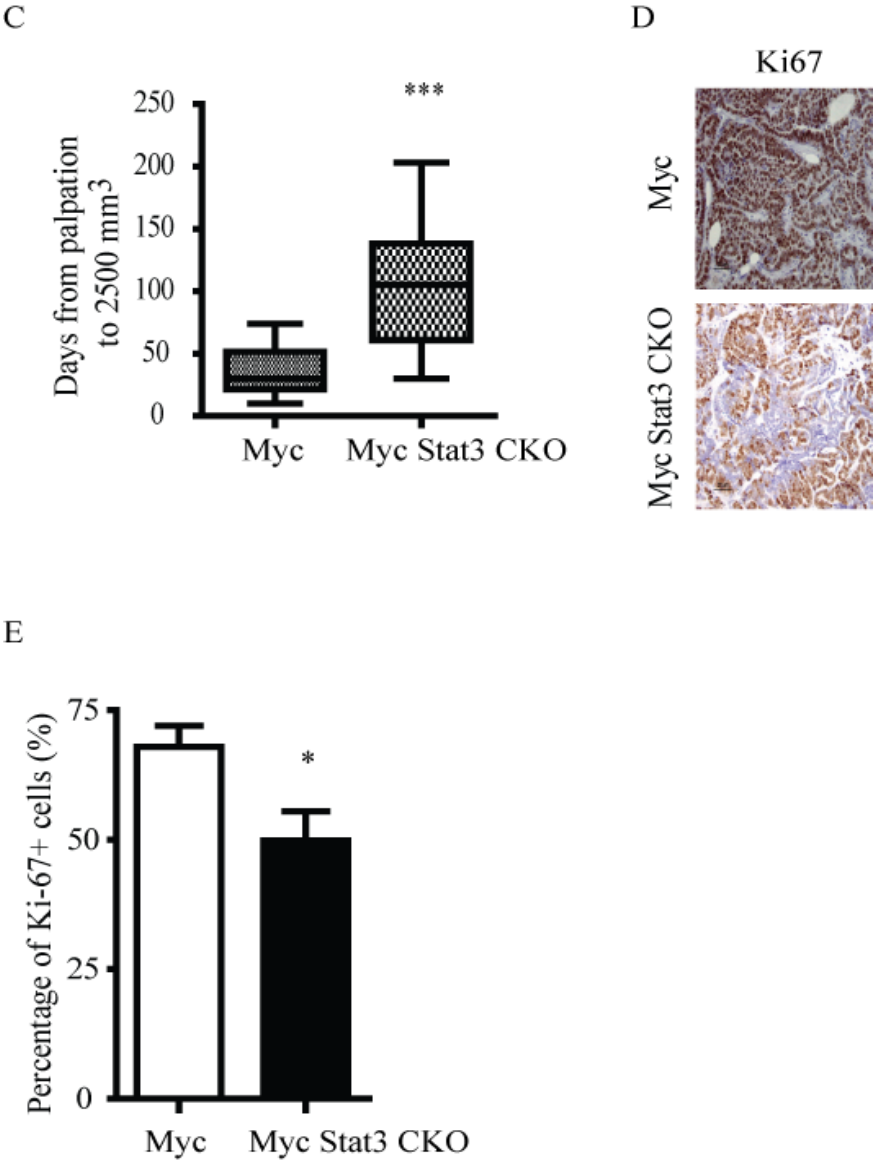

(C) A box plot of days from palpation to 2500 mm^3 reveals slowed tumor growth in the Myc Stat3 CKO mice with an average of 36 days from palpation to endpoint in MMTV-Myc mice (n=32), and 109 days in the Myc Stat3 CKO mice (n=20). ***p<0.001. (D) Ki67 staining of mammary tumors in MMTV-Myc and Myc Stat3 CKO mice reveals a reduction in Ki67 staining. Representative pictures (D) and quantification results (E) are shown. Data are mean ± S.D.*p<0.05. ***p<0.001, two-tailed Student's t test.

Figure 4.5. Incomplete excision of Stat3 in mammary tumors.

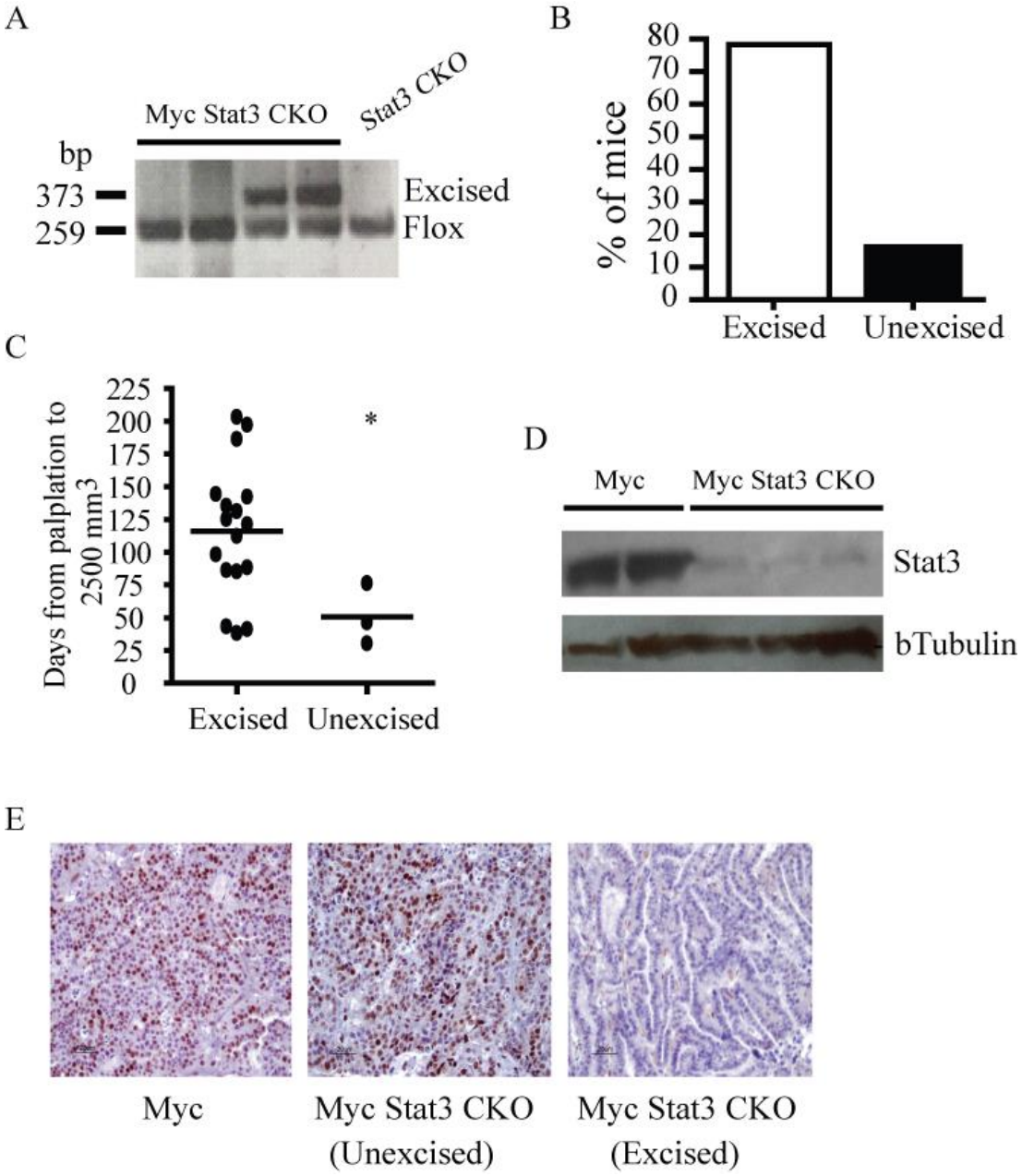

(A) Excision of Stat3 in tumors was tested using PCR with tail DNA of $STAT3^{Fl/Fl}$ mice as a control. (B) Excision PCR demonstrated that 16% (6 out of 37) tumors did not have detectable STAT3 excision. (C) Examination of tumor growth rate showed that excision of Stat3 in Myc induced tumors was associated with delayed growth rate. *p= 0.04, two-tailed Student's t test. (D) To ensure excision was associated with protein loss, western blot of STAT3 in mammary tumors from MMTV-Myc and Myc with excised Stat3 was conducted. (E) Representative images are shown from immunohistochemistry for pSTAT3 (Y705) conducted on Myc tumors and Myc Stat3 CKO tumors without and with excision.

Figure 4.6. Loss of Stat3 alters tumor histology.

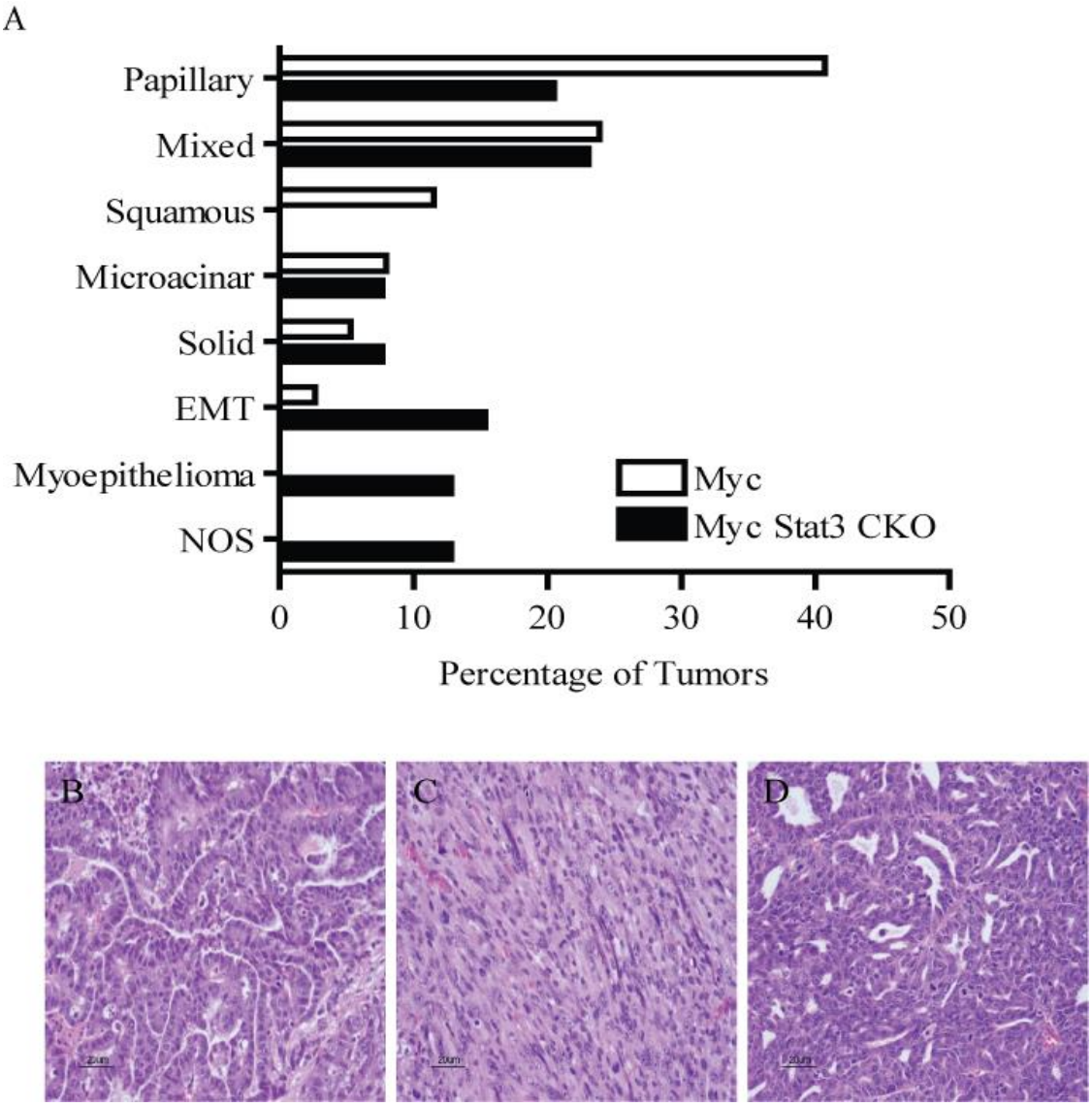

(A) Quantification of the histological subtypes of mammary tumors observed in MMTV-Myc and Myc Stat3 CKO mice reveals histological differences in Myc induced tumors lacking Stat3. EMT – Epithelial to Mesenchymal Transition, NOS – Not otherwise specified. Representative images with hematoxylin and eosin staining from various subtypes including papillary (B), EMT (C), and myoepithelioma (D) are shown.

Figure 4.7. STAT3 ablation affects angiogenesis and inflammation.

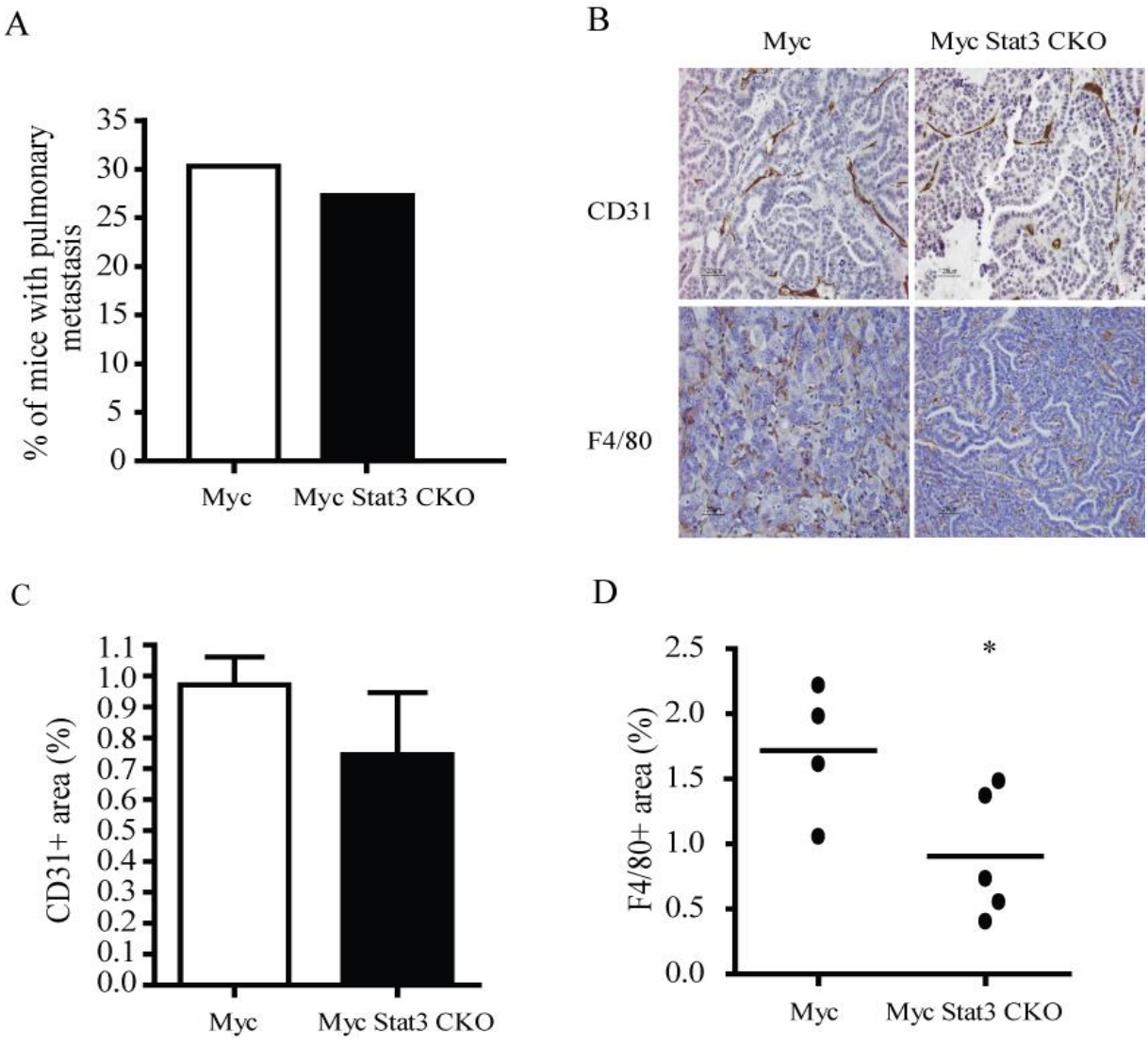

(A) The percentage of mice with lung metastases at end point (tumor volume reaches 2500 mm^3) did not reveal an alteration in metastatic capacity with loss of Stat3.
(B) Immunohistochemistry for CD31 in mammary tumors from MMTV-Myc and Myc Stat3 CKO mice reveals a decrease in CD31 staining. (C) Quantification of CD31 staining was determined by CD31+ per tumor area (mm^3). n=5 per genotype and n=5 per mouse. Data are mean ± S.D. (D) F4/80 staining of mammary tumors in MMTV-Myc and Myc Stat3 CKO mice revealed a reduction in F4/80 staining with the loss of Stat3. The percentage of F4/80 was calculated by F4/80+ per tumor area (mm^3) and quantification is shown (E). *$p<0.05$.

BIBLIOGRAPHY

BIBLIOGRAPHY

Aas, T., A. L. Borresen, S. Geisler, B. Smith-Sorensen, H. Johnsen, J. E. Varhaug, L. A. Akslen and P. E. Lonning (1996). "Specific P53 mutations are associated with de novo resistance to doxorubicin in breast cancer patients." Nat Med **2**(7): 811-814.

Aghib, D. F., J. M. Bishop, S. Ottolenghi, A. Guerrasio, A. Serra and G. Saglio (1990). "A 3' truncation of MYC caused by chromosomal translocation in a human T-cell leukemia increases mRNA stability." Oncogene **5**(5): 707-711.

Aleskandarany, M. A., D. Agarwal, O. H. Negm, G. Ball, A. Elmouna, I. Ashankyty, E. Nuglozeh, M. F. Fazaludeen, M. Diez-Rodriguez, C. C. Nolan, P. J. Tighe, A. R. Green, I. O. Ellis and E. A. Rakha (2016). "The prognostic significance of STAT3 in invasive breast cancer: analysis of protein and mRNA expressions in large cohorts." Breast Cancer Res Treat **156**(1): 9-20.

Alexander, W. S. and D. J. Hilton (2004). "The role of suppressors of cytokine signaling (SOCS) proteins in regulation of the immune response." Annu Rev Immunol **22**: 503-529.

Alexandrow, M. G., M. Kawabata, M. Aakre and H. L. Moses (1995). "Overexpression of the c-Myc oncoprotein blocks the growth-inhibitory response but is required for the mitogenic effects of transforming growth factor beta 1." Proc Natl Acad Sci U S A **92**(8): 3239-3243.

Amati, B., M. W. Brooks, N. Levy, T. D. Littlewood, G. I. Evan and H. Land (1993). "Oncogenic activity of the c-Myc protein requires dimerization with Max." Cell **72**(2): 233-245.

Andre, F., R. O'Regan, M. Ozguroglu, M. Toi, B. Xu, G. Jerusalem, N. Masuda, S. Wilks, F. Arena, C. Isaacs, Y. S. Yap, Z. Papai, I. Lang, A. Armstrong, G. Lerzo, M. White, K. Shen, J. Litton, D. Chen, Y. Zhang, S. Ali, T. Taran and L. Gianni (2014). "Everolimus for women with trastuzumab-resistant, HER2-positive, advanced breast cancer (BOLERO-3): a randomised, double-blind, placebo-controlled phase 3 trial." Lancet Oncol **15**(6): 580-591.

Andrechek, E. R., R. D. Cardiff, J. T. Chang, M. L. Gatza, C. R. Acharya, A. Potti and J. R. Nevins (2009). "Genetic heterogeneity of Myc-induced mammary tumors reflecting diverse phenotypes including metastatic potential." Proc Natl Acad Sci U S A **106**(38): 16387-16392.

Andrechek, E. R., S. Mori, R. E. Rempel, J. T. Chang and J. R. Nevins (2008). "Patterns of cell signaling pathway activation that characterize mammary development." Development **135**(14): 2403-2413.

Andres, A. C., C. A. Schonenberger, B. Groner, L. Hennighausen, M. LeMeur and P. Gerlinger (1987). "Ha-ras oncogene expression directed by a milk protein gene promoter: tissue specificity, hormonal regulation, and tumor induction in transgenic mice." Proc Natl Acad Sci U S A **84**(5): 1299-1303.

Aoki, Y., G. M. Feldman and G. Tosato (2003). "Inhibition of STAT3 signaling induces apoptosis and decreases survivin expression in primary effusion lymphoma." Blood **101**(4): 1535-1542.

Arap, W., R. Pasqualini and E. Ruoslahti (1998). "Cancer treatment by targeted drug delivery to tumor vasculature in a mouse model." Science **279**(5349): 377-380.

Arps, D. P., P. Healy, L. Zhao, C. G. Kleer and J. C. Pang (2013). "Invasive ductal carcinoma with lobular features: a comparison study to invasive ductal and invasive lobular carcinomas of the breast." Breast Cancer Res Treat **138**(3): 719-726.

Ayer, D. E., L. Kretzner and R. N. Eisenman (1993). "Mad: a heterodimeric partner for Max that antagonizes Myc transcriptional activity." Cell **72**(2): 211-222.

Bahram, F., N. von der Lehr, C. Cetinkaya and L. G. Larsson (2000). "c-Myc hot spot mutations in lymphomas result in inefficient ubiquitination and decreased proteasome-mediated turnover." Blood **95**(6): 2104-2110.

Balko, J. M., J. M. Giltnane, K. Wang, L. J. Schwarz, C. D. Young, R. S. Cook, P. Owens, M. E. Sanders, M. G. Kuba, V. Sanchez, R. Kurupi, P. D. Moore, J. A. Pinto, F. D. Doimi, H. Gomez, D. Horiuchi, A. Goga, B. D. Lehmann, J. A. Bauer, J. A. Pietenpol, J. S. Ross, G. A. Palmer, R. Yelensky, M. Cronin, V. A. Miller, P. J. Stephens and C. L. Arteaga (2014). "Molecular profiling of the residual disease of triple-negative breast cancers after neoadjuvant chemotherapy identifies actionable therapeutic targets." Cancer Discov **4**(2): 232-245.

Barry, S. P., P. A. Townsend, R. A. Knight, T. M. Scarabelli, D. S. Latchman and A. Stephanou (2010). "STAT3 modulates the DNA damage response pathway." Int J Exp Pathol **91**(6): 506-514.

Bartlett, J. M., J. Thomas, D. T. Ross, R. S. Seitz, B. Z. Ring, R. A. Beck, H. C. Pedersen, A. Munro, I. H. Kunkler, F. M. Campbell, W. Jack, G. R. Kerr, L. Johnstone, D. A. Cameron and U.

Chetty (2010). "Mammostrat as a tool to stratify breast cancer patients at risk of recurrence during endocrine therapy." Breast Cancer Res **12**(4): R47.

Baselga, J., J. Cortes, S. B. Kim, S. A. Im, R. Hegg, Y. H. Im, L. Roman, J. L. Pedrini, T. Pienkowski, A. Knott, E. Clark, M. C. Benyunes, G. Ross, S. M. Swain and C. S. Group (2012). "Pertuzumab plus trastuzumab plus docetaxel for metastatic breast cancer." N Engl J Med **366**(2): 109-119.

Baudino, T. A., C. McKay, H. Pendeville-Samain, J. A. Nilsson, K. H. Maclean, E. L. White, A. C. Davis, J. N. Ihle and J. L. Cleveland (2002). "c-Myc is essential for vasculogenesis and angiogenesis during development and tumor progression." Genes Dev **16**(19): 2530-2543.

Bean, J., C. Brennan, J. Y. Shih, G. Riely, A. Viale, L. Wang, D. Chitale, N. Motoi, J. Szoke, S. Broderick, M. Balak, W. C. Chang, C. J. Yu, A. Gazdar, H. Pass, V. Rusch, W. Gerald, S. F. Huang, P. C. Yang, V. Miller, M. Ladanyi, C. H. Yang and W. Pao (2007). "MET amplification occurs with or without T790M mutations in EGFR mutant lung tumors with acquired resistance to gefitinib or erlotinib." Proc Natl Acad Sci U S A **104**(52): 20932-20937.

Bear, H. D., G. Tang, P. Rastogi, C. E. Geyer, Jr., Q. Liu, A. Robidoux, L. Baez-Diaz, A. M. Brufsky, R. S. Mehta, L. Fehrenbacher, J. A. Young, F. M. Senecal, R. Gaur, R. G. Margolese, P. T. Adams, H. M. Gross, J. P. Costantino, S. Paik, S. M. Swain, E. P. Mamounas and N. Wolmark (2015). "Neoadjuvant plus adjuvant bevacizumab in early breast cancer (NSABP B-40 [NRG Oncology]): secondary outcomes of a phase 3, randomised controlled trial." Lancet Oncol **16**(9): 1037-1048.

Berishaj, M., S. P. Gao, S. Ahmed, K. Leslie, H. Al-Ahmadie, W. L. Gerald, W. Bornmann and J. F. Bromberg (2007). "Stat3 is tyrosine-phosphorylated through the interleukin-6/glycoprotein 130/Janus kinase pathway in breast cancer." Breast Cancer Res **9**(3): R32.

Berns, K., H. M. Horlings, B. T. Hennessy, M. Madiredjo, E. M. Hijmans, K. Beelen, S. C. Linn, A. M. Gonzalez-Angulo, K. Stemke-Hale, M. Hauptmann, R. L. Beijersbergen, G. B. Mills, M. J. van de Vijver and R. Bernards (2007). "A functional genetic approach identifies the PI3K pathway as a major determinant of trastuzumab resistance in breast cancer." Cancer Cell **12**(4): 395-402.

Bernstein, P. L., D. J. Herrick, R. D. Prokipcak and J. Ross (1992). "Control of c-myc mRNA half-life in vitro by a protein capable of binding to a coding region stability determinant." Genes Dev **6**(4): 642-654.

Beroukhim, R., C. H. Mermel, D. Porter, G. Wei, S. Raychaudhuri, J. Donovan, J. Barretina, J. S. Boehm, J. Dobson, M. Urashima, K. T. Mc Henry, R. M. Pinchback, A. H. Ligon, Y. J. Cho, L.

Haery, H. Greulich, M. Reich, W. Winckler, M. S. Lawrence, B. A. Weir, K. E. Tanaka, D. Y. Chiang, A. J. Bass, A. Loo, C. Hoffman, J. Prensner, T. Liefeld, Q. Gao, D. Yecies, S. Signoretti, E. Maher, F. J. Kaye, H. Sasaki, J. E. Tepper, J. A. Fletcher, J. Tabernero, J. Baselga, M. S. Tsao, F. Demichelis, M. A. Rubin, P. A. Janne, M. J. Daly, C. Nucera, R. L. Levine, B. L. Ebert, S. Gabriel, A. K. Rustgi, C. R. Antonescu, M. Ladanyi, A. Letai, L. A. Garraway, M. Loda, D. G. Beer, L. D. True, A. Okamoto, S. L. Pomeroy, S. Singer, T. R. Golub, E. S. Lander, G. Getz, W. R. Sellers and M. Meyerson (2010). "The landscape of somatic copy-number alteration across human cancers." Nature **463**(7283): 899-905.

Bertucci, F., M. Fekih, A. Autret, T. Petit, F. Dalenc, C. Levy, G. Romieu, J. Bonneterre, J. M. Ferrero, P. Kerbrat, P. Soulie, M. A. Mouret-Reynier, T. Bachelot, F. Lerebours, J. C. Eymard, M. Deblock, A. Lortholary, A. C. Hardy-Bessard, P. Barthelemy, H. Bonnefoi, E. Charafe-Jauffret, F. C. Bidard, P. Viens, J. Lemonnier and J. Y. Pierga (2016). "Bevacizumab plus neoadjuvant chemotherapy in patients with HER2-negative inflammatory breast cancer (BEVERLY-1): a multicentre, single-arm, phase 2 study." Lancet Oncol **17**(5): 600-611.

Bhatt, A. P., P. M. Bhende, S. H. Sin, D. Roy, D. P. Dittmer and B. Damania (2010). "Dual inhibition of PI3K and mTOR inhibits autocrine and paracrine proliferative loops in PI3K/Akt/mTOR-addicted lymphomas." Blood **115**(22): 4455-4463.

Bieche, I., I. Laurendeau, S. Tozlu, M. Olivi, D. Vidaud, R. Lidereau and M. Vidaud (1999). "Quantitation of MYC gene expression in sporadic breast tumors with a real-time reverse transcription-PCR assay." Cancer Res **59**(12): 2759-2765.

Bild, A. H., G. Yao, J. T. Chang, Q. Wang, A. Potti, D. Chasse, M. B. Joshi, D. Harpole, J. M. Lancaster, A. Berchuck, J. A. Olson, Jr., J. R. Marks, H. K. Dressman, M. West and J. R. Nevins (2006). "Oncogenic pathway signatures in human cancers as a guide to targeted therapies." Nature **439**(7074): 353-357.

Bines, J., D. M. Oleske and M. A. Cobleigh (1996). "Ovarian function in premenopausal women treated with adjuvant chemotherapy for breast cancer." J Clin Oncol **14**(5): 1718-1729.

Blackwell, K. L., H. J. Burstein, A. M. Storniolo, H. Rugo, G. Sledge, M. Koehler, C. Ellis, M. Casey, S. Vukelja, J. Bischoff, J. Baselga and J. O'Shaughnessy (2010). "Randomized study of Lapatinib alone or in combination with trastuzumab in women with ErbB2-positive, trastuzumab-refractory metastatic breast cancer." J Clin Oncol **28**(7): 1124-1130.

Blackwood, E. M. and R. N. Eisenman (1991). "Max: a helix-loop-helix zipper protein that forms a sequence-specific DNA-binding complex with Myc." Science **251**(4998): 1211-1217.

Blakely, C. M., L. Sintasath, C. M. D'Cruz, K. T. Hahn, K. D. Dugan, G. K. Belka and L. A. Chodosh (2005). "Developmental stage determines the effects of MYC in the mammary epithelium." Development **132**(5): 1147-1160.

Borowsky, A. D., R. Namba, L. J. Young, K. W. Hunter, J. G. Hodgson, C. G. Tepper, E. T. McGoldrick, W. J. Muller, R. D. Cardiff and J. P. Gregg (2005). "Syngeneic mouse mammary carcinoma cell lines: two closely related cell lines with divergent metastatic behavior." Clin Exp Metastasis **22**(1): 47-59.

Boxer, R. B., J. W. Jang, L. Sintasath and L. A. Chodosh (2004). "Lack of sustained regression of c-MYC-induced mammary adenocarcinomas following brief or prolonged MYC inactivation." Cancer Cell **6**(6): 577-586.

Bromberg, J. (2002). "Stat proteins and oncogenesis." J Clin Invest **109**(9): 1139-1142.

Bromberg, J. F., M. H. Wrzeszczynska, G. Devgan, Y. Zhao, R. G. Pestell, C. Albanese and J. E. Darnell, Jr. (1999). "Stat3 as an oncogene." Cell **98**(3): 295-303.

Brooks, M. D., M. L. Burness and M. S. Wicha (2015). "Therapeutic Implications of Cellular Heterogeneity and Plasticity in Breast Cancer." Cell Stem Cell **17**(3): 260-271.

Brooks, T. A. and L. H. Hurley (2010). "Targeting MYC Expression through G-Quadruplexes." Genes Cancer **1**(6): 641-649.

Buerger, C., K. Nagel-Wolfrum, C. Kunz, I. Wittig, K. Butz, F. Hoppe-Seyler and B. Groner (2003). "Sequence-specific peptide aptamers, interacting with the intracellular domain of the epidermal growth factor receptor, interfere with Stat3 activation and inhibit the growth of tumor cells." J Biol Chem **278**(39): 37610-37621.

Buzdar, A. U., N. K. Ibrahim, D. Francis, D. J. Booser, E. S. Thomas, R. L. Theriault, L. Pusztai, M. C. Green, B. K. Arun, S. H. Giordano, M. Cristofanilli, D. K. Frye, T. L. Smith, K. K. Hunt, S. E. Singletary, A. A. Sahin, M. S. Ewer, T. A. Buchholz, D. Berry and G. N. Hortobagyi (2005). "Significantly higher pathologic complete remission rate after neoadjuvant therapy with trastuzumab, paclitaxel, and epirubicin chemotherapy: results of a randomized trial in human epidermal growth factor receptor 2-positive operable breast cancer." J Clin Oncol **23**(16): 3676-3685.

Byrski, T., J. Gronwald, T. Huzarski, E. Grzybowska, M. Budryk, M. Stawicka, T. Mierzwa, M. Szwiec, R. Wisniowski, M. Siolek, R. Dent, J. Lubinski and S. Narod (2010). "Pathologic

complete response rates in young women with BRCA1-positive breast cancers after neoadjuvant chemotherapy." J Clin Oncol **28**(3): 375-379.

Cameron, D., J. Brown, R. Dent, C. Jackisch, J. Mackey, X. Pivot, G. G. Steger, T. M. Suter, M. Toi, M. Parmar, R. Laeufle, Y. H. Im, G. Romieu, V. Harvey, O. Lipatov, T. Pienkowski, P. Cottu, A. Chan, S. A. Im, P. S. Hall, L. Bubuteishvili-Pacaud, V. Henschel, R. J. Deurloo, C. Pallaud and R. Bell (2013). "Adjuvant bevacizumab-containing therapy in triple-negative breast cancer (BEATRICE): primary results of a randomised, phase 3 trial." Lancet Oncol **14**(10): 933-942.

Cancer Genome Atlas, N. (2012). "Comprehensive molecular portraits of human breast tumours." Nature **490**(7418): 61-70.

Carracedo, A., L. Ma, J. Teruya-Feldstein, F. Rojo, L. Salmena, A. Alimonti, A. Egia, A. T. Sasaki, G. Thomas, S. C. Kozma, A. Papa, C. Nardella, L. C. Cantley, J. Baselga and P. P. Pandolfi (2008). "Inhibition of mTORC1 leads to MAPK pathway activation through a PI3K-dependent feedback loop in human cancer." J Clin Invest **118**(9): 3065-3074.

Carvalho, C. M., J. Chang, J. E. Lucas, J. R. Nevins, Q. Wang and M. West (2008). "High-Dimensional Sparse Factor Modeling: Applications in Gene Expression Genomics." J Am Stat Assoc **103**(484): 1438-1456.

Cassidy, J. W., C. Caldas and A. Bruna (2015). "Maintaining Tumor Heterogeneity in Patient-Derived Tumor Xenografts." Cancer Res **75**(15): 2963-2968.

Catlett-Falcone, R., T. H. Landowski, M. M. Oshiro, J. Turkson, A. Levitzki, R. Savino, G. Ciliberto, L. Moscinski, J. L. Fernandez-Luna, G. Nunez, W. S. Dalton and R. Jove (1999). "Constitutive activation of Stat3 signaling confers resistance to apoptosis in human U266 myeloma cells." Immunity **10**(1): 105-115.

Chang, C. H., M. Zhang, K. Rajapakshe, C. Coarfa, D. Edwards, S. Huang and J. M. Rosen (2015). "Mammary Stem Cells and Tumor-Initiating Cells Are More Resistant to Apoptosis and Exhibit Increased DNA Repair Activity in Response to DNA Damage." Stem Cell Reports **5**(3): 378-391.

Chang, D. W., G. F. Claassen, S. R. Hann and M. D. Cole (2000). "The c-Myc transactivation domain is a direct modulator of apoptotic versus proliferative signals." Mol Cell Biol **20**(12): 4309-4319.

Chang, Q., E. Bournazou, P. Sansone, M. Berishaj, S. P. Gao, L. Daly, J. Wels, T. Theilen, S. Granitto, X. Zhang, J. Cotari, M. L. Alpaugh, E. de Stanchina, K. Manova, M. Li, M. Bonafe, C. Ceccarelli, M. Taffurelli, D. Santini, G. Altan-Bonnet, R. Kaplan, L. Norton, N. Nishimoto, D. Huszar, D. Lyden and J. Bromberg (2013). "The IL-6/JAK/Stat3 feed-forward loop drives tumorigenesis and metastasis." Neoplasia **15**(7): 848-862.

Chang, T. C., D. Yu, Y. S. Lee, E. A. Wentzel, D. E. Arking, K. M. West, C. V. Dang, A. Thomas-Tikhonenko and J. T. Mendell (2008). "Widespread microRNA repression by Myc contributes to tumorigenesis." Nat Genet **40**(1): 43-50.

Chapman, R. S., P. C. Lourenco, E. Tonner, D. J. Flint, S. Selbert, K. Takeda, S. Akira, A. R. Clarke and C. J. Watson (1999). "Suppression of epithelial apoptosis and delayed mammary gland involution in mice with a conditional knockout of Stat3." Genes Dev **13**(19): 2604-2616.

Cheang, M. C., S. K. Chia, D. Voduc, D. Gao, S. Leung, J. Snider, M. Watson, S. Davies, P. S. Bernard, J. S. Parker, C. M. Perou, M. J. Ellis and T. O. Nielsen (2009). "Ki67 index, HER2 status, and prognosis of patients with luminal B breast cancer." J Natl Cancer Inst **101**(10): 736-750.

Chou, T. Y. and G. W. Hart (2001). "O-linked N-acetylglucosamine and cancer: messages from the glycosylation of c-Myc." Adv Exp Med Biol **491**: 413-418.

Chung, C. D., J. Liao, B. Liu, X. Rao, P. Jay, P. Berta and K. Shuai (1997). "Specific inhibition of Stat3 signal transduction by PIAS3." Science **278**(5344): 1803-1805.

Ciriello, G., M. L. Gatza, A. H. Beck, M. D. Wilkerson, S. K. Rhie, A. Pastore, H. Zhang, M. McLellan, C. Yau, C. Kandoth, R. Bowlby, H. Shen, S. Hayat, R. Fieldhouse, S. C. Lester, G. M. Tse, R. E. Factor, L. C. Collins, K. H. Allison, Y. Y. Chen, K. Jensen, N. B. Johnson, S. Oesterreich, G. B. Mills, A. D. Cherniack, G. Robertson, C. Benz, C. Sander, P. W. Laird, K. A. Hoadley, T. A. King, T. R. Network and C. M. Perou (2015). "Comprehensive Molecular Portraits of Invasive Lobular Breast Cancer." Cell **163**(2): 506-519.

Claassen, G. F. and S. R. Hann (1999). "Myc-mediated transformation: the repression connection." Oncogene **18**(19): 2925-2933.

Cortez, D., Y. Wang, J. Qin and S. J. Elledge (1999). "Requirement of ATM-dependent phosphorylation of brca1 in the DNA damage response to double-strand breaks." Science **286**(5442): 1162-1166.

Cottu, P., I. Bieche, F. Assayag, R. El Botty, S. Chateau-Joubert, A. Thuleau, T. Bagarre, B. Albaud, A. Rapinat, D. Gentien, P. de la Grange, V. Sibut, S. Vacher, R. Hatem, J. L. Servely, J. J. Fontaine, D. Decaudin, J. Y. Pierga, S. Roman-Roman and E. Marangoni (2014). "Acquired resistance to endocrine treatments is associated with tumor-specific molecular changes in patient-derived luminal breast cancer xenografts." Clin Cancer Res **20**(16): 4314-4325.

Cottu, P., E. Marangoni, F. Assayag, P. de Cremoux, A. Vincent-Salomon, C. Guyader, L. de Plater, C. Elbaz, N. Karboul, J. J. Fontaine, S. Chateau-Joubert, P. Boudou-Rouquette, S. Alran, V. Dangles-Marie, D. Gentien, M. F. Poupon and D. Decaudin (2012). "Modeling of response to endocrine therapy in a panel of human luminal breast cancer xenografts." Breast Cancer Res Treat **133**(2): 595-606.

Cowin, P. and J. Wysolmerski (2010). "Molecular mechanisms guiding embryonic mammary gland development." Cold Spring Harb Perspect Biol **2**(6): a003251.

Cowling, V. H. and M. D. Cole (2010). "Myc Regulation of mRNA Cap Methylation." Genes Cancer **1**(6): 576-579.

Cronin, M., C. Sangli, M. L. Liu, M. Pho, D. Dutta, A. Nguyen, J. Jeong, J. Wu, K. C. Langone and D. Watson (2007). "Analytical validation of the Oncotype DX genomic diagnostic test for recurrence prognosis and therapeutic response prediction in node-negative, estrogen receptor-positive breast cancer." Clin Chem **53**(6): 1084-1091.

Curtis, C., S. P. Shah, S. F. Chin, G. Turashvili, O. M. Rueda, M. J. Dunning, D. Speed, A. G. Lynch, S. Samarajiwa, Y. Yuan, S. Graf, G. Ha, G. Haffari, A. Bashashati, R. Russell, S. McKinney, M. Group, A. Langerod, A. Green, E. Provenzano, G. Wishart, S. Pinder, P. Watson, F. Markowetz, L. Murphy, I. Ellis, A. Purushotham, A. L. Borresen-Dale, J. D. Brenton, S. Tavare, C. Caldas and S. Aparicio (2012). "The genomic and transcriptomic architecture of 2,000 breast tumours reveals novel subgroups." Nature **486**(7403): 346-352.

D'Alfonso, T. M., R. K. van Laar, L. T. Vahdat, W. Hussain, R. Flinchum, N. Brown, L. S. John and S. J. Shin (2013). "BreastPRS is a gene expression assay that stratifies intermediate-risk Oncotype DX patients into high- or low-risk for disease recurrence." Breast Cancer Res Treat **139**(3): 705-715.

D'Cruz, C. M., E. J. Gunther, R. B. Boxer, J. L. Hartman, L. Sintasath, S. E. Moody, J. D. Cox, S. I. Ha, G. K. Belka, A. Golant, R. D. Cardiff and L. A. Chodosh (2001). "c-MYC induces mammary tumorigenesis by means of a preferred pathway involving spontaneous Kras2 mutations." Nat Med **7**(2): 235-239.

DaCosta Byfield, S., C. Major, N. J. Laping and A. B. Roberts (2004). "SB-505124 is a selective inhibitor of transforming growth factor-beta type I receptors ALK4, ALK5, and ALK7." Mol Pharmacol **65**(3): 744-752.

Dancey, J. E. and H. X. Chen (2006). "Strategies for optimizing combinations of molecularly targeted anticancer agents." Nat Rev Drug Discov **5**(8): 649-659.

Dang, C. V. (1999). "c-Myc target genes involved in cell growth, apoptosis, and metabolism." Mol Cell Biol **19**(1): 1-11.

Dang, C. V., K. A. O'Donnell, K. I. Zeller, T. Nguyen, R. C. Osthus and F. Li (2006). "The c-Myc target gene network." Semin Cancer Biol **16**(4): 253-264.

Dani, C., J. M. Blanchard, M. Piechaczyk, S. El Sabouty, L. Marty and P. Jeanteur (1984). "Extreme instability of myc mRNA in normal and transformed human cells." Proc Natl Acad Sci U S A **81**(22): 7046-7050.

Dauer, D. J., B. Ferraro, L. Song, B. Yu, L. Mora, R. Buettner, S. Enkemann, R. Jove and E. B. Haura (2005). "Stat3 regulates genes common to both wound healing and cancer." Oncogene **24**(21): 3397-3408.

Davis, A. C., M. Wims, G. D. Spotts, S. R. Hann and A. Bradley (1993). "A null c-myc mutation causes lethality before 10.5 days of gestation in homozygotes and reduced fertility in heterozygous female mice." Genes Dev **7**(4): 671-682.

Davis, F. M., B. Lloyd-Lewis, O. B. Harris, S. Kozar, D. J. Winton, L. Muresan and C. J. Watson (2016). "Single-cell lineage tracing in the mammary gland reveals stochastic clonal dispersion of stem/progenitor cell progeny." Nat Commun **7**: 13053.

Dechow, T. N., L. Pedranzini, A. Leitch, K. Leslie, W. L. Gerald, I. Linkov and J. F. Bromberg (2004). "Requirement of matrix metalloproteinase-9 for the transformation of human mammary epithelial cells by Stat3-C." Proc Natl Acad Sci U S A **101**(29): 10602-10607.

Delmore, J. E., G. C. Issa, M. E. Lemieux, P. B. Rahl, J. Shi, H. M. Jacobs, E. Kastritis, T. Gilpatrick, R. M. Paranal, J. Qi, M. Chesi, A. C. Schinzel, M. R. McKeown, T. P. Heffernan, C. R. Vakoc, P. L. Bergsagel, I. M. Ghobrial, P. G. Richardson, R. A. Young, W. C. Hahn, K. C. Anderson, A. L. Kung, J. E. Bradner and C. S. Mitsiades (2011). "BET bromodomain inhibition as a therapeutic strategy to target c-Myc." Cell **146**(6): 904-917.

Deming, S. L., S. J. Nass, R. B. Dickson and B. J. Trock (2000). "C-myc amplification in breast cancer: a meta-analysis of its occurrence and prognostic relevance." Br J Cancer **83**(12): 1688-1695.

Dent, R., M. Trudeau, K. I. Pritchard, W. M. Hanna, H. K. Kahn, C. A. Sawka, L. A. Lickley, E. Rawlinson, P. Sun and S. A. Narod (2007). "Triple-negative breast cancer: clinical features and patterns of recurrence." Clin Cancer Res **13**(15 Pt 1): 4429-4434.

DeRose, Y. S., G. Wang, Y. C. Lin, P. S. Bernard, S. S. Buys, M. T. Ebbert, R. Factor, C. Matsen, B. A. Milash, E. Nelson, L. Neumayer, R. L. Randall, I. J. Stijleman, B. E. Welm and A. L. Welm (2011). "Tumor grafts derived from women with breast cancer authentically reflect tumor pathology, growth, metastasis and disease outcomes." Nat Med **17**(11): 1514-1520.

Diaz, N., S. Minton, C. Cox, T. Bowman, T. Gritsko, R. Garcia, I. Eweis, M. Wloch, S. Livingston, E. Seijo, A. Cantor, J. H. Lee, C. A. Beam, D. Sullivan, R. Jove and C. A. Muro-Cacho (2006). "Activation of stat3 in primary tumors from high-risk breast cancer patients is associated with elevated levels of activated SRC and survivin expression." Clin Cancer Res **12**(1): 20-28.

Dittrich, A., H. Gautrey, D. Browell and A. Tyson-Capper (2014). "The HER2 Signaling Network in Breast Cancer--Like a Spider in its Web." J Mammary Gland Biol Neoplasia **19**(3-4): 253-270.

Dolled-Filhart, M., R. L. Camp, D. P. Kowalski, B. L. Smith and D. L. Rimm (2003). "Tissue microarray analysis of signal transducers and activators of transcription 3 (Stat3) and phospho-Stat3 (Tyr705) in node-negative breast cancer shows nuclear localization is associated with a better prognosis." Clin Cancer Res **9**(2): 594-600.

Dong, J., M. Naito and T. Tsuruo (1997). "c-Myc plays a role in cellular susceptibility to death receptor-mediated and chemotherapy-induced apoptosis in human monocytic leukemia U937 cells." Oncogene **15**(6): 639-647.

Dossus, L. and P. R. Benusiglio (2015). "Lobular breast cancer: incidence and genetic and non-genetic risk factors." Breast Cancer Res **17**: 37.

Dowsett, M., J. Cuzick, C. Wale, J. Forbes, E. A. Mallon, J. Salter, E. Quinn, A. Dunbier, M. Baum, A. Buzdar, A. Howell, R. Bugarini, F. L. Baehner and S. Shak (2010). "Prediction of risk of distant recurrence using the 21-gene recurrence score in node-negative and node-positive postmenopausal patients with breast cancer treated with anastrozole or tamoxifen: a TransATAC study." J Clin Oncol **28**(11): 1829-1834.

Dubsky, P., J. C. Brase, R. Jakesz, M. Rudas, C. F. Singer, R. Greil, O. Dietze, I. Luisser, E. Klug, R. Sedivy, M. Bachner, D. Mayr, M. Schmidt, M. C. Gehrmann, C. Petry, K. E. Weber, K. Fisch, R. Kronenwett, M. Gnant, M. Filipits, B. Austrian and G. Colorectal Cancer Study (2013). "The EndoPredict score provides prognostic information on late distant metastases in ER+/HER2- breast cancer patients." Br J Cancer **109**(12): 2959-2964.

Dunn, G. P., A. T. Bruce, H. Ikeda, L. J. Old and R. D. Schreiber (2002). "Cancer immunoediting: from immunosurveillance to tumor escape." Nat Immunol **3**(11): 991-998.

Ecker, A., O. Simma, A. Hoelbl, L. Kenner, H. Beug, R. Moriggl and V. Sexl (2009). "The dark and the bright side of Stat3: proto-oncogene and tumor-suppressor." Front Biosci (Landmark Ed) **14**: 2944-2958.

Eichhorn, P. J., M. Gili, M. Scaltriti, V. Serra, M. Guzman, W. Nijkamp, R. L. Beijersbergen, V. Valero, J. Seoane, R. Bernards and J. Baselga (2008). "Phosphatidylinositol 3-kinase hyperactivation results in lapatinib resistance that is reversed by the mTOR/phosphatidylinositol 3-kinase inhibitor NVP-BEZ235." Cancer Res **68**(22): 9221-9230.

Eilers, M., D. Picard, K. R. Yamamoto and J. M. Bishop (1989). "Chimaeras of myc oncoprotein and steroid receptors cause hormone-dependent transformation of cells." Nature **340**(6228): 66-68.

Ellwood-Yen, K., T. G. Graeber, J. Wongvipat, M. L. Iruela-Arispe, J. Zhang, R. Matusik, G. V. Thomas and C. L. Sawyers (2003). "Myc-driven murine prostate cancer shares molecular features with human prostate tumors." Cancer Cell **4**(3): 223-238.

Emery, C. M., K. G. Vijayendran, M. C. Zipser, A. M. Sawyer, L. Niu, J. J. Kim, C. Hatton, R. Chopra, P. A. Oberholzer, M. B. Karpova, L. E. MacConaill, J. Zhang, N. S. Gray, W. R. Sellers, R. Dummer and L. A. Garraway (2009). "MEK1 mutations confer resistance to MEK and B-RAF inhibition." Proc Natl Acad Sci U S A **106**(48): 20411-20416.

Epling-Burnette, P. K., J. H. Liu, R. Catlett-Falcone, J. Turkson, M. Oshiro, R. Kothapalli, Y. Li, J. M. Wang, H. F. Yang-Yen, J. Karras, R. Jove and T. P. Loughran, Jr. (2001). "Inhibition of STAT3 signaling leads to apoptosis of leukemic large granular lymphocytes and decreased Mcl-1 expression." J Clin Invest **107**(3): 351-362.

Esserman, L. J., D. A. Berry, M. C. Cheang, C. Yau, C. M. Perou, L. Carey, A. DeMichele, J. W. Gray, K. Conway-Dorsey, M. E. Lenburg, M. B. Buxton, S. E. Davis, L. J. van't Veer, C. Hudis, K. Chin, D. Wolf, H. Krontiras, L. Montgomery, D. Tripathy, C. Lehman, M. C. Liu, O. I. Olopade, H. S. Rugo, J. T. Carpenter, C. Livasy, L. Dressler, D. Chhieng, B. Singh, C. Mies, J. Rabban, Y. Y. Chen, D. Giri, A. Au, N. Hylton and I. S. T. Investigators (2012). "Chemotherapy

response and recurrence-free survival in neoadjuvant breast cancer depends on biomarker profiles: results from the I-SPY 1 TRIAL (CALGB 150007/150012; ACRIN 6657)." Breast Cancer Res Treat **132**(3): 1049-1062.

Esteva, F. J., D. Yu, M. C. Hung and G. N. Hortobagyi (2010). "Molecular predictors of response to trastuzumab and lapatinib in breast cancer." Nat Rev Clin Oncol **7**(2): 98-107.

Evan, G. I., A. H. Wyllie, C. S. Gilbert, T. D. Littlewood, H. Land, M. Brooks, C. M. Waters, L. Z. Penn and D. C. Hancock (1992). "Induction of apoptosis in fibroblasts by c-myc protein." Cell **69**(1): 119-128.

Facchini, L. M. and L. Z. Penn (1998). "The molecular role of Myc in growth and transformation: recent discoveries lead to new insights." FASEB J **12**(9): 633-651.

Fan, L., G. Peng, N. Sahgal, L. Fazli, M. Gleave, Y. Zhang, A. Hussain and J. Qi (2016). "Regulation of c-Myc expression by the histone demethylase JMJD1A is essential for prostate cancer cell growth and survival." Oncogene **35**(19): 2441-2452.

Farmer, H., N. McCabe, C. J. Lord, A. N. Tutt, D. A. Johnson, T. B. Richardson, M. Santarosa, K. J. Dillon, I. Hickson, C. Knights, N. M. Martin, S. P. Jackson, G. C. Smith and A. Ashworth (2005). "Targeting the DNA repair defect in BRCA mutant cells as a therapeutic strategy." Nature **434**(7035): 917-921.

Felsher, D. W. and J. M. Bishop (1999). "Transient excess of MYC activity can elicit genomic instability and tumorigenesis." Proc Natl Acad Sci U S A **96**(7): 3940-3944.

Ferrajoli, A., S. Faderl, Q. Van, P. Koch, D. Harris, Z. Liu, I. Hazan-Halevy, Y. Wang, H. M. Kantarjian, W. Priebe and Z. Estrov (2007). "WP1066 disrupts Janus kinase-2 and induces caspase-dependent apoptosis in acute myelogenous leukemia cells." Cancer Res **67**(23): 11291-11299.

Filipits, M., M. Rudas, R. Jakesz, P. Dubsky, F. Fitzal, C. F. Singer, O. Dietze, R. Greil, A. Jelen, P. Sevelda, C. Freibauer, V. Muller, F. Janicke, M. Schmidt, H. Kolbl, A. Rody, M. Kaufmann, W. Schroth, H. Brauch, M. Schwab, P. Fritz, K. E. Weber, I. S. Feder, G. Hennig, R. Kronenwett, M. Gehrmann, M. Gnant and E. P. Investigators (2011). "A new molecular predictor of distant recurrence in ER-positive, HER2-negative breast cancer adds independent information to conventional clinical risk factors." Clin Cancer Res **17**(18): 6012-6020.

Fillmore, C. M. and C. Kuperwasser (2008). "Human breast cancer cell lines contain stem-like cells that self-renew, give rise to phenotypically diverse progeny and survive chemotherapy." Breast Cancer Res **10**(2): R25.

Finn, R. S., J. P. Crown, I. Lang, K. Boer, I. M. Bondarenko, S. O. Kulyk, J. Ettl, R. Patel, T. Pinter, M. Schmidt, Y. Shparyk, A. R. Thummala, N. L. Voytko, C. Fowst, X. Huang, S. T. Kim, S. Randolph and D. J. Slamon (2015). "The cyclin-dependent kinase 4/6 inhibitor palbociclib in combination with letrozole versus letrozole alone as first-line treatment of oestrogen receptor-positive, HER2-negative, advanced breast cancer (PALOMA-1/TRIO-18): a randomised phase 2 study." Lancet Oncol **16**(1): 25-35.

Fleming, J. M., T. C. Miller, M. J. Meyer, E. Ginsburg and B. K. Vonderhaar (2010). "Local regulation of human breast xenograft models." J Cell Physiol **224**(3): 795-806.

Folkman, J. (1974). "Proceedings: Tumor angiogenesis factor." Cancer Res **34**(8): 2109-2113.

Folkman, J. (2002). "Role of angiogenesis in tumor growth and metastasis." Semin Oncol **29**(6 Suppl 16): 15-18.

Ford, D., D. F. Easton, M. Stratton, S. Narod, D. Goldgar, P. Devilee, D. T. Bishop, B. Weber, G. Lenoir, J. Chang-Claude, H. Sobol, M. D. Teare, J. Struewing, A. Arason, S. Scherneck, J. Peto, T. R. Rebbeck, P. Tonin, S. Neuhausen, R. Barkardottir, J. Eyfjord, H. Lynch, B. A. Ponder, S. A. Gayther, M. Zelada-Hedman and et al. (1998). "Genetic heterogeneity and penetrance analysis of the BRCA1 and BRCA2 genes in breast cancer families. The Breast Cancer Linkage Consortium." Am J Hum Genet **62**(3): 676-689.

Fukada, T., M. Hibi, Y. Yamanaka, M. Takahashi-Tezuka, Y. Fujitani, T. Yamaguchi, K. Nakajima and T. Hirano (1996). "Two signals are necessary for cell proliferation induced by a cytokine receptor gp130: involvement of STAT3 in anti-apoptosis." Immunity **5**(5): 449-460.

Gao, S. P., K. G. Mark, K. Leslie, W. Pao, N. Motoi, W. L. Gerald, W. D. Travis, W. Bornmann, D. Veach, B. Clarkson and J. F. Bromberg (2007). "Mutations in the EGFR kinase domain mediate STAT3 activation via IL-6 production in human lung adenocarcinomas." J Clin Invest **117**(12): 3846-3856.

Gartel, A. L., X. Ye, E. Goufman, P. Shianov, N. Hay, F. Najmabadi and A. L. Tyner (2001). "Myc represses the p21(WAF1/CIP1) promoter and interacts with Sp1/Sp3." Proc Natl Acad Sci U S A **98**(8): 4510-4515.

Gatza, M. L., J. E. Lucas, W. T. Barry, J. W. Kim, Q. Wang, M. D. Crawford, M. B. Datto, M. Kelley, B. Mathey-Prevot, A. Potti and J. R. Nevins (2010). "A pathway-based classification of human breast cancer." Proc Natl Acad Sci U S A **107**(15): 6994-6999.

Geisler, S., P. E. Lonning, T. Aas, H. Johnsen, O. Fluge, D. F. Haugen, J. R. Lillehaug, L. A. Akslen and A. L. Borresen-Dale (2001). "Influence of TP53 gene alterations and c-erbB-2 expression on the response to treatment with doxorubicin in locally advanced breast cancer." Cancer Res **61**(6): 2505-2512.

Gillet, J. P., A. M. Calcagno, S. Varma, M. Marino, L. J. Green, M. I. Vora, C. Patel, J. N. Orina, T. A. Eliseeva, V. Singal, R. Padmanabhan, B. Davidson, R. Ganapathi, A. K. Sood, B. R. Rueda, S. V. Ambudkar and M. M. Gottesman (2011). "Redefining the relevance of established cancer cell lines to the study of mechanisms of clinical anti-cancer drug resistance." Proc Natl Acad Sci U S A **108**(46): 18708-18713.

Gluck, S., F. de Snoo, J. Peeters, L. Stork-Sloots and G. Somlo (2013). "Molecular subtyping of early-stage breast cancer identifies a group of patients who do not benefit from neoadjuvant chemotherapy." Breast Cancer Res Treat **139**(3): 759-767.

Goel, S., Q. Wang, A. C. Watt, S. M. Tolaney, D. A. Dillon, W. Li, S. Ramm, A. C. Palmer, H. Yuzugullu, V. Varadan, D. Tuck, L. N. Harris, K. K. Wong, X. S. Liu, P. Sicinski, E. P. Winer, I. E. Krop and J. J. Zhao (2016). "Overcoming Therapeutic Resistance in HER2-Positive Breast Cancers with CDK4/6 Inhibitors." Cancer Cell **29**(3): 255-269.

Gomez-Roman, N., C. Grandori, R. N. Eisenman and R. J. White (2003). "Direct activation of RNA polymerase III transcription by c-Myc." Nature **421**(6920): 290-294.

Gonzalez-Angulo, A. M., K. M. Timms, S. Liu, H. Chen, J. K. Litton, J. Potter, J. S. Lanchbury, K. Stemke-Hale, B. T. Hennessy, B. K. Arun, G. N. Hortobagyi, K. A. Do, G. B. Mills and F. Meric-Bernstam (2011). "Incidence and outcome of BRCA mutations in unselected patients with triple receptor-negative breast cancer." Clin Cancer Res **17**(5): 1082-1089.

Gottlicher, M., S. Minucci, P. Zhu, O. H. Kramer, A. Schimpf, S. Giavara, J. P. Sleeman, F. Lo Coco, C. Nervi, P. G. Pelicci and T. Heinzel (2001). "Valproic acid defines a novel class of HDAC inhibitors inducing differentiation of transformed cells." EMBO J **20**(24): 6969-6978.

Grabner, B., H. P. Moll and E. Casanova (2016). "Unexpected oncosuppressive role for STAT3 in KRAS-induced lung tumorigenesis." Mol Cell Oncol **3**(3): e1036199.

Grimm, S. L. and S. K. Nordeen (1998). "Mouse mammary tumor virus sequences responsible for activating cellular oncogenes." J Virol **72**(12): 9428-9435.

Gritsko, T., A. Williams, J. Turkson, S. Kaneko, T. Bowman, M. Huang, S. Nam, I. Eweis, N. Diaz, D. Sullivan, S. Yoder, S. Enkemann, S. Eschrich, J. H. Lee, C. A. Beam, J. Cheng, S. Minton, C. A. Muro-Cacho and R. Jove (2006). "Persistent activation of stat3 signaling induces survivin gene expression and confers resistance to apoptosis in human breast cancer cells." Clin Cancer Res **12**(1): 11-19.

Grob, J. J., M. M. Amonkar, B. Karaszewska, J. Schachter, R. Dummer, A. Mackiewicz, D. Stroyakovskiy, K. Drucis, F. Grange, V. Chiarion-Sileni, P. Rutkowski, M. Lichinitser, E. Levchenko, P. Wolter, A. Hauschild, G. V. Long, P. Nathan, A. Ribas, K. Flaherty, P. Sun, J. J. Legos, D. O. McDowell, B. Mookerjee, D. Schadendorf and C. Robert (2015). "Comparison of dabrafenib and trametinib combination therapy with vemurafenib monotherapy on health-related quality of life in patients with unresectable or metastatic cutaneous BRAF Val600-mutation-positive melanoma (COMBI-v): results of a phase 3, open-label, randomised trial." Lancet Oncol **16**(13): 1389-1398.

Gunther, E. J., G. K. Belka, G. B. Wertheim, J. Wang, J. L. Hartman, R. B. Boxer and L. A. Chodosh (2002). "A novel doxycycline-inducible system for the transgenic analysis of mammary gland biology." FASEB J **16**(3): 283-292.

Hann, S. R. and R. N. Eisenman (1984). "Proteins encoded by the human c-myc oncogene: differential expression in neoplastic cells." Mol Cell Biol **4**(11): 2486-2497.

Hanson, K. D., M. Shichiri, M. R. Follansbee and J. M. Sedivy (1994). "Effects of c-myc expression on cell cycle progression." Mol Cell Biol **14**(9): 5748-5755.

Harris, D. A., R. A. Burns and R. Ali (1988). "Evaluation of infant formula protein quality: comparison of in vitro with in vivo methods." J Assoc Off Anal Chem **71**(2): 353-357.

Harris, L. N., N. Ismaila, L. M. McShane, F. Andre, D. E. Collyar, A. M. Gonzalez-Angulo, E. H. Hammond, N. M. Kuderer, M. C. Liu, R. G. Mennel, C. Van Poznak, R. C. Bast, D. F. Hayes and O. American Society of Clinical (2016). "Use of Biomarkers to Guide Decisions on Adjuvant Systemic Therapy for Women With Early-Stage Invasive Breast Cancer: American Society of Clinical Oncology Clinical Practice Guideline." J Clin Oncol **34**(10): 1134-1150.

Hatzis, C., L. Pusztai, V. Valero, D. J. Booser, L. Esserman, A. Lluch, T. Vidaurre, F. Holmes, E. Souchon, H. Wang, M. Martin, J. Cotrina, H. Gomez, R. Hubbard, J. I. Chacon, J. Ferrer-Lozano, R. Dyer, M. Buxton, Y. Gong, Y. Wu, N. Ibrahim, E. Andreopoulou, N. T. Ueno, K. Hunt, W. Yang, A. Nazario, A. DeMichele, J. O'Shaughnessy, G. N. Hortobagyi and W. F. Symmans

(2011). "A genomic predictor of response and survival following taxane-anthracycline chemotherapy for invasive breast cancer." JAMA **305**(18): 1873-1881.

Hayakawa, F., K. Sugimoto, Y. Harada, N. Hashimoto, N. Ohi, S. Kurahashi and T. Naoe (2013). "A novel STAT inhibitor, OPB-31121, has a significant antitumor effect on leukemia with STAT-addictive oncokinases." Blood Cancer J **3**: e166.

He, B., L. You, K. Uematsu, K. Zang, Z. Xu, A. Y. Lee, J. F. Costello, F. McCormick and D. M. Jablons (2003). "SOCS-3 is frequently silenced by hypermethylation and suppresses cell growth in human lung cancer." Proc Natl Acad Sci U S A **100**(24): 14133-14138.

He, C., H. Hu, R. Braren, S. Y. Fong, A. Trumpp, T. R. Carlson and R. A. Wang (2008). "c-myc in the hematopoietic lineage is crucial for its angiogenic function in the mouse embryo." Development **135**(14): 2467-2477.

He, D. X., F. Gu, F. Gao, J. J. Hao, D. Gong, X. T. Gu, A. Q. Mao, J. Jin, L. Fu and X. Ma (2016). "Genome-wide profiles of methylation, microRNAs, and gene expression in chemoresistant breast cancer." Sci Rep **6**: 24706.

Heikkila, R., G. Schwab, E. Wickstrom, S. L. Loke, D. H. Pluznik, R. Watt and L. M. Neckers (1987). "A c-myc antisense oligodeoxynucleotide inhibits entry into S phase but not progress from G0 to G1." Nature **328**(6129): 445-449.

Heinrich, P. C., I. Behrmann, G. Muller-Newen, F. Schaper and L. Graeve (1998). "Interleukin-6-type cytokine signalling through the gp130/Jak/STAT pathway." Biochem J **334 (Pt 2)**: 297-314.

Henrard, D. and S. R. Ross (1988). "Endogenous mouse mammary tumor virus is expressed in several organs in addition to the lactating mammary gland." J Virol **62**(8): 3046-3049.

Herrick, D. J. and J. Ross (1994). "The half-life of c-myc mRNA in growing and serum-stimulated cells: influence of the coding and 3' untranslated regions and role of ribosome translocation." Mol Cell Biol **14**(3): 2119-2128.

Herschkowitz, J. I., K. Simin, V. J. Weigman, I. Mikaelian, J. Usary, Z. Hu, K. E. Rasmussen, L. P. Jones, S. Assefnia, S. Chandrasekharan, M. G. Backlund, Y. Yin, A. I. Khramtsov, R. Bastein, J. Quackenbush, R. I. Glazer, P. H. Brown, J. E. Green, L. Kopelovich, P. A. Furth, J. P. Palazzo, O. I. Olopade, P. S. Bernard, G. A. Churchill, T. Van Dyke and C. M. Perou (2007). "Identification of conserved gene expression features between murine mammary carcinoma models and human breast tumors." Genome Biol **8**(5): R76.

Hipfner, D. R. and S. M. Cohen (2004). "Connecting proliferation and apoptosis in development and disease." Nat Rev Mol Cell Biol **5**(10): 805-815.

Hoefflin, R., B. Lahrmann, G. Warsow, D. Hubschmann, C. Spath, B. Walter, X. Chen, L. Hofer, S. Macher-Goeppinger, Y. Tolstov, N. Korzeniewski, A. Duensing, C. Grullich, D. Jager, S. Perner, G. Schonberg, J. Nyarangi-Dix, S. Isaac, G. Hatiboglu, D. Teber, B. Hadaschik, S. Pahernik, W. Roth, R. Eils, M. Schlesner, H. Sultmann, M. Hohenfellner, N. Grabe and S. Duensing (2016). "Spatial niche formation but not malignant progression is a driving force for intratumoural heterogeneity." Nat Commun **7**: ncomms11845.

Hoffman, B. and D. A. Liebermann (2008). "Apoptotic signaling by c-MYC." Oncogene **27**(50): 6462-6472.

Hollern, D. P. and E. R. Andrechek (2014). "A genomic analysis of mouse models of breast cancer reveals molecular features of mouse models and relationships to human breast cancer." Breast Cancer Res **16**(3): R59.

Hollern, D. P., I. Yuwanita and E. R. Andrechek (2013). "A mouse model with T58A mutations in Myc reduces the dependence on KRas mutations and has similarities to claudin-low human breast cancer." Oncogene **32**(10): 1296-1304.

Hsu, P. Y., H. K. Hsu, X. Lan, L. Juan, P. S. Yan, J. Labanowska, N. Heerema, T. H. Hsiao, Y. C. Chiu, Y. Chen, Y. Liu, L. Li, R. Li, I. M. Thompson, K. P. Nephew, Z. D. Sharp, N. B. Kirma, V. X. Jin and T. H. Huang (2013). "Amplification of distant estrogen response elements deregulates target genes associated with tamoxifen resistance in breast cancer." Cancer Cell **24**(2): 197-212.

Huang, E., S. Ishida, J. Pittman, H. Dressman, A. Bild, M. Kloos, M. D'Amico, R. G. Pestell, M. West and J. R. Nevins (2003). "Gene expression phenotypic models that predict the activity of oncogenic pathways." Nat Genet **34**(2): 226-230.

Huang, M. J., Y. C. Cheng, C. R. Liu, S. Lin and H. E. Liu (2006). "A small-molecule c-Myc inhibitor, 10058-F4, induces cell-cycle arrest, apoptosis, and myeloid differentiation of human acute myeloid leukemia." Exp Hematol **34**(11): 1480-1489.

Humphreys, R. C., B. Bierie, L. Zhao, R. Raz, D. Levy and L. Hennighausen (2002). "Deletion of Stat3 blocks mammary gland involution and extends functional competence of the secretory epithelium in the absence of lactogenic stimuli." Endocrinology **143**(9): 3641-3650.

Hurlin, P. J., C. Queva and R. N. Eisenman (1997). "Mnt, a novel Max-interacting protein is coexpressed with Myc in proliferating cells and mediates repression at Myc binding sites." Genes Dev **11**(1): 44-58.

Hutchinson, J. N. and W. J. Muller (2000). "Transgenic mouse models of human breast cancer." Oncogene **19**(53): 6130-6137.

Ihle, J. N. (2001). "The Stat family in cytokine signaling." Curr Opin Cell Biol **13**(2): 211-217.

Inman, J. L., C. Robertson, J. D. Mott and M. J. Bissell (2015). "Mammary gland development: cell fate specification, stem cells and the microenvironment." Development **142**(6): 1028-1042.

Irie-Sasaki, J., T. Sasaki, W. Matsumoto, A. Opavsky, M. Cheng, G. Welstead, E. Griffiths, C. Krawczyk, C. D. Richardson, K. Aitken, N. Iscove, G. Koretzky, P. Johnson, P. Liu, D. M. Rothstein and J. M. Penninger (2001). "CD45 is a JAK phosphatase and negatively regulates cytokine receptor signalling." Nature **409**(6818): 349-354.

Iwamaru, A., S. Szymanski, E. Iwado, H. Aoki, T. Yokoyama, I. Fokt, K. Hess, C. Conrad, T. Madden, R. Sawaya, S. Kondo, W. Priebe and Y. Kondo (2007). "A novel inhibitor of the STAT3 pathway induces apoptosis in malignant glioma cells both in vitro and in vivo." Oncogene **26**(17): 2435-2444.

Iyer, V., I. Klebba, J. McCready, L. M. Arendt, M. Betancur-Boissel, M. F. Wu, X. Zhang, M. T. Lewis and C. Kuperwasser (2012). "Estrogen promotes ER-negative tumor growth and angiogenesis through mobilization of bone marrow-derived monocytes." Cancer Res **72**(11): 2705-2713.

Jager, R., U. Herzer, J. Schenkel and H. Weiher (1997). "Overexpression of Bcl-2 inhibits alveolar cell apoptosis during involution and accelerates c-myc-induced tumorigenesis of the mammary gland in transgenic mice." Oncogene **15**(15): 1787-1795.

Janicke, R. U., F. H. Lee and A. G. Porter (1994). "Nuclear c-Myc plays an important role in the cytotoxicity of tumor necrosis factor alpha in tumor cells." Mol Cell Biol **14**(9): 5661-5670.

Jones, L. M., M. L. Broz, J. J. Ranger, J. Ozcelik, R. Ahn, D. Zuo, J. Ursini-Siegel, M. T. Hallett, M. Krummel and W. J. Muller (2016). "STAT3 Establishes an Immunosuppressive Microenvironment during the Early Stages of Breast Carcinogenesis to Promote Tumor Growth and Metastasis." Cancer Res **76**(6): 1416-1428.

Jones, T. R. and M. D. Cole (1987). "Rapid cytoplasmic turnover of c-myc mRNA: requirement of the 3' untranslated sequences." Mol Cell Biol **7**(12): 4513-4521.

Junttila, T. T., R. W. Akita, K. Parsons, C. Fields, G. D. Lewis Phillips, L. S. Friedman, D. Sampath and M. X. Sliwkowski (2009). "Ligand-independent HER2/HER3/PI3K complex is disrupted by trastuzumab and is effectively inhibited by the PI3K inhibitor GDC-0941." Cancer Cell **15**(5): 429-440.

Kamemura, K., B. K. Hayes, F. I. Comer and G. W. Hart (2002). "Dynamic interplay between O-glycosylation and O-phosphorylation of nucleocytoplasmic proteins: alternative glycosylation/phosphorylation of THR-58, a known mutational hot spot of c-Myc in lymphomas, is regulated by mitogens." J Biol Chem **277**(21): 19229-19235.

Kandioler-Eckersberger, D., C. Ludwig, M. Rudas, S. Kappel, E. Janschek, C. Wenzel, H. Schlagbauer-Wadl, M. Mittlbock, M. Gnant, G. Steger and R. Jakesz (2000). "TP53 mutation and p53 overexpression for prediction of response to neoadjuvant treatment in breast cancer patients." Clin Cancer Res **6**(1): 50-56.

Kanehisa, M. and S. Goto (2000). "KEGG: kyoto encyclopedia of genes and genomes." Nucleic Acids Res **28**(1): 27-30.

Kang, J., C. M. Sergio, R. L. Sutherland and E. A. Musgrove (2014). "Targeting cyclin-dependent kinase 1 (CDK1) but not CDK4/6 or CDK2 is selectively lethal to MYC-dependent human breast cancer cells." BMC Cancer **14**: 32.

Kao, J., K. Salari, M. Bocanegra, Y. L. Choi, L. Girard, J. Gandhi, K. A. Kwei, T. Hernandez-Boussard, P. Wang, A. F. Gazdar, J. D. Minna and J. R. Pollack (2009). "Molecular profiling of breast cancer cell lines defines relevant tumor models and provides a resource for cancer gene discovery." PLoS One **4**(7): e6146.

Kessler, J. D., K. T. Kahle, T. Sun, K. L. Meerbrey, M. R. Schlabach, E. M. Schmitt, S. O. Skinner, Q. Xu, M. Z. Li, Z. C. Hartman, M. Rao, P. Yu, R. Dominguez-Vidana, A. C. Liang, N. L. Solimini, R. J. Bernardi, B. Yu, T. Hsu, I. Golding, J. Luo, C. K. Osborne, C. J. Creighton, S. G. Hilsenbeck, R. Schiff, C. A. Shaw, S. J. Elledge and T. F. Westbrook (2012). "A SUMOylation-dependent transcriptional subprogram is required for Myc-driven tumorigenesis." Science **335**(6066): 348-353.

Kim, H. H., Y. Kuwano, S. Srikantan, E. K. Lee, J. L. Martindale and M. Gorospe (2009). "HuR recruits let-7/RISC to repress c-Myc expression." Genes Dev **23**(15): 1743-1748.

Kim, S. Y., A. Herbst, K. A. Tworkowski, S. E. Salghetti and W. P. Tansey (2003). "Skp2 regulates Myc protein stability and activity." Mol Cell **11**(5): 1177-1188.

Kiuchi, N., K. Nakajima, M. Ichiba, T. Fukada, M. Narimatsu, K. Mizuno, M. Hibi and T. Hirano (1999). "STAT3 is required for the gp130-mediated full activation of the c-myc gene." J Exp Med **189**(1): 63-73.

Knauer, M., S. Mook, E. J. Rutgers, R. A. Bender, M. Hauptmann, M. J. van de Vijver, R. H. Koornstra, J. M. Bueno-de-Mesquita, S. C. Linn and L. J. van 't Veer (2010). "The predictive value of the 70-gene signature for adjuvant chemotherapy in early breast cancer." Breast Cancer Res Treat **120**(3): 655-661.

Kokai, E., F. Voss, F. Fleischer, S. Kempe, D. Marinkovic, H. Wolburg, F. Leithauser, V. Schmidt, U. Deutsch and T. Wirth (2009). "Myc regulates embryonic vascular permeability and remodeling." Circ Res **104**(10): 1151-1159.

Kortylewski, M., M. Kujawski, T. Wang, S. Wei, S. Zhang, S. Pilon-Thomas, G. Niu, H. Kay, J. Mule, W. G. Kerr, R. Jove, D. Pardoll and H. Yu (2005). "Inhibiting Stat3 signaling in the hematopoietic system elicits multicomponent antitumor immunity." Nat Med **11**(12): 1314-1321.

Kress, T. R., A. Sabo and B. Amati (2015). "MYC: connecting selective transcriptional control to global RNA production." Nat Rev Cancer **15**(10): 593-607.

Kreuzaler, P. A., A. D. Staniszewska, W. Li, N. Omidvar, B. Kedjouar, J. Turkson, V. Poli, R. A. Flavell, R. W. Clarkson and C. J. Watson (2011). "Stat3 controls lysosomal-mediated cell death in vivo." Nat Cell Biol **13**(3): 303-309.

Krijgsman, O., P. Roepman, W. Zwart, J. S. Carroll, S. Tian, F. A. de Snoo, R. A. Bender, R. Bernards and A. M. Glas (2012). "A diagnostic gene profile for molecular subtyping of breast cancer associated with treatment response." Breast Cancer Res Treat **133**(1): 37-47.

Kritikou, E. A., A. Sharkey, K. Abell, P. J. Came, E. Anderson, R. W. Clarkson and C. J. Watson (2003). "A dual, non-redundant, role for LIF as a regulator of development and STAT3-mediated cell death in mammary gland." Development **130**(15): 3459-3468.

Lacroix, M. and G. Leclercq (2004). "Relevance of breast cancer cell lines as models for breast tumours: an update." Breast Cancer Res Treat **83**(3): 249-289.

Lamb, J., E. D. Crawford, D. Peck, J. W. Modell, I. C. Blat, M. J. Wrobel, J. Lerner, J. P. Brunet, A. Subramanian, K. N. Ross, M. Reich, H. Hieronymus, G. Wei, S. A. Armstrong, S. J. Haggarty, P. A. Clemons, R. Wei, S. A. Carr, E. S. Lander and T. R. Golub (2006). "The Connectivity Map: using gene-expression signatures to connect small molecules, genes, and disease." Science **313**(5795): 1929-1935.

Land, H., L. F. Parada and R. A. Weinberg (1983). "Tumorigenic conversion of primary embryo fibroblasts requires at least two cooperating oncogenes." Nature **304**(5927): 596-602.

Leder, A., P. K. Pattengale, A. Kuo, T. A. Stewart and P. Leder (1986). "Consequences of widespread deregulation of the c-myc gene in transgenic mice: multiple neoplasms and normal development." Cell **45**(4): 485-495.

Lee, H., J. Deng, M. Kujawski, C. Yang, Y. Liu, A. Herrmann, M. Kortylewski, D. Horne, G. Somlo, S. Forman, R. Jove and H. Yu (2010). "STAT3-induced S1PR1 expression is crucial for persistent STAT3 activation in tumors." Nat Med **16**(12): 1421-1428.

Lee, S. J., L. R. Schover, A. H. Partridge, P. Patrizio, W. H. Wallace, K. Hagerty, L. N. Beck, L. V. Brennan, K. Oktay and O. American Society of Clinical (2006). "American Society of Clinical Oncology recommendations on fertility preservation in cancer patients." J Clin Oncol **24**(18): 2917-2931.

Lehmann, B. D., J. A. Bauer, X. Chen, M. E. Sanders, A. B. Chakravarthy, Y. Shyr and J. A. Pietenpol (2011). "Identification of human triple-negative breast cancer subtypes and preclinical models for selection of targeted therapies." J Clin Invest **121**(7): 2750-2767.

Lemm, I. and J. Ross (2002). "Regulation of c-myc mRNA decay by translational pausing in a coding region instability determinant." Mol Cell Biol **22**(12): 3959-3969.

Leone, G., J. DeGregori, R. Sears, L. Jakoi and J. R. Nevins (1997). "Myc and Ras collaborate in inducing accumulation of active cyclin E/Cdk2 and E2F." Nature **387**(6631): 422-426.

Leong, P. L., G. A. Andrews, D. E. Johnson, K. F. Dyer, S. Xi, J. C. Mai, P. D. Robbins, S. Gadiparthi, N. A. Burke, S. F. Watkins and J. R. Grandis (2003). "Targeted inhibition of Stat3 with a decoy oligonucleotide abrogates head and neck cancer cell growth." Proc Natl Acad Sci U S A **100**(7): 4138-4143.

Li, D., L. Ambrogio, T. Shimamura, S. Kubo, M. Takahashi, L. R. Chirieac, R. F. Padera, G. I. Shapiro, A. Baum, F. Himmelsbach, W. J. Rettig, M. Meyerson, F. Solca, H. Greulich and K. K.

Wong (2008). "BIBW2992, an irreversible EGFR/HER2 inhibitor highly effective in preclinical lung cancer models." Oncogene **27**(34): 4702-4711.

Li, L. and P. E. Shaw (2002). "Autocrine-mediated activation of STAT3 correlates with cell proliferation in breast carcinoma lines." J Biol Chem **277**(20): 17397-17405.

Li, S., D. Shen, J. Shao, R. Crowder, W. Liu, A. Prat, X. He, S. Liu, J. Hoog, C. Lu, L. Ding, O. L. Griffith, C. Miller, D. Larson, R. S. Fulton, M. Harrison, T. Mooney, J. F. McMichael, J. Luo, Y. Tao, R. Goncalves, C. Schlosberg, J. F. Hiken, L. Saied, C. Sanchez, T. Giuntoli, C. Bumb, C. Cooper, R. T. Kitchens, A. Lin, C. Phommaly, S. R. Davies, J. Zhang, M. S. Kavuri, D. McEachern, Y. Y. Dong, C. Ma, T. Pluard, M. Naughton, R. Bose, R. Suresh, R. McDowell, L. Michel, R. Aft, W. Gillanders, K. DeSchryver, R. K. Wilson, S. Wang, G. B. Mills, A. Gonzalez-Angulo, J. R. Edwards, C. Maher, C. M. Perou, E. R. Mardis and M. J. Ellis (2013). "Endocrine-therapy-resistant ESR1 variants revealed by genomic characterization of breast-cancer-derived xenografts." Cell Rep **4**(6): 1116-1130.

Li, Z., S. Van Calcar, C. Qu, W. K. Cavenee, M. Q. Zhang and B. Ren (2003). "A global transcriptional regulatory role for c-Myc in Burkitt's lymphoma cells." Proc Natl Acad Sci U S A **100**(14): 8164-8169.

Liang, K., F. J. Esteva, C. Albarracin, K. Stemke-Hale, Y. Lu, G. Bianchini, C. Y. Yang, Y. Li, X. Li, C. T. Chen, G. B. Mills, G. N. Hortobagyi, J. Mendelsohn, M. C. Hung and Z. Fan (2010). "Recombinant human erythropoietin antagonizes trastuzumab treatment of breast cancer cells via Jak2-mediated Src activation and PTEN inactivation." Cancer Cell **18**(5): 423-435.

Liedtke, C., C. Hatzis, W. F. Symmans, C. Desmedt, B. Haibe-Kains, V. Valero, H. Kuerer, G. N. Hortobagyi, M. Piccart-Gebhart, C. Sotiriou and L. Pusztai (2009). "Genomic grade index is associated with response to chemotherapy in patients with breast cancer." J Clin Oncol **27**(19): 3185-3191.

Liedtke, C., C. Mazouni, K. R. Hess, F. Andre, A. Tordai, J. A. Mejia, W. F. Symmans, A. M. Gonzalez-Angulo, B. Hennessy, M. Green, M. Cristofanilli, G. N. Hortobagyi and L. Pusztai (2008). "Response to neoadjuvant therapy and long-term survival in patients with triple-negative breast cancer." J Clin Oncol **26**(8): 1275-1281.

Lim, E., F. Vaillant, D. Wu, N. C. Forrest, B. Pal, A. H. Hart, M. L. Asselin-Labat, D. E. Gyorki, T. Ward, A. Partanen, F. Feleppa, L. I. Huschtscha, H. J. Thorne, kConFab, S. B. Fox, M. Yan, J. D. French, M. A. Brown, G. K. Smyth, J. E. Visvader and G. J. Lindeman (2009). "Aberrant luminal progenitors as the candidate target population for basal tumor development in BRCA1 mutation carriers." Nat Med **15**(8): 907-913.

Linderholm, B. K., H. Hellborg, U. Johansson, G. Elmberger, L. Skoog, J. Lehtio and R. Lewensohn (2009). "Significantly higher levels of vascular endothelial growth factor (VEGF) and shorter survival times for patients with primary operable triple-negative breast cancer." Ann Oncol **20**(10): 1639-1646.

Liu, X., H. Holstege, H. van der Gulden, M. Treur-Mulder, J. Zevenhoven, A. Velds, R. M. Kerkhoven, M. H. van Vliet, L. F. Wessels, J. L. Peterse, A. Berns and J. Jonkers (2007). "Somatic loss of BRCA1 and p53 in mice induces mammary tumors with features of human BRCA1-mutated basal-like breast cancer." Proc Natl Acad Sci U S A **104**(29): 12111-12116.

Loibl, S., G. von Minckwitz, A. Schneeweiss, S. Paepke, A. Lehmann, M. Rezai, D. M. Zahm, P. Sinn, F. Khandan, H. Eidtmann, K. Dohnal, C. Heinrichs, J. Huober, B. Pfitzner, P. A. Fasching, F. Andre, J. L. Lindner, C. Sotiriou, A. Dykgers, S. Guo, S. Gade, V. Nekljudova, S. Loi, M. Untch and C. Denkert (2014). "PIK3CA mutations are associated with lower rates of pathologic complete response to anti-human epidermal growth factor receptor 2 (her2) therapy in primary HER2-overexpressing breast cancer." J Clin Oncol **32**(29): 3212-3220.

Long, X. and K. P. Nephew (2006). "Fulvestrant (ICI 182,780)-dependent interacting proteins mediate immobilization and degradation of estrogen receptor-alpha." J Biol Chem **281**(14): 9607-9615.

Look, M. P., W. L. van Putten, M. J. Duffy, N. Harbeck, I. J. Christensen, C. Thomssen, R. Kates, F. Spyratos, M. Ferno, S. Eppenberger-Castori, C. G. Sweep, K. Ulm, J. P. Peyrat, P. M. Martin, H. Magdelenat, N. Brunner, C. Duggan, B. W. Lisboa, P. O. Bendahl, V. Quillien, A. Daver, G. Ricolleau, M. E. Meijer-van Gelder, P. Manders, W. E. Fiets, M. A. Blankenstein, P. Broet, S. Romain, G. Daxenbichler, G. Windbichler, T. Cufer, S. Borstnar, W. Kueng, L. V. Beex, J. G. Klijn, N. O'Higgins, U. Eppenberger, F. Janicke, M. Schmitt and J. A. Foekens (2002). "Pooled analysis of prognostic impact of urokinase-type plasminogen activator and its inhibitor PAI-1 in 8377 breast cancer patients." J Natl Cancer Inst **94**(2): 116-128.

Lu, Y., X. Zi, Y. Zhao, D. Mascarenhas and M. Pollak (2001). "Insulin-like growth factor-I receptor signaling and resistance to trastuzumab (Herceptin)." J Natl Cancer Inst **93**(24): 1852-1857.

Lutterbach, B. and S. R. Hann (1994). "Hierarchical phosphorylation at N-terminal transformation-sensitive sites in c-Myc protein is regulated by mitogens and in mitosis." Mol Cell Biol **14**(8): 5510-5522.

Ma, C. X., S. Cai, S. Li, C. E. Ryan, Z. Guo, W. T. Schaiff, L. Lin, J. Hoog, R. J. Goiffon, A. Prat, R. L. Aft, M. J. Ellis and H. Piwnica-Worms (2012). "Targeting Chk1 in p53-deficient

triple-negative breast cancer is therapeutically beneficial in human-in-mouse tumor models." J Clin Invest **122**(4): 1541-1552.

Ma, X. J., R. Salunga, S. Dahiya, W. Wang, E. Carney, V. Durbecq, A. Harris, P. Goss, C. Sotiriou, M. Erlander and D. Sgroi (2008). "A five-gene molecular grade index and HOXB13:IL17BR are complementary prognostic factors in early stage breast cancer." Clin Cancer Res **14**(9): 2601-2608.

Macias, H. and L. Hinck (2012). "Mammary gland development." Wiley Interdiscip Rev Dev Biol **1**(4): 533-557.

Maira, S. M., F. Stauffer, J. Brueggen, P. Furet, C. Schnell, C. Fritsch, S. Brachmann, P. Chene, A. De Pover, K. Schoemaker, D. Fabbro, D. Gabriel, M. Simonen, L. Murphy, P. Finan, W. Sellers and C. Garcia-Echeverria (2008). "Identification and characterization of NVP-BEZ235, a new orally available dual phosphatidylinositol 3-kinase/mammalian target of rapamycin inhibitor with potent in vivo antitumor activity." Mol Cancer Ther **7**(7): 1851-1863.

Malhotra, G. K., X. Zhao, H. Band and V. Band (2010). "Histological, molecular and functional subtypes of breast cancers." Cancer Biol Ther **10**(10): 955-960.

Marangoni, E., A. Vincent-Salomon, N. Auger, A. Degeorges, F. Assayag, P. de Cremoux, L. de Plater, C. Guyader, G. De Pinieux, J. G. Judde, M. Rebucci, C. Tran-Perennou, X. Sastre-Garau, B. Sigal-Zafrani, O. Delattre, V. Dieras and M. F. Poupon (2007). "A new model of patient tumor-derived breast cancer xenografts for preclinical assays." Clin Cancer Res **13**(13): 3989-3998.

Marotta, L. L., V. Almendro, A. Marusyk, M. Shipitsin, J. Schemme, S. R. Walker, N. Bloushtain-Qimron, J. J. Kim, S. A. Choudhury, R. Maruyama, Z. Wu, M. Gonen, L. A. Mulvey, M. O. Bessarabova, S. J. Huh, S. J. Silver, S. Y. Kim, S. Y. Park, H. E. Lee, K. S. Anderson, A. L. Richardson, T. Nikolskaya, Y. Nikolsky, X. S. Liu, D. E. Root, W. C. Hahn, D. A. Frank and K. Polyak (2011). "The JAK2/STAT3 signaling pathway is required for growth of CD44(+)CD24(-) stem cell-like breast cancer cells in human tumors." J Clin Invest **121**(7): 2723-2735.

Maroulakou, I. G., M. Anver, L. Garrett and J. E. Green (1994). "Prostate and mammary adenocarcinoma in transgenic mice carrying a rat C3(1) simian virus 40 large tumor antigen fusion gene." Proc Natl Acad Sci U S A **91**(23): 11236-11240.

Mateyak, M. K., A. J. Obaya and J. M. Sedivy (1999). "c-Myc regulates cyclin D-Cdk4 and -Cdk6 activity but affects cell cycle progression at multiple independent points." Mol Cell Biol **19**(7): 4672-4683.

McCormack, S. J., Z. Weaver, S. Deming, G. Natarajan, J. Torri, M. D. Johnson, M. Liyanage, T. Ried and R. B. Dickson (1998). "Myc/p53 interactions in transgenic mouse mammary development, tumorigenesis and chromosomal instability." Oncogene **16**(21): 2755-2766.

Menssen, A. and H. Hermeking (2002). "Characterization of the c-MYC-regulated transcriptome by SAGE: identification and analysis of c-MYC target genes." Proc Natl Acad Sci U S A **99**(9): 6274-6279.

Mertz, J. A., A. R. Conery, B. M. Bryant, P. Sandy, S. Balasubramanian, D. A. Mele, L. Bergeron and R. J. Sims, 3rd (2011). "Targeting MYC dependence in cancer by inhibiting BET bromodomains." Proc Natl Acad Sci U S A **108**(40): 16669-16674.

Michels, S., M. Trautmann, E. Sievers, D. Kindler, S. Huss, M. Renner, N. Friedrichs, J. Kirfel, S. Steiner, E. Endl, P. Wurst, L. Heukamp, R. Penzel, O. Larsson, A. Kawai, S. Tanaka, H. Sonobe, P. Schirmacher, G. Mechtersheimer, E. Wardelmann, R. Buttner and W. Hartmann (2013). "SRC signaling is crucial in the growth of synovial sarcoma cells." Cancer Res **73**(8): 2518-2528.

Miles, D. W., V. Dieras, J. Cortes, A. A. Duenne, J. Yi and J. O'Shaughnessy (2013). "First-line bevacizumab in combination with chemotherapy for HER2-negative metastatic breast cancer: pooled and subgroup analyses of data from 2447 patients." Ann Oncol **24**(11): 2773-2780.

Miller, K., M. Wang, J. Gralow, M. Dickler, M. Cobleigh, E. A. Perez, T. Shenkier, D. Cella and N. E. Davidson (2007). "Paclitaxel plus bevacizumab versus paclitaxel alone for metastatic breast cancer." N Engl J Med **357**(26): 2666-2676.

Miller, T. W., J. M. Balko, Z. Ghazoui, A. Dunbier, H. Anderson, M. Dowsett, A. M. Gonzalez-Angulo, G. B. Mills, W. R. Miller, H. Wu, Y. Shyr and C. L. Arteaga (2011). "A gene expression signature from human breast cancer cells with acquired hormone independence identifies MYC as a mediator of antiestrogen resistance." Clin Cancer Res **17**(7): 2024-2034.

Nagata, Y., K. H. Lan, X. Zhou, M. Tan, F. J. Esteva, A. A. Sahin, K. S. Klos, P. Li, B. P. Monia, N. T. Nguyen, G. N. Hortobagyi, M. C. Hung and D. Yu (2004). "PTEN activation contributes to tumor inhibition by trastuzumab, and loss of PTEN predicts trastuzumab resistance in patients." Cancer Cell **6**(2): 117-127.

Nahta, R., L. X. Yuan, Y. Du and F. J. Esteva (2007). "Lapatinib induces apoptosis in trastuzumab-resistant breast cancer cells: effects on insulin-like growth factor I signaling." Mol Cancer Ther **6**(2): 667-674.

Nahta, R., L. X. Yuan, B. Zhang, R. Kobayashi and F. J. Esteva (2005). "Insulin-like growth factor-I receptor/human epidermal growth factor receptor 2 heterodimerization contributes to trastuzumab resistance of breast cancer cells." Cancer Res **65**(23): 11118-11128.

Naidu, R., N. A. Wahab, M. Yadav and M. K. Kutty (2002). "Protein expression and molecular analysis of c-myc gene in primary breast carcinomas using immunohistochemistry and differential polymerase chain reaction." Int J Mol Med **9**(2): 189-196.

Nakagawa, M., M. Koyanagi, K. Tanabe, K. Takahashi, T. Ichisaka, T. Aoi, K. Okita, Y. Mochiduki, N. Takizawa and S. Yamanaka (2008). "Generation of induced pluripotent stem cells without Myc from mouse and human fibroblasts." Nat Biotechnol **26**(1): 101-106.

Narayan, M., J. A. Wilken, L. N. Harris, A. T. Baron, K. D. Kimbler and N. J. Maihle (2009). "Trastuzumab-induced HER reprogramming in "resistant" breast carcinoma cells." Cancer Res **69**(6): 2191-2194.

Niu, G., R. Heller, R. Catlett-Falcone, D. Coppola, M. Jaroszeski, W. Dalton, R. Jove and H. Yu (1999). "Gene therapy with dominant-negative Stat3 suppresses growth of the murine melanoma B16 tumor in vivo." Cancer Res **59**(20): 5059-5063.

Niu, G., K. L. Wright, M. Huang, L. Song, E. Haura, J. Turkson, S. Zhang, T. Wang, D. Sinibaldi, D. Coppola, R. Heller, L. M. Ellis, J. Karras, J. Bromberg, D. Pardoll, R. Jove and H. Yu (2002). "Constitutive Stat3 activity up-regulates VEGF expression and tumor angiogenesis." Oncogene **21**(13): 2000-2008.

O'Donnell, K. A., E. A. Wentzel, K. I. Zeller, C. V. Dang and J. T. Mendell (2005). "c-Myc-regulated microRNAs modulate E2F1 expression." Nature **435**(7043): 839-843.

O'Reilly, K. E., F. Rojo, Q. B. She, D. Solit, G. B. Mills, D. Smith, H. Lane, F. Hofmann, D. J. Hicklin, D. L. Ludwig, J. Baselga and N. Rosen (2006). "mTOR inhibition induces upstream receptor tyrosine kinase signaling and activates Akt." Cancer Res **66**(3): 1500-1508.

O'Shaughnessy, J., C. Osborne, J. E. Pippen, M. Yoffe, D. Patt, C. Rocha, I. C. Koo, B. M. Sherman and C. Bradley (2011). "Iniparib plus chemotherapy in metastatic triple-negative breast cancer." N Engl J Med **364**(3): 205-214.

Pal, S. K., S. K. Lau, L. Kruper, U. Nwoye, C. Garberoglio, R. K. Gupta, B. Paz, L. Vora, E. Guzman, A. Artinyan and G. Somlo (2010). "Papillary carcinoma of the breast: an overview." Breast Cancer Res Treat **122**(3): 637-645.

Pang, B., X. Qiao, L. Janssen, A. Velds, T. Groothuis, R. Kerkhoven, M. Nieuwland, H. Ovaa, S. Rottenberg, O. van Tellingen, J. Janssen, P. Huijgens, W. Zwart and J. Neefjes (2013). "Drug-induced histone eviction from open chromatin contributes to the chemotherapeutic effects of doxorubicin." Nat Commun **4**: 1908.

Park, O. K., T. S. Schaefer and D. Nathans (1996). "In vitro activation of Stat3 by epidermal growth factor receptor kinase." Proc Natl Acad Sci U S A **93**(24): 13704-13708.

Parker, J. S., M. Mullins, M. C. Cheang, S. Leung, D. Voduc, T. Vickery, S. Davies, C. Fauron, X. He, Z. Hu, J. F. Quackenbush, I. J. Stijleman, J. Palazzo, J. S. Marron, A. B. Nobel, E. Mardis, T. O. Nielsen, M. J. Ellis, C. M. Perou and P. S. Bernard (2009). "Supervised risk predictor of breast cancer based on intrinsic subtypes." J Clin Oncol **27**(8): 1160-1167.

Patel, K. J., V. P. Yu, H. Lee, A. Corcoran, F. C. Thistlethwaite, M. J. Evans, W. H. Colledge, L. S. Friedman, B. A. Ponder and A. R. Venkitaraman (1998). "Involvement of Brca2 in DNA repair." Mol Cell **1**(3): 347-357.

Perou, C. M., S. S. Jeffrey, M. van de Rijn, C. A. Rees, M. B. Eisen, D. T. Ross, A. Pergamenschikov, C. F. Williams, S. X. Zhu, J. C. Lee, D. Lashkari, D. Shalon, P. O. Brown and D. Botstein (1999). "Distinctive gene expression patterns in human mammary epithelial cells and breast cancers." Proc Natl Acad Sci U S A **96**(16): 9212-9217.

Perou, C. M., T. Sorlie, M. B. Eisen, M. van de Rijn, S. S. Jeffrey, C. A. Rees, J. R. Pollack, D. T. Ross, H. Johnsen, L. A. Akslen, O. Fluge, A. Pergamenschikov, C. Williams, S. X. Zhu, P. E. Lonning, A. L. Borresen-Dale, P. O. Brown and D. Botstein (2000). "Molecular portraits of human breast tumours." Nature **406**(6797): 747-752.

Philp, J. A., T. G. Burdon and C. J. Watson (1996). "Differential activation of STATs 3 and 5 during mammary gland development." FEBS Lett **396**(1): 77-80.

Pilati, C., M. Amessou, M. P. Bihl, C. Balabaud, J. T. Nhieu, V. Paradis, J. C. Nault, T. Izard, P. Bioulac-Sage, G. Couchy, K. Poussin and J. Zucman-Rossi (2011). "Somatic mutations activating STAT3 in human inflammatory hepatocellular adenomas." J Exp Med **208**(7): 1359-1366.

Prat, A., J. S. Parker, O. Karginova, C. Fan, C. Livasy, J. I. Herschkowitz, X. He and C. M. Perou (2010). "Phenotypic and molecular characterization of the claudin-low intrinsic subtype of breast cancer." Breast Cancer Res **12**(5): R68.

Prat, A. and C. M. Perou (2009). "Mammary development meets cancer genomics." Nat Med **15**(8): 842-844.

Prat, A. and C. M. Perou (2011). "Deconstructing the molecular portraits of breast cancer." Mol Oncol **5**(1): 5-23.

Rabbitts, P. H., A. Forster, M. A. Stinson and T. H. Rabbitts (1985). "Truncation of exon 1 from the c-myc gene results in prolonged c-myc mRNA stability." EMBO J **4**(13B): 3727-3733.

Ramsay, G., G. I. Evan and J. M. Bishop (1984). "The protein encoded by the human proto-oncogene c-myc." Proc Natl Acad Sci U S A **81**(24): 7742-7746.

Ranger, J. J., D. E. Levy, S. Shahalizadeh, M. Hallett and W. J. Muller (2009). "Identification of a Stat3-dependent transcription regulatory network involved in metastatic progression." Cancer Res **69**(17): 6823-6830.

Raz, R., C. K. Lee, L. A. Cannizzaro, P. d'Eustachio and D. E. Levy (1999). "Essential role of STAT3 for embryonic stem cell pluripotency." Proc Natl Acad Sci U S A **96**(6): 2846-2851.

Riely, G. J., W. Pao, D. Pham, A. R. Li, N. Rizvi, E. S. Venkatraman, M. F. Zakowski, M. G. Kris, M. Ladanyi and V. A. Miller (2006). "Clinical course of patients with non-small cell lung cancer and epidermal growth factor receptor exon 19 and exon 21 mutations treated with gefitinib or erlotinib." Clin Cancer Res **12**(3 Pt 1): 839-844.

Roberts, P. J., J. E. Usary, D. B. Darr, P. M. Dillon, A. D. Pfefferle, M. C. Whittle, J. S. Duncan, S. M. Johnson, A. J. Combest, J. Jin, W. C. Zamboni, G. L. Johnson, C. M. Perou and N. E. Sharpless (2012). "Combined PI3K/mTOR and MEK inhibition provides broad antitumor activity in faithful murine cancer models." Clin Cancer Res **18**(19): 5290-5303.

Rody, A., T. Karn, C. Liedtke, L. Pusztai, E. Ruckhaeberle, L. Hanker, R. Gaetje, C. Solbach, A. Ahr, D. Metzler, M. Schmidt, V. Muller, U. Holtrich and M. Kaufmann (2011). "A clinically relevant gene signature in triple negative and basal-like breast cancer." Breast Cancer Res **13**(5): R97.

Romond, E. H., E. A. Perez, J. Bryant, V. J. Suman, C. E. Geyer, Jr., N. E. Davidson, E. Tan-Chiu, S. Martino, S. Paik, P. A. Kaufman, S. M. Swain, T. M. Pisansky, L. Fehrenbacher, L. A. Kutteh, V. G. Vogel, D. W. Visscher, G. Yothers, R. B. Jenkins, A. M. Brown, S. R. Dakhil, E. P. Mamounas, W. L. Lingle, P. M. Klein, J. N. Ingle and N. Wolmark (2005). "Trastuzumab plus adjuvant chemotherapy for operable HER2-positive breast cancer." N Engl J Med **353**(16): 1673-1684.

Ross, J. S., C. Hatzis, W. F. Symmans, L. Pusztai and G. N. Hortobagyi (2008). "Commercialized multigene predictors of clinical outcome for breast cancer." Oncologist **13**(5): 477-493.

Rupnow, B. A., A. D. Murtha, R. M. Alarcon, A. J. Giaccia and S. J. Knox (1998). "Direct evidence that apoptosis enhances tumor responses to fractionated radiotherapy." Cancer Res **58**(9): 1779-1784.

Rusnak, D. W., K. Lackey, K. Affleck, E. R. Wood, K. J. Alligood, N. Rhodes, B. R. Keith, D. M. Murray, W. B. Knight, R. J. Mullin and T. M. Gilmer (2001). "The effects of the novel, reversible epidermal growth factor receptor/ErbB-2 tyrosine kinase inhibitor, GW2016, on the growth of human normal and tumor-derived cell lines in vitro and in vivo." Mol Cancer Ther **1**(2): 85-94.

Sachdeva, M., S. Zhu, F. Wu, H. Wu, V. Walia, S. Kumar, R. Elble, K. Watabe and Y. Y. Mo (2009). "p53 represses c-Myc through induction of the tumor suppressor miR-145." Proc Natl Acad Sci U S A **106**(9): 3207-3212.

Sargeant, T. J., B. Lloyd-Lewis, H. K. Resemann, A. Ramos-Montoya, J. Skepper and C. J. Watson (2014). "Stat3 controls cell death during mammary gland involution by regulating uptake of milk fat globules and lysosomal membrane permeabilization." Nat Cell Biol **16**(11): 1057-1068.

Schmid, P., W. A. Schulz and H. Hameister (1989). "Dynamic expression pattern of the myc protooncogene in midgestation mouse embryos." Science **243**(4888): 226-229.

Schmidt, E. V. (1999). "The role of c-myc in cellular growth control." Oncogene **18**(19): 2988-2996.

Schoenenberger, C. A., A. C. Andres, B. Groner, M. van der Valk, M. LeMeur and P. Gerlinger (1988). "Targeted c-myc gene expression in mammary glands of transgenic mice induces mammary tumours with constitutive milk protein gene transcription." EMBO J **7**(1): 169-175.

Schuyer, M. and E. M. Berns (1999). "Is TP53 dysfunction required for BRCA1-associated carcinogenesis?" Mol Cell Endocrinol **155**(1-2): 143-152.

Scognamiglio, R., N. Cabezas-Wallscheid, M. C. Thier, S. Altamura, A. Reyes, A. M. Prendergast, D. Baumgartner, L. S. Carnevalli, A. Atzberger, S. Haas, L. von Paleske, T. Boroviak, P. Worsdorfer, M. A. Essers, U. Kloz, R. N. Eisenman, F. Edenhofer, P. Bertone, W.

Huber, F. van der Hoeven, A. Smith and A. Trumpp (2016). "Myc Depletion Induces a Pluripotent Dormant State Mimicking Diapause." Cell **164**(4): 668-680.

Sears, R., G. Leone, J. DeGregori and J. R. Nevins (1999). "Ras enhances Myc protein stability." Mol Cell **3**(2): 169-179.

Sears, R., F. Nuckolls, E. Haura, Y. Taya, K. Tamai and J. R. Nevins (2000). "Multiple Ras-dependent phosphorylation pathways regulate Myc protein stability." Genes Dev **14**(19): 2501-2514.

Sen, M., S. M. Thomas, S. Kim, J. I. Yeh, R. L. Ferris, J. T. Johnson, U. Duvvuri, J. Lee, N. Sahu, S. Joyce, M. L. Freilino, H. Shi, C. Li, D. Ly, S. Rapireddy, J. P. Etter, P. K. Li, L. Wang, S. Chiosea, R. R. Seethala, W. E. Gooding, X. Chen, N. Kaminski, K. Pandit, D. E. Johnson and J. R. Grandis (2012). "First-in-human trial of a STAT3 decoy oligonucleotide in head and neck tumors: implications for cancer therapy." Cancer Discov **2**(8): 694-705.

Serra, V., M. Scaltriti, L. Prudkin, P. J. Eichhorn, Y. H. Ibrahim, S. Chandarlapaty, B. Markman, O. Rodriguez, M. Guzman, S. Rodriguez, M. Gili, M. Russillo, J. L. Parra, S. Singh, J. Arribas, N. Rosen and J. Baselga (2011). "PI3K inhibition results in enhanced HER signaling and acquired ERK dependency in HER2-overexpressing breast cancer." Oncogene **30**(22): 2547-2557.

Seth, A., F. A. Gonzalez, S. Gupta, D. L. Raden and R. J. Davis (1992). "Signal transduction within the nucleus by mitogen-activated protein kinase." J Biol Chem **267**(34): 24796-24804.

Shattuck, D. L., J. K. Miller, K. L. Carraway, 3rd and C. Sweeney (2008). "Met receptor contributes to trastuzumab resistance of Her2-overexpressing breast cancer cells." Cancer Res **68**(5): 1471-1477.

Siegel, R. L., K. D. Miller and A. Jemal (2016). "Cancer statistics, 2016." CA Cancer J Clin **66**(1): 7-30.

Simons, J. P., M. McClenaghan and A. J. Clark (1987). "Alteration of the quality of milk by expression of sheep beta-lactoglobulin in transgenic mice." Nature **328**(6130): 530-532.

Singel, S. M., C. Cornelius, K. Batten, G. Fasciani, W. E. Wright, L. Lum and J. W. Shay (2013). "A targeted RNAi screen of the breast cancer genome identifies KIF14 and TLN1 as genes that modulate docetaxel chemosensitivity in triple-negative breast cancer." Clin Cancer Res **19**(8): 2061-2070.

Sinn, E., W. Muller, P. Pattengale, I. Tepler, R. Wallace and P. Leder (1987). "Coexpression of MMTV/v-Ha-ras and MMTV/c-myc genes in transgenic mice: synergistic action of oncogenes in vivo." Cell **49**(4): 465-475.

Slamon, D. J., B. Leyland-Jones, S. Shak, H. Fuchs, V. Paton, A. Bajamonde, T. Fleming, W. Eiermann, J. Wolter, M. Pegram, J. Baselga and L. Norton (2001). "Use of chemotherapy plus a monoclonal antibody against HER2 for metastatic breast cancer that overexpresses HER2." N Engl J Med **344**(11): 783-792.

Snyder, M., X. Y. Huang and J. J. Zhang (2008). "Identification of novel direct Stat3 target genes for control of growth and differentiation." J Biol Chem **283**(7): 3791-3798.

Sorlie, T., C. M. Perou, R. Tibshirani, T. Aas, S. Geisler, H. Johnsen, T. Hastie, M. B. Eisen, M. van de Rijn, S. S. Jeffrey, T. Thorsen, H. Quist, J. C. Matese, P. O. Brown, D. Botstein, P. E. Lonning and A. L. Borresen-Dale (2001). "Gene expression patterns of breast carcinomas distinguish tumor subclasses with clinical implications." Proc Natl Acad Sci U S A **98**(19): 10869-10874.

Sorlie, T., R. Tibshirani, J. Parker, T. Hastie, J. S. Marron, A. Nobel, S. Deng, H. Johnsen, R. Pesich, S. Geisler, J. Demeter, C. M. Perou, P. E. Lonning, P. O. Brown, A. L. Borresen-Dale and D. Botstein (2003). "Repeated observation of breast tumor subtypes in independent gene expression data sets." Proc Natl Acad Sci U S A **100**(14): 8418-8423.

Sotiriou, C., P. Wirapati, S. Loi, A. Harris, S. Fox, J. Smeds, H. Nordgren, P. Farmer, V. Praz, B. Haibe-Kains, C. Desmedt, D. Larsimont, F. Cardoso, H. Peterse, D. Nuyten, M. Buyse, M. J. Van de Vijver, J. Bergh, M. Piccart and M. Delorenzi (2006). "Gene expression profiling in breast cancer: understanding the molecular basis of histologic grade to improve prognosis." J Natl Cancer Inst **98**(4): 262-272.

Soucek, L., R. Jucker, L. Panacchia, R. Ricordy, F. Tato and S. Nasi (2002). "Omomyc, a potential Myc dominant negative, enhances Myc-induced apoptosis." Cancer Res **62**(12): 3507-3510.

Stein, T., N. Salomonis and B. A. Gusterson (2007). "Mammary gland involution as a multi-step process." J Mammary Gland Biol Neoplasia **12**(1): 25-35.

Stewart, T. A., P. K. Pattengale and P. Leder (1984). "Spontaneous mammary adenocarcinomas in transgenic mice that carry and express MTV/myc fusion genes." Cell **38**(3): 627-637.

Stoelzle, T., P. Schwarb, A. Trumpp and N. E. Hynes (2009). "c-Myc affects mRNA translation, cell proliferation and progenitor cell function in the mammary gland." BMC Biol **7**: 63.

Stone, J., T. de Lange, G. Ramsay, E. Jakobovits, J. M. Bishop, H. Varmus and W. Lee (1987). "Definition of regions in human c-myc that are involved in transformation and nuclear localization." Mol Cell Biol **7**(5): 1697-1709.

Subramanian, A., P. Tamayo, V. K. Mootha, S. Mukherjee, B. L. Ebert, M. A. Gillette, A. Paulovich, S. L. Pomeroy, T. R. Golub, E. S. Lander and J. P. Mesirov (2005). "Gene set enrichment analysis: a knowledge-based approach for interpreting genome-wide expression profiles." Proc Natl Acad Sci U S A **102**(43): 15545-15550.

Sun, C., S. Hobor, A. Bertotti, D. Zecchin, S. Huang, F. Galimi, F. Cottino, A. Prahallad, W. Grernrum, A. Tzani, A. Schlicker, L. F. Wessels, E. F. Smit, E. Thunnissen, P. Halonen, C. Lieftink, R. L. Beijersbergen, F. Di Nicolantonio, A. Bardelli, L. Trusolino and R. Bernards (2014). "Intrinsic resistance to MEK inhibition in KRAS mutant lung and colon cancer through transcriptional induction of ERBB3." Cell Rep **7**(1): 86-93.

Sutherland, K. D., F. Vaillant, W. S. Alexander, T. M. Wintermantel, N. C. Forrest, S. L. Holroyd, E. J. McManus, G. Schutz, C. J. Watson, L. A. Chodosh, G. J. Lindeman and J. E. Visvader (2006). "c-myc as a mediator of accelerated apoptosis and involution in mammary glands lacking Socs3." EMBO J **25**(24): 5805-5815.

Takahashi, K. and S. Yamanaka (2006). "Induction of pluripotent stem cells from mouse embryonic and adult fibroblast cultures by defined factors." Cell **126**(4): 663-676.

Takeda, K., T. Kaisho, N. Yoshida, J. Takeda, T. Kishimoto and S. Akira (1998). "Stat3 activation is responsible for IL-6-dependent T cell proliferation through preventing apoptosis: generation and characterization of T cell-specific Stat3-deficient mice." J Immunol **161**(9): 4652-4660.

Takeda, K., K. Noguchi, W. Shi, T. Tanaka, M. Matsumoto, N. Yoshida, T. Kishimoto and S. Akira (1997). "Targeted disruption of the mouse Stat3 gene leads to early embryonic lethality." Proc Natl Acad Sci U S A **94**(8): 3801-3804.

Tang, Y., X. Wu, W. Lei, L. Pang, C. Wan, Z. Shi, L. Zhao, T. R. Nagy, X. Peng, J. Hu, X. Feng, W. Van Hul, M. Wan and X. Cao (2009). "TGF-beta1-induced migration of bone mesenchymal stem cells couples bone resorption with formation." Nat Med **15**(7): 757-765.

Taub, R., I. Kirsch, C. Morton, G. Lenoir, D. Swan, S. Tronick, S. Aaronson and P. Leder (1982). "Translocation of the c-myc gene into the immunoglobulin heavy chain locus in human Burkitt lymphoma and murine plasmacytoma cells." Proc Natl Acad Sci U S A **79**(24): 7837-7841.

Thomas, E. S., H. L. Gomez, R. K. Li, H. C. Chung, L. E. Fein, V. F. Chan, J. Jassem, X. B. Pivot, J. V. Klimovsky, F. H. de Mendoza, B. Xu, M. Campone, G. L. Lerzo, R. A. Peck, P. Mukhopadhyay, L. T. Vahdat and H. H. Roche (2007). "Ixabepilone plus capecitabine for metastatic breast cancer progressing after anthracycline and taxane treatment." J Clin Oncol **25**(33): 5210-5217.

Timofeeva, O. A., N. I. Tarasova, X. Zhang, S. Chasovskikh, A. K. Cheema, H. Wang, M. L. Brown and A. Dritschilo (2013). "STAT3 suppresses transcription of proapoptotic genes in cancer cells with the involvement of its N-terminal domain." Proc Natl Acad Sci U S A **110**(4): 1267-1272.

Toyoshima, M., H. L. Howie, M. Imakura, R. M. Walsh, J. E. Annis, A. N. Chang, J. Frazier, B. N. Chau, A. Loboda, P. S. Linsley, M. A. Cleary, J. R. Park and C. Grandori (2012). "Functional genomics identifies therapeutic targets for MYC-driven cancer." Proc Natl Acad Sci U S A **109**(24): 9545-9550.

Turke, A. B., Y. Song, C. Costa, R. Cook, C. L. Arteaga, J. M. Asara and J. A. Engelman (2012). "MEK inhibition leads to PI3K/AKT activation by relieving a negative feedback on ERBB receptors." Cancer Res **72**(13): 3228-3237.

Turkson, J., T. Bowman, R. Garcia, E. Caldenhoven, R. P. De Groot and R. Jove (1998). "Stat3 activation by Src induces specific gene regulation and is required for cell transformation." Mol Cell Biol **18**(5): 2545-2552.

Turkson, J., D. Ryan, J. S. Kim, Y. Zhang, Z. Chen, E. Haura, A. Laudano, S. Sebti, A. D. Hamilton and R. Jove (2001). "Phosphotyrosyl peptides block Stat3-mediated DNA binding activity, gene regulation, and cell transformation." J Biol Chem **276**(48): 45443-45455.

Turkson, J., S. Zhang, J. Palmer, H. Kay, J. Stanko, L. B. Mora, S. Sebti, H. Yu and R. Jove (2004). "Inhibition of constitutive signal transducer and activator of transcription 3 activation by novel platinum complexes with potent antitumor activity." Mol Cancer Ther **3**(12): 1533-1542.

Turner, N., A. Tutt and A. Ashworth (2004). "Hallmarks of 'BRCAness' in sporadic cancers." Nat Rev Cancer **4**(10): 814-819.

Turner, N. C., C. J. Lord, E. Iorns, R. Brough, S. Swift, R. Elliott, S. Rayter, A. N. Tutt and A. Ashworth (2008). "A synthetic lethal siRNA screen identifying genes mediating sensitivity to a PARP inhibitor." EMBO J **27**(9): 1368-1377.

Tusher, V. G., R. Tibshirani and G. Chu (2001). "Significance analysis of microarrays applied to the ionizing radiation response." Proc Natl Acad Sci U S A **98**(9): 5116-5121.

Tutt, A., M. Robson, J. E. Garber, S. M. Domchek, M. W. Audeh, J. N. Weitzel, M. Friedlander, B. Arun, N. Loman, R. K. Schmutzler, A. Wardley, G. Mitchell, H. Earl, M. Wickens and J. Carmichael (2010). "Oral poly(ADP-ribose) polymerase inhibitor olaparib in patients with BRCA1 or BRCA2 mutations and advanced breast cancer: a proof-of-concept trial." Lancet **376**(9737): 235-244.

Usary, J., W. Zhao, D. Darr, P. J. Roberts, M. Liu, L. Balletta, O. Karginova, J. Jordan, A. Combest, A. Bridges, A. Prat, M. C. Cheang, J. I. Herschkowitz, J. M. Rosen, W. Zamboni, N. E. Sharpless and C. M. Perou (2013). "Predicting drug responsiveness in human cancers using genetically engineered mice." Clin Cancer Res **19**(17): 4889-4899.

Vafa, O., M. Wade, S. Kern, M. Beeche, T. K. Pandita, G. M. Hampton and G. M. Wahl (2002). "c-Myc can induce DNA damage, increase reactive oxygen species, and mitigate p53 function: a mechanism for oncogene-induced genetic instability." Mol Cell **9**(5): 1031-1044.

Van Keymeulen, A., A. S. Rocha, M. Ousset, B. Beck, G. Bouvencourt, J. Rock, N. Sharma, S. Dekoninck and C. Blanpain (2011). "Distinct stem cells contribute to mammary gland development and maintenance." Nature **479**(7372): 189-193.

Vargo-Gogola, T. and J. M. Rosen (2007). "Modelling breast cancer: one size does not fit all." Nat Rev Cancer **7**(9): 659-672.

Veltmaat, J. M., A. A. Mailleux, J. P. Thiery and S. Bellusci (2003). "Mouse embryonic mammogenesis as a model for the molecular regulation of pattern formation." Differentiation **71**(1): 1-17.

Verma, S., C. H. Bartlett, P. Schnell, A. M. DeMichele, S. Loi, J. Ro, M. Colleoni, H. Iwata, N. Harbeck, M. Cristofanilli, K. Zhang, A. Thiele, N. C. Turner and H. S. Rugo (2016). "Palbociclib in Combination With Fulvestrant in Women With Hormone Receptor-Positive/HER2-Negative Advanced Metastatic Breast Cancer: Detailed Safety Analysis From a Multicenter, Randomized, Placebo-Controlled, Phase III Study (PALOMA-3)." Oncologist.

Visvader, J. E. and G. J. Lindeman (2006). "Mammary stem cells and mammopoiesis." Cancer Res **66**(20): 9798-9801.

Vogel, C. L., M. A. Cobleigh, D. Tripathy, J. C. Gutheil, L. N. Harris, L. Fehrenbacher, D. J. Slamon, M. Murphy, W. F. Novotny, M. Burchmore, S. Shak, S. J. Stewart and M. Press (2002). "Efficacy and safety of trastuzumab as a single agent in first-line treatment of HER2-overexpressing metastatic breast cancer." J Clin Oncol **20**(3): 719-726.

Wang, S. E., A. Narasanna, M. Perez-Torres, B. Xiang, F. Y. Wu, S. Yang, G. Carpenter, A. F. Gazdar, S. K. Muthuswamy and C. L. Arteaga (2006). "HER2 kinase domain mutation results in constitutive phosphorylation and activation of HER2 and EGFR and resistance to EGFR tyrosine kinase inhibitors." Cancer Cell **10**(1): 25-38.

Wang, T., G. Niu, M. Kortylewski, L. Burdelya, K. Shain, S. Zhang, R. Bhattacharya, D. Gabrilovich, R. Heller, D. Coppola, W. Dalton, R. Jove, D. Pardoll and H. Yu (2004). "Regulation of the innate and adaptive immune responses by Stat-3 signaling in tumor cells." Nat Med **10**(1): 48-54.

Wang, X., M. Cunningham, X. Zhang, S. Tokarz, B. Laraway, M. Troxell and R. C. Sears (2011). "Phosphorylation regulates c-Myc's oncogenic activity in the mammary gland." Cancer Res **71**(3): 925-936.

Wang, Y. H., S. Liu, G. Zhang, C. Q. Zhou, H. X. Zhu, X. B. Zhou, L. P. Quan, J. F. Bai and N. Z. Xu (2005). "Knockdown of c-Myc expression by RNAi inhibits MCF-7 breast tumor cells growth in vitro and in vivo." Breast Cancer Res **7**(2): R220-228.

Wasylishen, A. R., M. Chan-Seng-Yue, C. Bros, D. Dingar, W. B. Tu, M. Kalkat, P. K. Chan, P. J. Mullen, L. Huang, N. Meyer, B. Raught, P. C. Boutros and L. Z. Penn (2013). "MYC phosphorylation at novel regulatory regions suppresses transforming activity." Cancer Res **73**(21): 6504-6515.

Watson, C. J. (2006). "Involution: apoptosis and tissue remodelling that convert the mammary gland from milk factory to a quiescent organ." Breast Cancer Res **8**(2): 203.

Watson, C. J. and W. R. Miller (1995). "Elevated levels of members of the STAT family of transcription factors in breast carcinoma nuclear extracts." Br J Cancer **71**(4): 840-844.

Weidensdorfer, D., N. Stohr, A. Baude, M. Lederer, M. Kohn, A. Schierhorn, S. Buchmeier, E. Wahle and S. Huttelmaier (2009). "Control of c-myc mRNA stability by IGF2BP1-associated cytoplasmic RNPs." RNA **15**(1): 104-115.

Weigelt, B., A. T. Lo, C. C. Park, J. W. Gray and M. J. Bissell (2010). "HER2 signaling pathway activation and response of breast cancer cells to HER2-targeting agents is dependent strongly on the 3D microenvironment." Breast Cancer Res Treat **122**(1): 35-43.

Welcker, M. and B. E. Clurman (2008). "FBW7 ubiquitin ligase: a tumour suppressor at the crossroads of cell division, growth and differentiation." Nat Rev Cancer **8**(2): 83-93.

Wernig, M., A. Meissner, R. Foreman, T. Brambrink, M. Ku, K. Hochedlinger, B. E. Bernstein and R. Jaenisch (2007). "In vitro reprogramming of fibroblasts into a pluripotent ES-cell-like state." Nature **448**(7151): 318-324.

West, M., C. Blanchette, H. Dressman, E. Huang, S. Ishida, R. Spang, H. Zuzan, J. A. Olson, Jr., J. R. Marks and J. R. Nevins (2001). "Predicting the clinical status of human breast cancer by using gene expression profiles." Proc Natl Acad Sci U S A **98**(20): 11462-11467.

White, J. D., E. J. Junor, J. McGarva, J. McManners and I. S. Holland (2004). "Adenocarcinoma of the salivary gland? A chemo-sensitive disease." Clin Oncol (R Coll Radiol) **16**(2): 159-160.

Wierstra, I. and J. Alves (2008). "The c-myc promoter: still MysterY and challenge." Adv Cancer Res **99**: 113-333.

Wisdom, R. and W. Lee (1991). "The protein-coding region of c-myc mRNA contains a sequence that specifies rapid mRNA turnover and induction by protein synthesis inhibitors." Genes Dev **5**(2): 232-243.

Wiseman, B. S. and Z. Werb (2002). "Stromal effects on mammary gland development and breast cancer." Science **296**(5570): 1046-1049.

Wistuba, II, C. Behrens, S. Milchgrub, S. Syed, M. Ahmadian, A. K. Virmani, V. Kurvari, T. H. Cunningham, R. Ashfaq, J. D. Minna and A. F. Gazdar (1998). "Comparison of features of human breast cancer cell lines and their corresponding tumors." Clin Cancer Res **4**(12): 2931-2938.

Wooster, R., S. L. Neuhausen, J. Mangion, Y. Quirk, D. Ford, N. Collins, K. Nguyen, S. Seal, T. Tran, D. Averill and et al. (1994). "Localization of a breast cancer susceptibility gene, BRCA2, to chromosome 13q12-13." Science **265**(5181): 2088-2090.

Wright, J. B., S. J. Brown and M. D. Cole (2010). "Upregulation of c-MYC in cis through a large chromatin loop linked to a cancer risk-associated single-nucleotide polymorphism in colorectal cancer cells." Mol Cell Biol **30**(6): 1411-1420.

Xia, W., I. Husain, L. Liu, S. Bacus, S. Saini, J. Spohn, K. Pry, R. Westlund, S. H. Stein and N. L. Spector (2007). "Lapatinib antitumor activity is not dependent upon phosphatase and tensin homologue deleted on chromosome 10 in ErbB2-overexpressing breast cancers." Cancer Res **67**(3): 1170-1175.

Xiong, H., W. Du, Y. J. Zhang, J. Hong, W. Y. Su, J. T. Tang, Y. C. Wang, R. Lu and J. Y. Fang (2012). "Trichostatin A, a histone deacetylase inhibitor, suppresses JAK2/STAT3 signaling via inducing the promoter-associated histone acetylation of SOCS1 and SOCS3 in human colorectal cancer cells." Mol Carcinog **51**(2): 174-184.

Xu, Q., J. Briggs, S. Park, G. Niu, M. Kortylewski, S. Zhang, T. Gritsko, J. Turkson, H. Kay, G. L. Semenza, J. Q. Cheng, R. Jove and H. Yu (2005). "Targeting Stat3 blocks both HIF-1 and VEGF expression induced by multiple oncogenic growth signaling pathways." Oncogene **24**(36): 5552-5560.

Yakes, F. M., W. Chinratanalab, C. A. Ritter, W. King, S. Seelig and C. L. Arteaga (2002). "Herceptin-induced inhibition of phosphatidylinositol-3 kinase and Akt Is required for antibody-mediated effects on p27, cyclin D1, and antitumor action." Cancer Res **62**(14): 4132-4141.

Yamaguchi, T., R. Kakefuda, N. Tajima, Y. Sowa and T. Sakai (2011). "Antitumor activities of JTP-74057 (GSK1120212), a novel MEK1/2 inhibitor, on colorectal cancer cell lines in vitro and in vivo." Int J Oncol **39**(1): 23-31.

Yan, C. and P. J. Higgins (2013). "Drugging the undruggable: transcription therapy for cancer." Biochim Biophys Acta **1835**(1): 76-85.

Yanagawa, M., K. Ikemot, S. Kawauchi, T. Furuya, S. Yamamoto, M. Oka, A. Oga, Y. Nagashima and K. Sasaki (2012). "Luminal A and luminal B (HER2 negative) subtypes of breast cancer consist of a mixture of tumors with different genotype." BMC Res Notes **5**: 376.

Yang, D., H. Liu, A. Goga, S. Kim, M. Yuneva and J. M. Bishop (2010). "Therapeutic potential of a synthetic lethal interaction between the MYC proto-oncogene and inhibition of aurora-B kinase." Proc Natl Acad Sci U S A **107**(31): 13836-13841.

Yardley, D. A., R. Weaver, M. E. Melisko, M. N. Saleh, F. P. Arena, A. Forero, T. Cigler, A. Stopeck, D. Citrin, I. Oliff, R. Bechhold, R. Loutfi, A. A. Garcia, S. Cruickshank, E. Crowley, J.

Green, T. Hawthorne, M. J. Yellin, T. A. Davis and L. T. Vahdat (2015). "EMERGE: A Randomized Phase II Study of the Antibody-Drug Conjugate Glembatumumab Vedotin in Advanced Glycoprotein NMB-Expressing Breast Cancer." J Clin Oncol **33**(14): 1609-1619.

Yates, L. R., M. Gerstung, S. Knappskog, C. Desmedt, G. Gundem, P. Van Loo, T. Aas, L. B. Alexandrov, D. Larsimont, H. Davies, Y. Li, Y. S. Ju, M. Ramakrishna, H. K. Haugland, P. K. Lilleng, S. Nik-Zainal, S. McLaren, A. Butler, S. Martin, D. Glodzik, A. Menzies, K. Raine, J. Hinton, D. Jones, L. J. Mudie, B. Jiang, D. Vincent, A. Greene-Colozzi, P. Y. Adnet, A. Fatima, M. Maetens, M. Ignatiadis, M. R. Stratton, C. Sotiriou, A. L. Richardson, P. E. Lonning, D. C. Wedge and P. J. Campbell (2015). "Subclonal diversification of primary breast cancer revealed by multiregion sequencing." Nat Med **21**(7): 751-759.

Yeh, E., M. Cunningham, H. Arnold, D. Chasse, T. Monteith, G. Ivaldi, W. C. Hahn, P. T. Stukenberg, S. Shenolikar, T. Uchida, C. M. Counter, J. R. Nevins, A. R. Means and R. Sears (2004). "A signalling pathway controlling c-Myc degradation that impacts oncogenic transformation of human cells." Nat Cell Biol **6**(4): 308-318.

Yokogami, K., S. Wakisaka, J. Avruch and S. A. Reeves (2000). "Serine phosphorylation and maximal activation of STAT3 during CNTF signaling is mediated by the rapamycin target mTOR." Curr Biol **10**(1): 47-50.

Yu, H., M. Kortylewski and D. Pardoll (2007). "Crosstalk between cancer and immune cells: role of STAT3 in the tumour microenvironment." Nat Rev Immunol **7**(1): 41-51.

Yuwanita, I., D. Barnes, M. D. Monterey, S. O'Reilly and E. R. Andrechek (2015). "Increased metastasis with loss of E2F2 in Myc-driven tumors." Oncotarget **6**(35): 38210-38224.

Zhang, H., A. L. Cohen, S. Krishnakumar, I. L. Wapnir, S. Veeriah, G. Deng, M. A. Coram, C. M. Piskun, T. A. Longacre, M. Herrler, D. O. Frimannsson, M. L. Telli, F. M. Dirbas, A. C. Matin, S. H. Dairkee, B. Larijani, G. V. Glinsky, A. H. Bild and S. S. Jeffrey (2014). "Patient-derived xenografts of triple-negative breast cancer reproduce molecular features of patient tumors and respond to mTOR inhibition." Breast Cancer Res **16**(2): R36.

Zhang, S., W. C. Huang, P. Li, H. Guo, S. B. Poh, S. W. Brady, Y. Xiong, L. M. Tseng, S. H. Li, Z. Ding, A. A. Sahin, F. J. Esteva, G. N. Hortobagyi and D. Yu (2011). "Combating trastuzumab resistance by targeting SRC, a common node downstream of multiple resistance pathways." Nat Med **17**(4): 461-469.

Zhang, X., S. Claerhout, A. Prat, L. E. Dobrolecki, I. Petrovic, Q. Lai, M. D. Landis, L. Wiechmann, R. Schiff, M. Giuliano, H. Wong, S. W. Fuqua, A. Contreras, C. Gutierrez, J. Huang, S. Mao, A. C. Pavlick, A. M. Froehlich, M. F. Wu, A. Tsimelzon, S. G. Hilsenbeck, E. S.

Chen, P. Zuloaga, C. A. Shaw, M. F. Rimawi, C. M. Perou, G. B. Mills, J. C. Chang and M. T. Lewis (2013). "A renewable tissue resource of phenotypically stable, biologically and ethnically diverse, patient-derived human breast cancer xenograft models." Cancer Res **73**(15): 4885-4897.

Zhao, D., C. Pan, J. Sun, C. Gilbert, K. Drews-Elger, D. J. Azzam, M. Picon-Ruiz, M. Kim, W. Ullmer, D. El-Ashry, C. J. Creighton and J. M. Slingerland (2015). "VEGF drives cancer-initiating stem cells through VEGFR-2/Stat3 signaling to upregulate Myc and Sox2." Oncogene **34**(24): 3107-3119.

Zhou, J., J. Wulfkuhle, H. Zhang, P. Gu, Y. Yang, J. Deng, J. B. Margolick, L. A. Liotta, E. Petricoin, 3rd and Y. Zhang (2007). "Activation of the PTEN/mTOR/STAT3 pathway in breast cancer stem-like cells is required for viability and maintenance." Proc Natl Acad Sci U S A **104**(41): 16158-16163.

Zimmermann, S. and K. Moelling (1999). "Phosphorylation and regulation of Raf by Akt (protein kinase B)." Science **286**(5445): 1741-1744.